Functional characterization of peroxisomes in the heart and the role of *Pex11α* and *Pex14* in cardiomyocytes

Inaugural Dissertation

submitted to the

Faculty of Medicine

in partial fulfillment of the requirements

for the PhD degree

of the Faculties of Veterinary Medicine and Medicine

of the Justus Liebig University Giessen

By

Chen, Jiangping

of

Zhejiang, China

Giessen 2017

From the Institute for Anatomy and Cell Biology II

of the Faculty of Medicine of the Justus Liebig University of Giessen

Director / Chairperson: Prof. Dr. Eveline Baumgart-Vogt

First Supervisor and Committee Member: Prof. Dr. Eveline Baumgart-Vogt

Second Supervisor and Committee Member: Prof. Dr. Christiane Herden

Examination chair and Committee Member: Prof. Dr. Norbert Weißmann

Committee Member:

Declaration

“I declare that I have completed this dissertation single-handedly without the unauthorized help of a second party and only with the assistance acknowledged therein. I have appropriately acknowledged and referenced all text passages that are derived literally from or are based on the content of published or unpublished work of others, and all information that relates to verbal communications. I have abided by the principles of good scientific conduct laid down in the charter of the Justus Liebig University of Giessen in carrying out the investigations described in the dissertation.”

Date:

Place:

Functional characterization of peroxisomes in the heart and the role of *Pex11α* and *Pex14* in cardiomyocytes

1. Introduction

1.1. The peroxisome and its functions in cellular metabolism

1.1.1. The history of peroxisomes

The organelles now known as peroxisomes were discovered by (Rhodin, 1954) and were initially named microbodies. Two years later, similar structures, 0.2–1 µm in diameter and bound by a single membrane, were also found in rat liver parenchymal cells, and featured a characteristic dense core in the matrix with a regular crystalloid structure (Bernhard and Rouiller, 1956). Later studies revealed that the crystalloid core, which contains urate oxidase, is not present in all cell types, but is found in human and rodent liver cells, and in the bovine kidney (Zaar et al., 1987). Twelve years after their discovery, microbodies were renamed peroxisomes (De Duve and Baudhuin, 1966).

Peroxisomes were initially identified by cytochemical staining, exploiting the ability of catalase to oxidize 3,3′-diaminobenzidine (DAB) (Fahimi, 1969). This method is still widely used to characterize peroxisomes (Fahimi and Baumgart, 1999). However, as information about additional peroxisome enzymes has accumulated, other techniques have been developed, such as the cerium technique that detects oxidase activity. Moreover, immunocytochemical techniques based on peroxisome-specific antibodies have been used to study the heterogeneous protein composition of peroxisomal compartments, which also enabled detailed functional analysis of the peroxisome in different organ systems (Fahimi et al., 1999).

1.1.2. Peroxisome metabolic pathways

Peroxisomes contain more than 130 different proteins which are involved in a variety of metabolic pathways (Karnati and Baumgart-Vogt, 2008). The most important

functions are the β-oxidation of very-long-chain fatty acids (VLCFAs) and the metabolism of reactive oxygen species (ROS) (Moser et al., 1984). Other metabolic pathways include etherphospholipid synthesis, docosahexaenoic acid (DHA) synthesis, glyoxylate metabolism, amino acid degradation, and bile acid synthesis (Wanders et al., 2016).

1.1.2.1. Peroxisomal β-oxidation of fatty acids

The peroxisomal fatty acid β-oxidation pathway is found in most of cell types and organisms (Waterham et al., 2016). In humans, β-oxidation occurs in both peroxisomes and mitochondria (Waterham et al., 2016). Fatty acids with a methyl group at the 3-position (e.g. phytanic acid) need prior α-oxidation in peroxisomes, which requires the enzymes phytanoyl-CoA 2-hydroxylase, 2-hydroxyphytanoyl-coenzyme A (CoA) lyase, and pristanal dehydrogenase, before β-oxidation takes place (Waterham et al., 2016). The peroxisomes and mitochondria share the principal catalytic mechanism of β-oxidation, which is the shortening of fatty acid chains by removing two carbons via dehydrogenation, hydration, dehydrogenation, and thiolytic cleavage (Waterham et al., 2016). Different pathways in each organelle produce flavin adenine dinucleotide (FAD/$FADH_2$) (Waterham et al., 2016). In peroxisomes, the $FADH_2$ reacts with dioxygen (O_2) to produce hydrogen peroxide (H_2O_2), which is degraded by peroxisomal catalase into water (H_2O) and O_2, whereas in mitochondria the re-oxidation of $FADH_2$ is coupled to the electron transport chain to produce energy (Van Veldhoven, 2010; Wanders, 2004; Wanders et al., 2010; Waterham et al., 2016).

Peroxisomal fatty acid β-oxidation requires an acyl-CoA oxidase (dehydrogenation step), a bifunctional enzyme (hydration and dehydrogenation steps), and a thiolase (for thiolytic cleavage) (Reddy and Hashimoto, 2001). Unlike mitochondria, which can fully oxidize fatty acids to carbon dioxide (CO_2) and H_2O, peroxisomes can only shorten fatty acid chains (C>8). The end products of peroxisomal β-oxidation must therefore be shuttled to the mitochondria (Wanders, 2014). On the other hand, VLCFAs (C>20) are exclusively degraded in peroxisomes (Sassa and Kihara, 2014).

1.1.2.2. Cellular redox mechanisms

Human peroxisomes contain many pro-oxidant and antioxidant enzymes (Del Río and López-Huertas, 2016; Stolz et al., 2002). These include enzymes that produce H_2O_2 (e.g. FAD oxidases) or degrade it (e.g. catalases) (Del Río et al., 2016), and enzymes that produce superoxide (e.g. xanthine oxidase) or degrade it (e.g. xanthine dehydrogenase, Cu/Zn superoxide dismutase, and superoxide dismutase 1). Peroxisomes also contain enzymes that generate nitric oxide (NO), such as inducible nitric oxide synthase (iNOS) (Antonenkov et al., 2010), and enzymes that degrade peroxynitrite ($ONOO^-$) such as peroxiredoxins 1 and 5, and enzymes that degrade epoxides (e.g. epoxide hydrolase 2), and lipid peroxides (e.g. peroxiredoxin 1, peroxiredoxin 5 and glutathione S-transferase kappa) (Fransen et al., 2012; Nordgren and Fransen, 2014). Peroxisomes therefore play a key role in the maintenance of the cellular redox balance.

Most of the ROS inside peroxisomes cannot diffuse across the membrane freely (Bienert et al., 2006), helping to maintain the normal enzymatic function of cells. Peroxisomal lipid synthesis plays a central role in the maintenance of intact cellular membranes (Fransen et al., 2012). Many membrane lipid composites are partly synthesized or recycled in the peroxisomes, which include VLCFAs, DHA, plasmalogens, and cholesterol precursors (Van Veldhoven, 2010). Plasmalogens not only regulate the physiological properties of membranes but also trap some free radicals (Wallner and Schmitz, 2011).

It is increasingly clear that changes in peroxisomal metabolism can have a profound impact on cellular processes by modulating the composition and concentration of specific lipids and redox-derived signaling mediators (Beach et al., 2012; Del Río et al., 2016). H_2O_2 and NO are thought to act as signaling molecules in many diseases (A. Fisher, 2009). However, it is unclear whether these signals originate from peroxisomes and their precise role in terms of intracellular and intercellular signaling are not understood.

1.1.3. Peroxisome biogenesis

At present, 31 proteins are known to be required for the biogenesis and maintenance of functional peroxisomes (Islinger et al., 2010). Fourteen different peroxins have been

characterized in mammals, including PEX11, which exists as three isoforms (Islinger et al., 2010). Peroxisome biogenesis genes can be sorted into three groups (Table 1 and Figure 1) reflecting the three major tasks of the peroxisome: proliferation, membrane assembly and matrix protein import (Fujiki et al., 2014).

Table 1. Functions of peroxins and other peroxisomal proteins in mammals

Function	Peroxins
Matrix protein import	PEX1, PEX2, PEX5, PEX6, PEX7,PEX10, PEX12, PEX13, PEX14, PEX26
Membrane assembly	PEX3, PEX16, PEX19
Proliferation	PEX11, DDPs, FIS, MFF

Reproduced from Islinger et al. (2010)

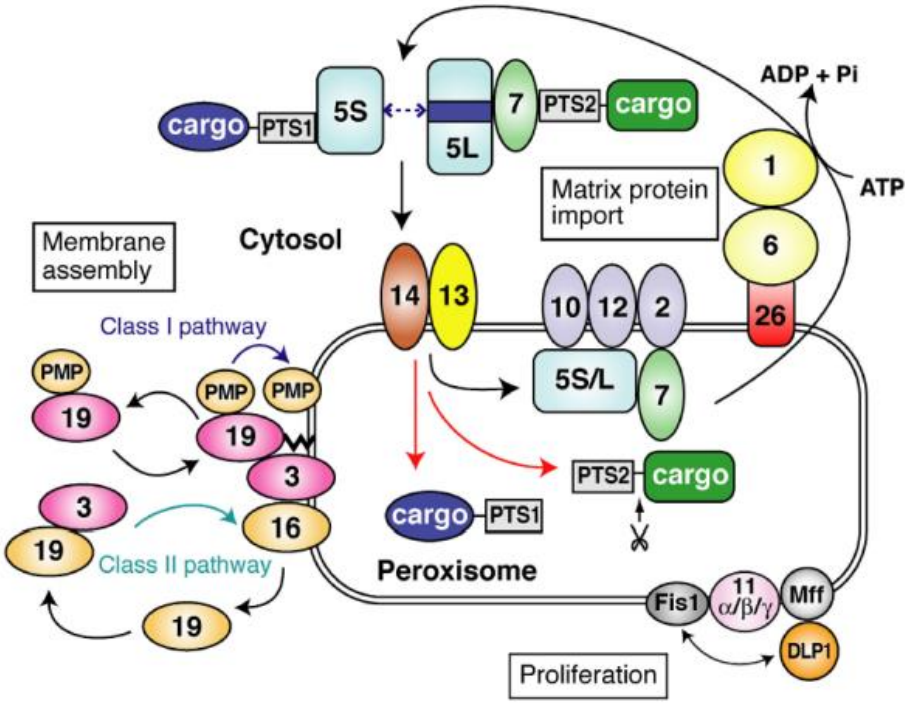

Fig.1. A schematic view of peroxisome biogenesis in mammals (Fujiki et al., 2014). PTS: peroxisomal targeting sequence.

The import of peroxisomal matrix proteins is mediated by several types of specific peroxisomal targeting sequence (PTS) (Waterham et al., 2016). Matrix proteins with PTS type 1 or 2 are recognized by the receptors PEX5p or PEX7p in the cytoplasm

and are imported by the peroxisomal translocation machinery (Waterham et al., 2016). PEX13p and PEX14p together form the peroxisomal docking complex on the peroxisomal membrane, which receive the cargo-loaded receptor proteins (Dammai et al., 2001; Dodt and Gould, 1996). After docking, the matrix proteins are imported into the peroxisomal lumen and the receptor proteins are released from membrane for another import cycle, or are directed to the proteasome for degradation (Chang et al., 1999; Dammai et al., 2001; Waterham et al., 2016).

PEX3p, PEX16p and PEX19p are responsible for peroxisome membrane biogenesis (Waterham et al., 2016). The proliferation of peroxisomes occurs in three stages: elongation, constriction, and fission (Schrader and Fahimi, 2006). PEX11 is required for elongation and constriction (Koch et al., 2010; Opaliński et al., 2011) and there are three isoforms of this protein in humans (PEX11α, PEX11β and PEX11γ) with distinct functions (Koch et al., 2012). DLP1/DRP1, FIS1, MFF and GDAP1 are required for peroxisome fission (Schrader et al., 2013, 2016).

1.1.4. Metabolic link between peroxisomes and mitochondria

Mitochondria and peroxisomes share several characteristics: they are small, ubiquitous organelles, they demonstrate behavioral plasticity and are highly adaptable in terms of structure and abundance according to cellular requirements (Demarquoy and Le Borgne, 2015). They are also metabolically linked in at least five ways: (1) cooperation in fatty acid β-oxidation to maintain lipid homeostasis; (2) a ROS-related sensitive relationship (Fransen et al., 2012); (3) coordinated biogenesis, by sharing key proteins of the organelle division machinery (Schrader et al., 2013); (4) potential exchange of materials via a vesicular trafficking pathway (Neuspiel et al., 2008), and (5) cooperation in anti-viral signaling (Dixit et al., 2010). The β-oxidation products of medium chain fatty acids in peroxisomes must be shuttled to mitochondria for further oxidation and ATP production (Wanders, 2004). This is the most important metabolic connection between these organelles.

Peroxisomal dysfunction is accompanied by morphological and functional changes in the mitochondria, as seen in the peroxisome biogenesis disorder Zellweger syndrome and the related knockout mouse models (Baumgart et al., 2001; Dirkx et al., 2005). In the cardiomyocytes of PEX5$^{-/-}$ mice, routine electron microscopy revealed an increase in the size and number of mitochondrial granules and the presence of

megamitochondria (Baumgart et al., 2001). In a diabetes mouse model, catalase deficiency increased mitochondrial ROS production in response to fatty acids (Hwang et al., 2012).

Mitochondria and peroxisomes also have a common division mechanism. In mammals, components of this mechanism include the dynamin-like protein DLP1/Drp1, which forms ring-like oligomeric structures around membrane constructions (Schrader et al., 2013). The tail-anchored membrane proteins FIS1 and MFF are DLP1 receptors on the organelle membranes (Bonekamp et al., 2012; Huybrechts et al., 2009). In the abovementioned inter-organelle vesicular trafficking pathway (Neuspiel et al., 2008), mitochondria generate small transportation vesicles known as mitochondria-derived vesicles (MDVs) containing the mitochondrial anchored protein ligase MAPL, which specifically targets peroxisomes (A. Sugiura et al., 2014). However, the physiological function of the peroxisome target transportation pathway is not clear. It may play a major role in the communication and cooperation of the two organelles or may represent the parking control pathway, which senses and responds to abnormalities in mitochondrial and peroxisomal functions.

1.1.5. Link between peroxisomes and the endoplasmic reticulum

The connection between the endoplasmic reticulum (ER) and peroxisomes is both physical and functional. During early peroxisome research, peroxisomes were through to be formed from the terminal ER (Novikoff and Shin, 1964). However, the discovery that peroxisomal enzymes were synthesized on free polyribosomes and directly imported from the cytosol supported an autonomous, self-replicating organelle model (Lazarow and Fujiki, 1985). Smooth ER segments surround peroxisomes and are often laterally affected by each other (Baumgart et al., 1989). PEX3p, a biogenesis peroxin, is initially localized in the ER (Hoepfner et al., 2005).

This metabolic interaction between the peroxisomes and ER is highlighted by the phenotype of conditional hepatic Pex5 knockout mice, which feature peroxisome ghosts rather than functional peroxisomes (Dirkx et al., 2005). Severe morphological alterations were also apparent in the mitochondria of these mice, and significant proliferation of the smooth ER was observed. In cases of peroxisome deficiency, ER stress pathways are activated, which leads to the deregulation of endogenous sterol response pathways (Kovacs et al., 2009, 2012).

The most common peroxisome–ER metabolic linkage may involve the biosynthesis of ether-phospholipids, which is initiated in the peroxisomes and completed in the ER (Braverman and Moser, 2012). For example, the key rate-limiting enzyme in the cholesterol biosynthesis pathway is 3-hydroxymethyl glutaryl-CoA reductase (HMG-CoA reductase), which is localized in peroxisomes (Keller et al., 1986).

The interaction between the ER and peroxisomes may also regulate calcium homeostasis. The smooth ER is known to control free and bound Ca^{2+} levels in all parts of the cell (Krebs et al., 2015). High intracellular concentrations of Ca^{2+} can lead to acute responses, including cell death (Krebs, 1998). Moreover, abnormal Ca^{2+} levels in the long-term can also results in the remodeling of the heart (Schreckenberg et al., 2015). In rat hepatocytes, the attachment of mature peroxisomes to the ER has been observed by three-dimensional (3D) image reconstruction (Grabenbauer et al., 2000), suggesting that metabolites are shuttled between these organelles to maintain calcium homeostasis. Peroxisomes may also function as calcium reservoirs, thus highlighting their role in calcium regulation (Lasorsa et al., 2008).

1.1.6. Peroxisome proliferators and peroxisome proliferator-activated receptors

1.1.6.1. Peroxisome proliferators

Various compounds can induce peroxisome proliferation, including certain phthalate ester plasticizers, herbicides, leukotriene D4 receptor antagonists, and lipid-lowering drugs such as WY-14.643 and ciprofibrate (Lalwani et al., 1983; Reddy and Krishnakantha, 1975). In the normal adult rat liver, peroxisomes make up less than 2% of the total cytoplasmic volume under physiological conditions (Loud, 1968). After treatment with peroxisome proliferators, the peroxisome fraction can rapidly increase to 25% (Rao et al., 1988). Peroxisome proliferation is therefore considered protective in many diseases because antioxidant enzymes become more abundant (Beier et al., 1997). However, prolonged exposure to peroxisome proliferators in the liver leads to the development of hepatocellular carcinomas in rats and mice (Reddy et al., 1976).

Table 2. Classification of peroxisome proliferators. Classification depends on chemical structures or moieties (Misra et al., 2013)

Fibrate class	Clofibrate analogs: methyl clofenapate, nafenopin, fenofibrate, gemfibrozil, ciprofibrate
Acid class	Hypolipidic compounds: [4-chloro-6-(2,3-xylidino)-2-pyrimidinylthio] acetic acid (WY-14.643), 2-chloro-5-(3, 5 dimethylpiperidinosulfonyl) benzoic acid (tibric acid)
Phthalate class	Phthalate-ester plasticizers: di-(2-ethylhexyl)-phthalate (DEHP), di-(2-ethylhexyl) adipate (DEHA)

1.1.6.2. Peroxisome proliferator-activated receptors

Peroxisome proliferator-activated receptors (PPARs) belong to the nuclear receptor superfamily of ligand-activated transcription factors and include three members (α, β/δ and γ) encoded by distinct genes located on different chromosomes with a high degree of interspecies sequence conservation (Colasante et al., 2015; Desvergne and Wahli, 1999; Lee and Kim, 2015). Following interaction with PPAR agonists, PPARs are translocated to the nucleus and heterodimerize with the retinoid X receptor (RXR) which is a promiscuous dimerization partner (Lee et al., 2015). The specific DNA targets bound by PPARs are peroxisome proliferator hormone response elements (PPREs) (Berger and Moller, 2002). PPARs regulate genes that control cell differentiation and metabolic processes such as lipid and glucose homeostasis (Tyagi et al., 2011).

1.1.7. Peroxisomal dysfunction and its associated diseases

The first human diseases linked to peroxisomal dysfunction were discovered by the analysis of liver biopsies of Zellweger patients, revealing that the hepatocytes of such patients lack functional peroxisomes and to contain abnormal mitochondria (Goldfischer et al., 1973). Patients with Zellweger syndrome display a variety of symptoms, including impaired brain development, craniofacial abnormalities, chondrodysplasia punctata, hypotonia, and liver cirrhosis, and most do not survive beyond 1 year of age (Yik et al., 2009). Peroxisomal disorders are classified into two groups: disorders of peroxisome biogenesis and single enzyme dysfunction diseases (Wanders, 2014).

1.1.7.1. Disorders of peroxisome biogenesis

Pathological mutations in 14 PEX genes lead to disorders of peroxisomal biogenesis, with only PEX11α and PEX11γ not associated with any known disorders (Braverman et al., 2013). The term Zellweger spectrum disorders (ZSD), which include Zellweger syndrome, neonatal adrenoleukodystrophy (NALD) and infantile Refsum disease (IRD), has been introduced since these disorders were recognized as a clinical spectrum of varying severity (Steinberg et al., 2006).

The metabolic abnormalities common among these disorders include the accumulation of VLCFAs and phytanic acid, elevated bile acid intermediates, and deficient plasmalogen biosynthesis (Braverman et al., 2013). Peroxisomes are almost completely absent from hepatocytes and fibroblasts, although peroxisomal membrane ghosts can be found (Santos et al., 2000). Zellweger syndrome is usually associated with death in infancy, but children with NALD may live to school age. Survival to adulthood is more likely in IRD (Braverman et al., 2013). Rhizomelic chondrodysplasia punctata (RCDP) presents in the neonatal period, with a characteristic skeletal dysplasia (Braverman et al., 2013).

Table 3. Pex genes involved in peroxisome diseases. ZS = Zellweger syndrome, NALD = neonatal adrenoleukodystrophy, IRD = infantile Refsum disease, RCDP = rhizomelic chondrodysplasia punctata (after (Fujiki et al., 2014).

Gene	Phenotype	Peroxisome ghosts
Pex1	ZS, NALD, IRD	+
Pex2	ZS, IRD	+
Pex3	ZS	-
Pex5	ZS, NALD	+
Pex6	ZS, NALD	+
Pex7	RCDP	+
Pex10	ZS, NALD	+
Pex11β	ZS	+
Pex12	ZS, NALD, IRD	+
Pex13	ZS, NALD	+
Pex14	ZS	+
Pex16	ZS	-
Pex19	ZS	-
Pex26	ZS, NALD, IRD	+

1.1.7.2. Peroxisomal single enzyme deficiencies

Five different genetic diseases are associated with peroxisomal fatty acid β-oxidation deficiency (Wanders, 2014). The most common disorder of peroxisomal β-oxidation is X-linked adrenoleukodystrophy (X-ALD), which is caused by mutations in the *ABCD1* gene encoding adrenoleukodystrophy protein (ALDP) (Johannes Berger and Gärtner, 2006). X-ALD patients are characterized by the accumulation of VLCFAs, especially C24:0 and C26:0 in their blood and organs (Ofman et al., 2010). The second most common disorder of peroxisomal β-oxidation is D-bifunctional protein (DBP) deficiency, which in its severe form mimics Zellweger syndrome in all aspects, including craniofacial dysmorphia, neuronal migration defects, and early death (Nascimento et al., 2015). Peroxisomal acyl-CoA oxidase deficiency, 2-methylacyl-CoA racemase (AMACR) deficiency, and sterol-carrier-protein X (SCPx) deficiency have also been reported (Wanders, 2014). Other dysfunctions of peroxisomes are listed in Table 4.

Table 4. Peroxisomal single enzyme dysfunction (Wanders, 2014)

Gene	Disorders	Altered function
Abcd1	X-linked adrenoleukodystrophy	Fatty acid β-oxidation
Acox1	Acyl-CoA oxidase deficiency	Fatty acid β-oxidation
Hsd17b4 *Mfp1*	D-Bifunctional protein deficiency	Fatty acid β-oxidation
Scp	Sterol-carrier-protein X deficiency	Fatty acid β-oxidation
Amacr	2-Methylacyl-CoA racemase deficiency	Fatty acid β-oxidation
Gnpat	Rhizomelic chondrodysplasia puncatata Type 2	Etherphospholipid biosynthesis
Agps	Rhizomelic chondrodysplasia puncatata Type 3	Etherphospholipid biosynthesis
Phyh/Pahx	Refsum disease	Fatty acid α-oxidation
Agtx	Hyperoxaluria type 1	Glyoxylate metabolism
Baat	Bile acid-CoA: amino acid *N*-acyltransferase deficiency	Bile acid synthesis
Cat	Acatalasemia	H_2O_2 metabolism

1.1.7.3. Peroxisomal disease management

Peroxisomal diseases cannot yet be cured and management is restricted to palliative care, including surveillance and developmental assessments (Braverman et al., 2013). Oral bile acid supplements ahve improved hepatic function in several ZS patients (Maeda et al., 2002; Setchell et al., 1992). However, only anecdotal reports are found in the literature (Braverman et al., 2013). Given the benefit of dietary phytanic acid restriction in adult Refusm disease, this treatment is often prescribed for surviving peroxisome biogenesis disorder (PBD) patients (Braverman et al., 2013). Oral supplements of plasmalogen precursors or DHA have not shown evidence of therapeutic efficacy (Noguer and Martinez, 2010; Paker et al., 2010).

1.2. Peroxisomes and the heart

1.2.1. The heart and cardiovascular diseases

The heart is a muscular organ consisting mainly of cardiomyocytes (Mendis et al., 2015). Studies on the heart date back more than one century, and at that time it was already recognized that the heart requires large amounts of calcium, nutrients and oxygen (Langendorff, 1895; Winterstein, 1904). Although living standards have improved greatly and people are generally more healthy than they were a century ago, cardiovascular disease (CVD) remains the most significant cause of death worldwide (Mendis et al., 2015). The mechanisms underlying the development of CVDs are still poorly understood, leading to unsatisfactory treatments (Mendis et al., 2015).

1.2.2. Metabolic function of the heart

The energy demands of the heart are enormous, but this organ has limited energy reserves. The heart continuously produces adenosine triphosphate (ATP) in its mitochondria and can utilize all classes of energy substrates for this purpose, including carbohydrates, lipids, amino acids, and ketone bodies (Neely and Morgan, 1974; Opie, 2004). The main energy resource is the utilization of free fatty acids (D. Fisher et al., 1980). Glycolysis supports the energy supply to a variable extent. A shift from fatty acid β-oxidation to glycolysis has been observed in different disease conditions (Bishop and Altschuld, 1970; D. Fisher et al., 1980; Goodwin and Taegtmeyer, 2000).

1.2.2.1. Fatty acid utilization

The cardiac energy supply may comprise up to 90% fatty acids, or a balanced supply may be available in which fatty acids are mixed with other substrates (Grynberg and Demaison, 1996). Before fatty acids enter the β-oxidation process, free fatty acids are esterified by acyl-coenzyme A (CoA) on the cytoplasmic face of organelle membranes (Cheng et al., 2004). Esterified free fatty acids are either transported directly to the myocardial triglyceride pool for storage or are converted to long-chain acylcarnitine by carnitine palmitoyltransferase (CPT) I in the mitochondria (Lopaschuk et al., 2010; van der Vusse et al., 2000). Esterified fatty acids can also be imported via peroxisomal ABCD transporters if mitochondria are overloaded with fatty acids (Baker et al., 2015). Some fatty acids, including VLCFAs, cannot be used directly by mitochondria because

these organelles do not contain VLCFA-CoA synthetase. For example, C24:0 and C26:0 are not substrates of carnitine palmitoyltransferase (CPT) I (Vluggens et al., 2010) and must be first digested in peroxisomes (Schrader et al., 2013).

1.2.2.2. Glucose utilization

Cardiomyocytes can utilize intracellular glucose stores or external glucose (Doenst et al., 2013). There are several glucose transporters (GLUTs) with diverse expression profiles. GLUT1 is the major transporter in the young heart whereas GLUT4 is the predominant isoform in the adult heart (Abel, 2004; Aerni-Flessner et al., 2012). Following glucose uptake, free glucose is rapidly converted to glucose 6-phosphate (G6P) in the smooth ER, and subsequently feeds into many metabolic pathways (Doenst et al., 2013).

1.2.2.3. Shift from glycolysis and lactate oxidation (fetal) to fatty acid oxidation (adult) in postnatal development

The fetal heart exists in a relatively hypoxic environment and mainly uses glucose and lactate for energy (Scholz and Segar, 2008). Additionally, the workload of the fetal heart is relatively low, and the energy derived from glycolysis and lactate oxidation is enough to maintain its activity. There is a switch to mitochondrial fatty acid β-oxidation after birth in order to accommodate the increased energy demand (Breckenridge, 2014; Minners et al., 2000). This switch occurs at both the mRNA and protein levels. For example, some genes encoding fatty acid β-oxidation enzymes are significantly upregulated in adult rat hearts compared to the neonatal organ (Marín-García and Goldenthal, 2002; Minners et al., 2000).

1.2.3. Heart disease markers

1.2.3.1. Natriuretic peptides

Atrial natriuretic peptide (ANP), brain (B-type) natriuretic peptide (BNP), and C-type natriuretic peptide (CNP) are circulating hormones that regulate blood pressure and blood volume (Nishikimi et al., 2006). ANP is synthesized mainly in the atrium, BNP

mainly in the ventricle and CNP throughout the central nervous system (Nishikimi et al., 2006).

Natriuretic peptides are wildly used as diagnostic markers. In patients with acute heart infarction and chronic heart failure, plasma ANP and BNP levels are markedly increased (Morita et al., 1993; Yasue et al., 1994). Higher ANP and BNP levels in plasma are believed to compensate for heart failure (Burnett et al., 1986; Mukoyama et al., 1991). Furthermore, natriuretic peptides may be involved in the modulation of cardiac hypertrophy. Knocking out the *Nppa* gene encoding ANP in mice leads to cardiac hypertrophy, suggesting that ANP also plays a role in the regulation of cardiac remodeling (Oliver et al., 1997).

1.2.3.2. Myosin heavy chains

Myosin heavy chains (MHC) α and β are two cardiac MHC isoforms with distinct functions (Krenz and Robbins, 2004). Whereas α-MHC is almost exclusively expressed in cardiac tissue, β-MHC is expressed in both cardiac and skeletal muscle (Krenz et al., 2004).

The expression levels of α-MHC and β-MHC are altered in pathological conditions, such as cardiac failure or hypertrophy (Krenz et al., 2004), which make these markers useful indicators for many cardiac diseases. The predominant isoform in the normal mouse heart is α-MHC, but a shift to β-MHC is observed in a mouse heart failure model (Harada et al., 1999). The downregulation of α-MHC expression in human hypertrophic hearts has also been reported (Miyata et al., 2000; Reiser et al., 2001). The upregulation of β-MHC in heart tissue is believed to be detrimental because it inhibits cardiomyocyte contractile function (T. Sugiura et al., 1992).

1.2.3.3. Extracellular matrix surrounding cardiomyocytes

The cardiac extracellular matrix (ECM) is a complex network of matrix proteins in which cardiomyocytes, fibroblasts and other cells are embedded (Rienks et al., 2014). The ECM not only provides structural support, but also a dynamic and plastic network that plays an important role in the regulation of diverse cellular functions. The ECM is involved in cell signaling/communication, cell proliferation/differentiation, and cell migration (Daley et al., 2008; Lockhart et al., 2011). The cardiac ECM consists

predominantly of fibrillar collagen types I and III, as well as collagen types IV, V and VI (Fan et al., 2012). Other components of the ECM include laminin, fibronectin, elastin, fibrillin, proteoglycans and glycoproteins (Fan et al., 2012).

1.2.4. Potential metabolic causes of heart diseases

1.2.4.1. Fatty acid metabolic dysfunction affects cardiac structure and function

Peroxisomal β-oxidation has a critical role in the degradation of long-chain fatty acids (LCFAs) and VLCFAs. The accumulation of free fatty acids in cardiomyocytes, which often occurs in diabetic or obese individuals, can lead to heart failure (Lopaschuk et al., 2010). Fatty acid accumulation can also induce apoptosis in cardiomyocytes (Marín-García et al., 2002). The inability to metabolize LCFAs and VLCFAs can lead to cardiomyopathy (Marín-García et al., 2002; Strauss et al., 1995). Fatty acids accumulating in cardiomyocytes disrupt mitochondrial activity and ATP generation, causing the accumulation of ROS (Colasante et al., 2015; Lopaschuk et al., 2010). Peroxisomes are actively involved in the protection of the heart by continuously and efficiently degrading excess lipid metabolites under pathological conditions.

1.2.4.2. ROS and cardiac diseases

Lower levels of ROS production can lead to chronic remodeling of the heart, whereas high levels of ROS can directly lead to apoptosis in the cardiomyocytes (Sugamura and Keaney, 2011). It is therefore interesting that catalase overexpression inhibits cardiomyocyte apoptosis by protecting the cells from ROS (Qin et al., 2010). Peroxisomal antioxidant enzymes and plasmalogens protect cardiomyocytes via the degradation and trapping of ROS and the maintenance of ROS homeostasis.

1.2.5. Peroxisome discovery in the heart

The main energy source in the adult mammalian heart is fatty acid β-oxidation, and a balanced level of ROS is needed for normal heart activity (Colasante et al., 2015; Lopaschuk et al., 2010). Peroxisomes are very important in cardiomyocytes because they play a central role in fatty acid β-oxidation under fatty acid overload conditions and they maintain the ROS balance. It is therefore surprising that few studies have

addressed the functions of peroxisomes in the heart and this organ was neglected for a long time in terms of peroxisome research. One very important reason for this lack of research is that it is difficult to visualize peroxisomes in cardiomyocytes. The first systematic descriptions of peroxisomes in the myocardium of rats and mice were published 20 years after the discovery of peroxisomes, and were reported at about the same time by two different groups (Hand, 1974; Herzog and Fahimi, 1974).

1.2.6. Peroxisomal morphology in the heart

As is the case for mitochondria, the number of peroxisomes in cardiomyocytes can vary (Herzog et al., 1974). Longitudinal sections of cardiomyocytes are optimal for the analysis of peroxisome distribution, because these organelles are often found at the junction of A and I bands (Herzog et al., 1974). Peroxisomes in cardiomyocytes may also be found in the proximity of mitochondria, lipid droplets, the sarcoplasmic reticulum, or T-tubules (Colasante et al., 2015). Peroxisomes in the heart share characteristics with other peroxisomes, such as an oval shape and a size range of 0.2–0.5 μm (Colasante et al., 2015; Herzog et al., 1974), but they lack the crystalline nucleoids seen in murine liver and kidney cells (Herzog et al., 1974) (Fig. 2).

Peroxisomal β-oxidation and catalase activity, and peroxisomal proliferation, can be stimulated in the rat heart by feeding the animals on a diet containing high levels of unsaturated LCFAs (De Craemer et al., 1994; Fahimi et al., 1979; Kvannes et al., 1995).

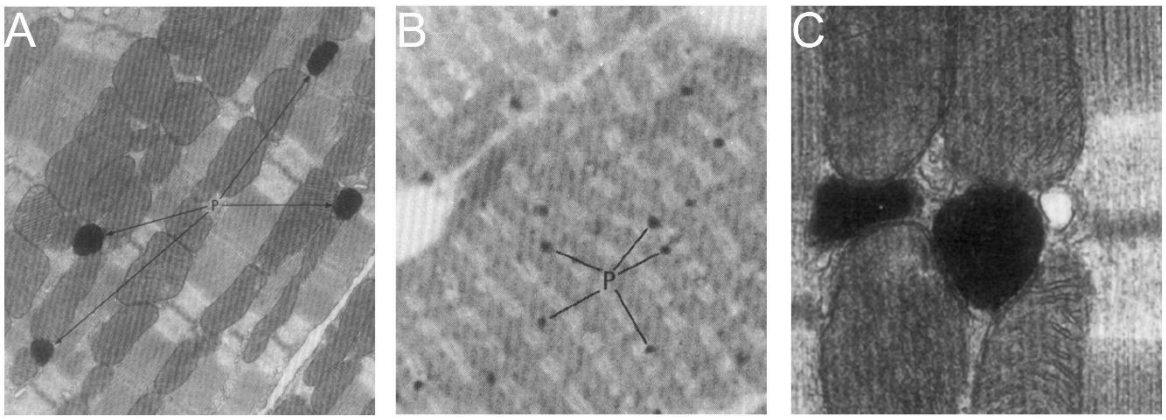

Fig. 2. Morphology of peroxisomes in cardiomyocytes (from Herzog and Fahimi 1975). The peroxisomes in the rat heart are oval in shape (A) and their numbers vary in cardiomyocytes (B). The peroxisomes are localized at the junction of A and I bands (B) and in the proximity of mitochondria (C).

1.2.7. Functions of peroxisomes in the heart

Peroxisomes may protect the function of the heart (Fahimi et al., 1979). Mice fed on an ethanol-rich diet were compared with a control group, revealing an increase in catalase activity in the control group, but no significant differences in cardiac function parameters. This suggested that higher catalase activity could maintain the normal function of the heart against ethanol exposure (Fahimi et al., 1979). This hypothesis was supported by experiments in which rats fed on an ethanol-rich diet and also administrated a catalase inhibitor (aminotriazole) showed characteristics of cardiac damage (Kino et al., 1981). Peroxisomes contain many antioxidants, in addition to catalase, such as superoxide dismutase 1, peroxiredoxin I and V, and glutathione peroxidase, all of which may be important in cardiomyocytes for scavenging ROS (Karnati et al., 2013). Peroxisomes may therefore protect the heart by degrading excess fatty acids under pathological conditions (Liepinsh et al., 2013).

1.2.8. Potential role of peroxisomes in heart ischemia

Acute myocardial ischemia is a pathological condition caused by an insufficient supply of blood to the heart, which leads to a sudden reduction in the quantity of nutrients and oxygen delivered to heart tissue (Raedschelders et al., 2012). ROS play a key role among the many mechanisms of ischemia-reperfusion injury, because ROS generation is detrimental to cardiomyocytes during both the ischemic and reperfusion phases (Raedschelders et al., 2012). Efficient reperfusion of the heart tissue during the early stage of ischemia is necessary to limit the damaged area and to rescue viable cardiomyocytes, but secondary damage may arise due to the sudden burst of ROS and the delayed ROS clearance (Raedschelders et al., 2012).

During an ischemic episode, complete glucose and fatty acid oxidation are inhibited as mitochondrial respiration is restricted by the reduced oxygen supply (Kantor et al., 1999). Glycogenolysis and anaerobic glycolysis briefly continue to produce a small amount of ATP until the accumulation of metabolites and end products leads to toxic acidosis (Stanley et al., 1997). These factors cause the progressive inhibition and disruption of the heart's normal function. Cardiomyocytes begin to die after 20 minutes of ischemia, and the damage becomes irreversible after 6 hours (Jennings and Reimer, 1991).

It has now a consensus that immediate reopening of the obstructed vessels via percutaneous coronary intervention (PCI) is among the most effective treatments for cardiac ischemia (Saia et al., 2010). After reperfusion, a larger fraction of cellular enzymes is released, even more than in the period of hypoxia (Hearse, 1990). Because peroxisomes play a central role in the production and scavenging of ROS, they may play an important role in cardiac ischemia-reperfusion injury. Studies of peroxisomes during ischemia-reperfusion could provide new insights that allow the protection of cardiomyocytes from damage.

1.2.9. Regulation by peroxisome proliferator-activated receptors

PPAR agonists have been used to treat a variety of metabolic disorders, such as diabetes and hyperlipidemia (Pol et al., 2015). PPARs are central modulators of peroxisomal proliferation and β-oxidation (Cheng et al., 2004; Dreyer et al., 1992). However, the functions of PPAR agonists in the heart are unclear. Both beneficial functions and adverse effects have been reported, and many PPARs knockout models have been studied (Table 5).

Table 5. PPAR knockout and overexpression models and their effects (from Christine et al., 2015)

Target	Model	Cardiac metabolism alterations	Cardiac function alterations	Reference
PPARα	PPAR$\alpha^{-/-}$	Defective lipid and glucose homeostasis	Not indicated	(Djouadi et al., 1998)
		Decreased fatty acid oxidation, abnormal mitochondria	Fibrosis, progressed during aging	(Watanabe et al., 2000)
		Substrate switch from fatty acid to glucose, inefficient ATP generation	Normal cardiac function	(Luptak et al., 2005)
		Not indicated	Systolic ventricular dysfunction, fibrosis	(Loichot et al., 2006)
		Not indicated	Increased oxidative stress, left ventricular dysfunction	(Guellich et al., 2013)
		Decreased fatty acid oxidation, increased glucose oxidation	Normal cardiac function	(Liu et al., 2011)
		Increased fatty acid oxidation, decreased glucose oxidation and uptake	Ventricular hypertrophy, systolic ventricular dysfunction	(Finck, 2007)
	αMHC-PPARα	Not indicated	Impaired development	(Peters et al., 2000)
PPARβ	PPAR$\beta^{-/-}$	Not indicated	Embryonic lethality	(Barak et al., 2002)
		Decreased fatty acid oxidation and increased glucose oxidation, lipid accumulation	Cardiac dysfunction, hypertrophy, and reduced survival	(Cheng et al., 2004)
	αMHC-PPAR$\beta^{-/-}$	Decreased fatty acid oxidation and normal glucose oxidation	Hypertrophy, mitochondrial abnormalities, and cardiac dysfunction	(Liu et al., 2011)
		Decreased fatty acid oxidation and glucose oxidation, mitochondrial abnormalities	Cardiac dysfunction, oxidative damage, and hypertrophy	(Wang et al., 2010)
	Inducible αMHC-PPAR$\beta^{-/-}$	Normal fatty acid oxidation, increased glucose oxidation	Normal cardiac function	(Burkart et al., 2007)
	αMHC-PPARβ	Increased fatty acid oxidation and glucose oxidation, increased mtDNA	Enhanced cardiac contractility	(Liu et al., 2011)
	Inducible αMHC-PPARβ	Not indicated	Embryonic lethality	(Barak et al., 1999)
PPARγ	Inducible αMHC-PPARγ−/−	Decreased fatty acid oxidation, normal glucose oxidation	Decreased cardiac contractility, modest hypertrophy	(Luo et al., 2010)
	αMHC-PPARγ1	Increased triglyceride uptake, increased lipid and glycogen stores, and abnormal mitochondria	Dilated cardiomyopathy	(Son et al., 2007)

1.2.10. Tools to study heart function and heart disease

1.2.10.1. Cell lines and models to study peroxisomes in cardiomyocytes

The mouse atrial cardiomyocyte cell line called HL-1 was derived from AT-1 cells, which can be serially passaged and differentiated while maintaining characteristics of adult mouse atrial cardiomyocytes (Claycomb et al., 1998) However, the potential to study peroxisomes in these cells has not been evaluated.

1.2.10.2. Knockout mouse models of peroxisome deficiency

Constitutive knockout mouse models have facilitated the investigation of pathogenic mechanisms underlying peroxisomal diseases (Baes and Van Veldhoven, 2012a). In knockouts of the peroxisomal biogenesis genes *Pex2*, *Pex5* and *Pex13*, normal peroxisomes were replaced with incompetent peroxisomal ghosts (Baes et al., 1997; Faust and Hatten, 1997; Maxwell et al., 2003). *Pex11* (*Pex11α* and *Pex11β*) knockout mice have also been generated (Li and Gould, 2002). Interestingly, the *Pex11β* knockout mice had a very similar phenotype to the *Pex2*, *Pex5* and *Pex13* knockouts and did not survive to adulthood, whereas *Pex11α* knockout mice had a normal lifespan (Li et al., 2002). In the latter model, peroxisomes were present but could not proliferate. This model would be suitable to study the role of *Pex11α* deficiency on cardiomyocytes in the adult heart.

Tissue-specific knockouts have been created by crossing *Pex5*-loxP and *Pex13*-loxP mice with lines expressing Cre in specific tissues, although not the heart (Baes et al., 2002; Bjorkman et al., 2002). Tissue-specific knockouts are useful not only to decipher the function of peroxisomes in particular cell types and tissues, they are also powerful tools to study disease mechanisms when combined with specific disease models (Baes et al., 2002).

Various knockouts of peroxisomal β-oxidation enzymes have been reported (Baes et al., 2002). Similar to mice lacking Pex11α, mice lacking the abundant peroxisomal membrane protein PMP34 (Van Veldhoven and Mannaerts, 1994) developed normally and were fertile, but female mice fed on diets supplemented with phytol showed delayed mammary gland development (Baes and Van Veldhoven, 2012b).

1.2.10.3. Analysis of heart function in peroxisomal deficiency models

The Langendorff perfusion system has been widely used to analyze the physiological function of the heart *in vitro* and to establish disease models, such as the ischemia-reperfusion model. Moreover, an improved cardiomyocyte isolation technique has allowed the function of individual murine cardiomyocytes to be analyzed in detail (Schlüter and Schreiber, 2005). Because most peroxisomal gene knockout models do not survive long after birth, only those with a minor phenotype (e.g. *Pex11α*) are suitable for physiological measurements of cardiac and cardiomyocyte function, given that these techniques require a mature heart and fully differentiated cardiomyocytes that contract normally.

1.2.11. Peroxisomes as targets for the treatment of cardiac diseases

There is now a large body of evidence indicating that metabolic disturbance in the heart and a disruption of the ROS balance are the principal factors underlying many heart diseases (Doenst et al., 2013). Peroxisomes play a central role in fatty acid β-oxidation, ROS production and scavenging, and calcium hemostasis, and also appear to maintain the activity of mitochondria as well as protecting cardiomyocytes from ROS injury and the accumulation of lipid end products. Investigating the role of peroxisomes in the heart may therefore provide novel insights into the pathogenic mechanisms of CVD, ultimately providing new treatment routes. Given the complex functional classification of peroxisomal proteins, experiments are needed to determine the roles of proteins from each of the functional groups.

2. Outline and aims of the study

At the beginning of the research described in this thesis, only limited information was available on the morphology and distribution of peroxisomes in the heart. Therefore, the first aim of the study was the comparative functional characterization of the peroxisomes and the expression of peroxisomal genes in atrial and ventricular cardiomyocytes of the normal heart.

The second aim was to investigate the role of peroxisomes in the heart by the knockout or knockdown of two peroxisomal genes with different roles in peroxisome biogenesis. The functional ablation of these genes in a mouse model and in a cardiomyocyte cell line should provide new insight into the consequences of peroxisomal deficiency in cardiomyocytes.

The first gene selected for analysis was *Pex11α*, which is known to play an important role in peroxisome proliferation. *Pex11α* knockout mice have been generated and used to investigate the function of this gene in the liver (X. Li, Baumgart, et al., 2002). Peroxisomes are present in these knockout animals but cannot proliferate under stress conditions. The research described in this thesis focused on differences in peroxisomal gene expression and morphology between *Pex11α* knockout mice and wide-type mice, and the specific effects of the *Pex11α* knockout in the heart (changes in molecular markers and cardiomyocyte physiological functions), under stress conditions.

The second gene selected for analysis was *Pex14*, which is involved in the import of cargo into peroxisomes. Three patients with *Pex14* mutations have been reported, all of whom suffered from severe symptoms and were not able to enjoy a normal life. In contrast to *Pex11α* deficiency, patients with *Pex14* deficiency do not possess metabolically functional peroxisomes (only membrane ghosts) and all peroxisomal metabolic pathways are dysfunctional. The consequences of such a deficiency in the heart remain unclear. Therefore, the effect of *Pex14* knockdown in HL-1 cardiomyocytes was investigated, focusing on the impact on cell viability, ECM components, and cardiac-specific markers.

3. Materials, Methods and Laboratory Animals

3.1. Materials used in the laboratory

3.1.1. Chemicals and reagents

General chemicals used during the research project are listed in Table 6, whereas specialized chemicals required for specific experiments are listed separately.

Table 6. General chemicals used during this research project

Chemical	Company and location
Acrylamide	Roth, Karlsruhe, Germany
Agarose LE	Roche, Grenzach-Wyhlen, Germany
Ammonium molybdate	Merck, Darmstadt, Germany
Ampicillin	Difco, Detroit, MI, USA
Ascorbic acid	Sigma-Aldrich, Steinheim, Germany
Bradford reagent	Sigma-Aldrich, Steinheim, Germany
Bromophenol blue	Riedel-de-Haën, Seelze, Germany
Citric acid	Merck, Darmstadt, Germany
Diethylpyrocarbonate (DEPC)	Sigma-Aldrich, Steinheim, Germany
Dimethylsulfoxide (DMSO)	Sigma-Aldrich, Steinheim, Germany
3-(4,5-dimethylthiazol-2-yl)-2,5-diphenyltetrazolium bromide (MTT)	Sigma-Aldrich, Steinheim, Germany
Dipotassium hydrogen phosphate	Merck, Darmstadt, Germany
Ethanol	Riedel-de-Haën, Seelze, Germany
Ethidium bromide	Fluka, Neu-Ulm, Germany
Ethylene diamine tetraacetic acid (EDTA)	Fluka, Neu-Ulm, Germany
Formamide	Merck, Darmstadt, Germany
Glycine	Roth, Karlsruhe, Germany
Glycerol	Sigma-Aldrich, Steinheim, Germany
Glycogen	Invitrogen, Karlsruhe, Germany
Hydrogen peroxide	Merck, Darmstadt, Germany
β-Mercaptoethanol	AppliChem, Darmstadt, Germany

Methanol	Sigma-Aldrich, Steinheim, Germany
Mowiol 4-88	Polysciences, Eppelheim, Germany
Paraformaldehyde (PFA)	Sigma-Aldrich, Steinheim, Germany
Penicillin/streptomycin	PAN Biotech, Aidenbach, Germany
Ponceau S	Serva, Heidelberg, Germany
Potassium dihydrogen phosphate	Merck, Darmstadt, Germany
Potassium hydroxide	Fluka, Neu-Ulm, Germany
Sodium carbonate	Merck, Darmstadt, Germany
Sodium chloride	Roth, Karlsruhe, Germany
Sodium hydrogen carbonate	Merck, Darmstadt, Germany
Sodium hydroxide	Merck, Darmstadt, Germany
Sucrose	Merck, Darmstadt, Germany
Sodium dodecylsulfate (SDS)	Sigma-Aldrich, Steinheim, Germany
Tetramethylethylenediamine (TEMED)	Roth, Karlsruhe, Germany
Trishydroxymethylaminomethane (Tris)	Merck, Darmstadt, Germany
Triton X-100	Sigma-Aldrich, Steinheim, Germany
Trypan blue	Sigma-Aldrich, Steinheim, Germany
Tween-20	Fluka, Steinheim, Germany
Uranyl acetate	Merck, Darmstadt, Germany
Xylene	Merck, Darmstadt, Germany

3.1.2. Laboratory instruments

3.1.2.1. General equipment and facilities

General equipment used during the research project is listed in Table 7, whereas specialized equipment required for specific experiments is listed separately.

Table 7. General machines and facilities used in the study

Instrument name	**Manufacturer**
Biocell A10 water system	Milli Q-Millipore, Schwalbach, Germany

Biofuge Fresco	Heraeus, Hanau, Germany
Biofuge Pico	Heraeus, Hanau, Germany
Bio-Rad electrophoresis apparatus (Sub Cell GT) system	Bio-Rad, Munich, Germany
Dishwashing machine (G 78 83 CD)	Miele, Gütersloh, Germany
Gel-Doc 2000 gel documentation system	Bio-Rad, Munich, Germany
Hera cell 240 incubator	Heraeus, Hanau, Germany
Hera safe, clean bench KS-12	Heraeus, Hanau, Germany
Ice machine	Manitowoc, Wisconsin, USA
I Cycler PCR machine MiQ2 optical module	Bio-Rad, Munich, Germany
Leica DMRD fluorescence microscope	Leica, Wetzlar, Germany
Leica DC 480 camera	Leica, Wetzlar, Germany
Leica TP1020 embedding machine	Leica, Wetzlar, Germany
Leica TCS SP2 confocal laser scanning microscope	Leica, Wetzlar, Germany
Leica SM 2000R rotation microtome	Leica, Wetzlar, Germany
Microwave oven MB-392445	LG, Willich, Germany
Mini-Protean 3 cell gel chamber	Bio-Rad, Munich, Germany
Microtome stretching water bath Type 1003	Vieth Enno, Wiesmoor, Germany
Multifuge 3 SR centrifuge	Heraeus, Hanau, Germany
MyiQTM2 two-color real-time PCR cycler and detection system	Bio-Rad, Munich, Germany
NanoDrop ND 2000	Thermo Fisher Scientific, Waltham, MA, USA
Oven HERAEUS T 5050 EKP	Heraeus, Hanau, Germany
PH-Meter E163649	IKA, Weilheim, Germany
Pipettes (0.1-2.5 µL, 0.5–10 µL, 2–20 µL, 10–100 µL, 20–200 µL, 100–1,000 µL)	Eppendorf, Hamburg, Germany
Potter-Elvehjem homogenizer 8533024	Braun, Melsungen, Germany
Power supply - 200, 300 and 3000 Xi	Bio-Rad, Munich, Germany

Pressure/Vacuum Autoclave FVA/3	Fedegari, Albuzzano, Italy
Pump Drive PD 5001	Heidolph Instruments, Schwabach, Germany
SmartspecTM 3000 spectrophotometer	Bio-Rad, Munich, Germany
Thermo plate HBT 130	Medax, Kiel, Germany
Thermo mixer HBT 130	HLC, BioTech, Bovenden, Germany
Trans-Blot SD semi dry transfer cell	Bio-Rad, Munich, Germany
TRIO-thermoblock	Biometra, Göttingen, Germany
Ultra balance LA120 S	Sartorius-Stedim Biotech, Göttingen, Germany
Ultra Turrax T25 basic homogenizer	Junke & Kunkel, Staufen, Germany
Vortex M10	VWR International, Darmstadt, Germany
Water bath shaker GFL 1083	GFL, Burgwedel, Germany

3.1.2.2. Measurement of cell contraction parameters (Department of Physiology, Faculty of Medicine, Justus-Liebig-University)

Equipment for the measurement of cardiomyocyte contraction is listed in Table 8.

Table 8. System for the measurement of cell contraction parameters

Instrument	**Company**
Interface INT4	Scientific Instruments GmbH, Heidelberg, Germany
Microscope TMS-F	Nikon, Tokyo, Japan
Monitor	Philips, Eindhoven, Holland
One-dimensional camera ZK4	Scientific Instruments GmbH, Heidelberg, Germany
Oscillograph	Scientific Instruments GmbH Heidelberg, Germany

3.1.3. Materials and chemicals for cell culture

3.1.3.1. Materials for HL-1 cell culture and analysis

The materials used to culture HL-1 cells are summarized in Table 9.

Table 9. Materials for HL-1 cell culture and analysis

General materials and culture medium	Company Name
Cover slips (12 mm, 15 mm)	Menzel-Gläser, Braunschweig, Germany
Culture flasks, 25 cm^2	Sigma-Aldrich, Steinheim, Germany
Filter tips and canules	Braun, Melsungen, Germany
Microtome blades A35	Feather, Köln, Germany
Molecular weight markers (DNA, RNA)	Fermentas, Baden-Württemberg, Germany
Multi-well cell culture plates (6/12/24-well)	BD Biosciences, Heidelberg, Germany
Needle (0.55 × 55 mm)	BD Biosciences, Heidelberg, Germany
Syringe (1 ml)	BD Biosciences, Heidelberg, Germany
Syringe (20 ml)	BD Drogheda, Drogheda, Ireland
Syringe filter (0.2 µm)	Thermo Fisher Scientific, Waltham, MA, USA
Penicillin/streptomycin (5000 U/ml)	Thermo Fisher Scientific, Waltham, MA, USA
Nunc-Immuno MicroWell 96-well solid plates	Thermo Fisher Scientific, Waltham, MA, USA

3.1.3.2. Chemicals for HL-1 cell culture

The HL-1 cells require specific media components to grow and maintain their cardiomyocyte characteristics, which are listed in Table 10.

Table 10. Media components required for the cultivation of HL-1 cells

Chemical	Vendor	Catalog #
Claycomb medium	Sigma-Aldrich, Steinheim, Germany	51800C
Fetal bovine serum	Sigma-Aldrich, Steinheim, Germany	F2442
Penicillin/streptomycin (104 U/ml and 104 g/ml, respectively)	Sigma-Aldrich, Steinheim, Germany	P4333
(±)-Norepinephrine (+)-bitartrate salt	Sigma-Aldrich, Steinheim, Germany	A0937
L-Ascorbic acid, sodium salt	Sigma-Aldrich, Steinheim, Germany	A7506
L-Glutamine, 200 mM	Sigma-Aldrich, Steinheim, Germany	G7513
Trypsin-EDTA (0.05% trypsin in 0.02% EDTA-Na)	Sigma-Aldrich, Steinheim, Germany	T3924
Trypsin inhibitor type I-S, saoybean	Sigma-Aldrich, Steinheim, Germany	T6522
Dulbecco's PBS (Ca^{2+} and Mg^{2+} free)	Sigma-Aldrich, Steinheim, Germany	D8537
Fibronectin (1 mg/ml)	Sigma-Aldrich, Steinheim, Germany	F-1141
Gelatin from bovine skin	Sigma-Aldrich, Steinheim, Germany	G9391
Distilled water, cell culture grade	Sigma-Aldrich, Steinheim, Germany	W3500
Cryovials, 2 ml round bottom	Corning, Corning, NY, USA	430289
Sterile acrodisc syringe filters, 0.2 µm	Gelman Sciences, Colorado, USA	4192
Mr. Frosty 18-tube freezing container	Nalgene Nunc, Rochester, NY, USA	7-5100-0001

3.1.3.3. Solutions for the preparation of mouse primary cardiomyocytes

The solutions used for the preparation of cardiomyocytes are listed in Table 11.

Table 11. Solutions for the preparation of mouse primary cardiomyocytes

Name	Composition
Calcium stock solution	$CaCl_2$ 100 mM
Powell medium	NaCl 110 mM $NaHCO_3$ 25 mM Glucose 11 mM KCl 2.6 mM KH_2PO_4 1.2 mM Mg_2SO_4 1.2 mM
Collagenase buffer	Powell Medium 40 ml Collagenase 20 mg Calcium stock solution 12.5 µl

3.1.4. Proteins and enzymes

Proteins (including enzymes) are listed alphabetically with the corresponding suppliers in Table 12.

Table 12. Proteins and enzymes used in the study

Proteins (including enzymes)	Company name and location
Bovine serum albumin (BSA)	Roth, Karlsruhe, Germany
DNase I	Sigma-Aldrich, Steinheim, Germany
Immunostar-alkaline phosphatase	Bio-Rad, Munich, Germany
Milk powder	Roth, Karlsruhe, Germany
Precision plus protein standards, dual color and unstained	Bio-Rad, Munich, Germany
Primary antibodies	Various companies, see Table 14
Secondary antibodies	Various companies, see Table 14

SuperScript II reverse transcriptase	Invitrogen, Karlsruhe, Germany
Taq DNA polymerase	Eppendorf, Hamburg, Germany
Protease-inhibitor Mix M (39102)	SERVA Electrophoresis GmbH, Heidelberg, Germany

3.1.5. Kits

All the kits used in this study are listed in Table 13.

Table 13. List of kits with corresponding suppliers

Kits Company name	**Kits Company name**
Fibrous tissues RNA isolation Kit	Qiagen, Hilden, Germany
RNeasy kit	Qiagen, Hilden, Germany
RT-PCR kit	Invitrogen, Karlsruhe, Germany
Maxima SYBR Green/ROX qPCR Master Mix	Thermo Fisher Scientific, Waltham, MA, USA
Lipofectamine 3000 Transfection Kit	Invitrogen, Karlsruhe, Germany
Amplite Fluorimetric H_2O_2 Assay Kit	AAT Bioquest, Sunnyvale, CA, USA
Plasmid Midi Kit (Cat No./ID 12143)	Qiagen, Hilden, Germany

3.1.6. Primary and secondary antibodies

The primary and secondary antibodies used in this study are listed in Table 14.

Table14. Primary and secondary antibodies used in this study. Ms = mouse; Rb = rabbit; WB = western blot analysis; IF = immunofluorescence analysis.

Target	**Host**	**Source; catalog number**	**Lot or Catalog number**	**Dilution WB**	**Dilution IF**
Catalase (CAT)	Rb	Gift from Denis I Crane, School of Biomolecular and Biophysical Science, Griffith University, Nathan, Brisbane, Australia	In house	1:10,000	1:2,000
GAPDH	Ms	HyTest Ltd, Intelligate, Turku, Finland; 5G4	09/10-G4-C5	1:20,000	-
Peroxisomal biogenesis factor 13 (Pex13p)	Rb	Gift from Denis I Crane (address see above)	In house	1:6,000	1:2,000
Peroxisomal biogenesis factor 14 (Pex14p)	Rb	Gift from Denis I Crane (address see above)	In house	1:20,000	1:4,000
PMP(peroxisomal membrane protein) 70	Rb	Gift from Alfred Völkl, Department of Anatomy and Cell Biology II, University of Heidelberg, Heidelberg, Germany	In house	1:250	-
Superoxide dismutase 2 (SOD2)	Rb	Research Diagnostics, Inc., Flanders, NJ, USA	RDI-RTSODMabR	1:6,000	1:5,000
Anti-mouse IgG alkaline phosphatase	Goat	Sigma-Aldrich, Steinheim, Germany	A3562	1:20,000	-
Anti-rabbit IgG alkaline phosphatase	Goat	Sigma-Aldrich, Steinheim, Germany	A3687	1:20,000	-
Anti-rabbit-IgG Alexa Fluor 488	Donkey	Molecular Probes/Invitrogen, Karlsruhe, Germany	A21206	-	1:600
Anti-mouse-IgG Alexa Fluor 555	Horse	Molecular Probes/Invitrogen, Karlsruhe, Germany	A21422	-	1:600

3.2. Software used for recording and analyzing data

The software used in this study is listed in Table 15.

Table 15. Software used for data recording and analysis

Function	Software
Text processing	Microsoft Word, Office 2010, Microsoft
Image process	Photoshop CS5, Adobe
Data analysis and Graph making	GraphPad Prism 6, Graphpad Software Microsoft Excel, Office 2010, Microsoft
Absorbance measurement, H_2O_2 assay	Mikro Win 2000, Mikrotek Laborsysteme GmbH
RNA concentration determination	Nanodrop 2000 software, Thermo Fisher Scientific
Quantitative PCR	iQ5 Optical System Software, Bio-Rad
Semi-quantitative PCR documentation	Gel Doc 2000 software, Bio-Rad
Cell shorting measurement	MUCEL, Scientific Instruments GmbH

3.3. Bioinformatics tools

3.3.1. GenBank

GenBank (http://www.ncbi.nlm.nih.gov) is a database that contains nucleotide sequences (Benson et al., 2016). PubMed is the integrated biomedical journal literature portal, which was used for literature searches in this study (https://www.ncbi.nlm.nih.gov/pubmed). The basic local alignment search tool (BLAST) allows sequence similarity searches against GenBank and other sequence databases (Benson et al., 2016). In this study, the specificity of primer binding sites was checked using BLAST.

3.3.2. Databases of expressed sequence tags

The database of expressed sequence tags (dbEST) is a collection of short cDNA clone fragments from diverse cDNA libraries (Boguski et al., 1993). These fragments can be

used to identify specific genes or gene transcripts (Adams et al., 1991). Expressed sequence tags (ESTs) are the primary source of data for gene expression and annotation studies, including species-restricted, organ/tissue-specific and cell type-specific expression profiles (Benson et al., 2016). EST sequence data in dbEST is annotated with the species and tissue of origin and the type of library.

3.3.3. UniGene

UniGene (http://www.bioinfo.org.cn/relative/NCBI-UniGene.htm) is a database of transcript sequences that partitions GenBank entries into gene-oriented clusters representing a unique gene. Each entry is linked to information such as the source species and tissue, and the genomic map location of the corresponding gene.

3.4. Mice

3.4.1. Wild-type mice

Wild-type C57BL/6J mice were obtained from the Central Animal Facility (Zentrales Tierlabor) of the Justus-Liebig-University Giessen, Germany. Breeding and handling was approved by the Regierungspraesidium (Governmental Commission of Animal Care), permit number V 54-19 C 20/15 c GI 20/23. Eight wild-type mice (19–24 weeks old) were used to analyze peroxisome distribution in different parts of the heart. Three newborn pups, four wild-type pups at postnatal day 2 (P2), and four mice aged 8 weeks were used to investigate the developmental changes of peroxisomes in mouse hearts.

3.4.2. *Pex11α* knockout mice

The *Pex11α* knockout mice were generated and described previously (X. Li, Baumgart, et al., 2002). Briefly, exon 2 and exon 3 of the *Pex11α* gene were replaced with a PGK-neo cassette by homologous recombination in embryonic stem cells. *Pex11α* knockout, heterozygotes and wild-type mice were identified by testing tail DNA. Breeding and handling was approved as above. Nine $Pex11\alpha^{+/+}$, three $Pex11\alpha^{+/-}$ and nine $Pex11\alpha^{-/-}$ mice (9–27 weeks old) were used in this study. Six wild-type mice and six *Pex11α* knockout mice (12–50 weeks old) were used to measure cell shorting. Six wild-type mice and five *Pex11α* knockout mice were used for ischemia-reperfusion experiments.

Animals were housed under standard conditions (12 h light and 12 h dark) in the Central Animal Facility of the Justus-Liebig University Giessen. All animal experiments were approved by the German Government Commission of Animal Care.

3.5. Methods

3.5.1. Data mining

For each peroxisomal gene of interest, data mining involved checking the dbEST profile for the heart and liver to find the transcripts per million (TPM) value. The liver was used as a reference given that this organ contains the largest number of peroxisomes in mammals (Islinger et al., 2010). The TPM values of peroxisome-related genes in the heart and liver libraries were acquired from the UniGene database, via the NCBI portal.

3.5.2. HL-1 cells

HL-1 atrial cardiomyocytes were obtained from Dr. William Claycomb (Louisiana State University Medical Center). Cells from passages 51–60 were used in this study. HL-1 cells are derived from the mouse atrial tumor lineage AT-1 and retain many characteristics of differentiated atrial cardiomyocytes (Claycomb et al., 1998). However, the cells used in this study did not display a beating phenotype.

3.5.2.1. HL-1 cell culture

HL-1 cells were grown in Claycomb medium supplemented with batch-specific 10% fetal bovine serum (FBS), 100 U/ml penicillin + 100 µg/ml streptomycin, 0.1 mM norepinephrine, and 2 mM L-glutamine. One day before seeding, the flasks were incubated overnight with 0.02% Bacto gelatin in 0.5% fibronectin. The cells were passaged twice per week, each time by seeding ~3 × 10^6 cells into a new 25 cm^2 flask, as previously described (Claycomb et al., 1998).

3.5.2.2. Transfection of HL-1 cardiomyocytes with *Pex14* siRNA

Cell culture plates (6/12/24 wells) with or without cover slips were coated with 0.02% Bacto gelatin in 0.5% fibronectin overnight. For six-well plates, 1.5–2×10^5 cells were seeded in each well. For 12/24-well plates, the cell number was reduced proportionally according to the surface area of the well. Once the cells had attached, transient transfection experiments were carried out using Lipofectamine 3000 reagent (Invitrogen) in Opti-MEM I Reduced Serum Medium (Thermo Fisher Scientific). For each well, a mixture of Lipofectamine/siRNA complex solution was prepared by mixing 10 µl of Lipofectamine 3000 reagent and 150 pmol *Pex14* siRNA in the Opti-MEM I medium, and a final volume of 250 µl was added to each well. The homogeneous dispersal of the complex was achieved by gentle shaking. Cells transfected with AllStars Negative Control siRNA (Qiagen) under the same conditions were used as the control group. After 48 h, 96 h and 6 days, the cells were collected for further analysis.

3.5.3. Cardiomyocyte cell shorting measurements

3.5.3.1. Isolation of adult mouse ventricular cardiomyocytes

Myocytes were prepared and their contraction was measured in the laboratory of Professor Schlüter, Department of Physiology, Faculty of Medicine, Justus-Liebig-University. Ventricular heart muscle cells were isolated from mice as previously described (Schlüter and Piper, 2005; Schlüter and Schreiber, 2005) with a slightly modified protocol. Briefly, operation scissors (Aesculap, Tuttlingen) and forceps (Eickemeyer, Tuttlingen) were disinfected before use. Mouse hearts were excised together with the lungs after cervical dislocation and transferred rapidly to physiological NaCl (0.9% w/v) (Braun Melsungen AG, Melsungen), followed by mounting on the cannula of a circulating constant-flow perfusion system (designed by the working group of Prof. Schlüter). The hearts were perfused with 5 ml calcium-free Powell medium (Section 3.1.3.3) in a non-re-circulating manner, then for 25 min in a re-circulating manner in Powell medium supplemented with type II collagenase (Type CLSII, Biochrom, Berlin) and calcium. Thereafter, the ventricular tissue was cut out, minced using a tissue chopper (HSE, March-Hugstetten), and incubated for another 5 min in re-circulating buffer at 37°C. After incubation, the cell solution was filtered through a 200-µm polyamide mesh (NeoLab, Heidelberg). The filtered material was centrifuged at 25 *g* (300 rpm) using a Megafuge 2.0 (Kendro, Hanau) and resuspended in buffer

with a gradually increasing calcium concentration to a final value of 1 mM, before transfer to the culture medium (Schlüter and Piper, 2005).

3.5.3.2. Cell shorting measurements

Isolated cells were separated in culture dishes (Falcon 3001/3004; Becton Dickinson, Heidelberg) and allowed to settle and adhere lightly for 1 h. Cell shortening was measured as previously described (Langer et al., 2003). Briefly, cardiomyocytes from the hearts of wild-type and *Pex11α* knockout mice were analyzed using a cell-edge detection system. Two AgCl electrodes sending out electrical stimuli were immersed in the culture medium. Four sets of cell shortening, contraction and relaxation velocity data (Table 16) were recorded, and the average was calculated (Hill et al., 2013).

Table 16. Cardiomyocyte parameters recorded and calculated in this study.

Parameters	**Definition**
Diastolic cell length	The maximum cell length when contracting
Systolic cell length	The minimum cell length when contracting
Time to peak	The time from the beginning of contraction to the maximum contraction
Con_{max} in µm/s	The maximum contraction velocity
Rel_{max} in µm/s	The maximum relaxation velocity
dL/L%	The dL is the change from diastolic to systolic cell length, and dL/L% is cell shortening as a percentage of diastolic cell length

3.5.4. Ischemia-reperfusion model in male Wister rat hearts

The following experiments were carried out in collaboration with Professor Böning (Department of Cardiovascular Surgery, University Hospital Giessen and Marburg, Campus Giessen, Giessen, Germany), who kindly provided us the rat samples ((Böning et al., 2014).

Wistar rats (Janvier Laboratories, France), 4–5 months of age and 464–597 g in weight were anesthetized with isoflurane (2.5% isoflurane and 97.5% oxygen) and killed by cervical dislocation. The hearts were rapidly excised, and the aorta was cannulated for

retrograde perfusion and connected to a Langendorff perfusion system as described by Böning et al. (Böning et al., 2014). The rat heart ischemia-reperfusion model used in this study was performed in two steps: (1) 90 min ischemia by aortic clamping and (2) reperfusion for 90 min. The heart was exposed to intervention for less than 4 h in total. Afterwards the hearts were stored at -80ºC and later processed for mRNA and protein isolation.

3.5.5. Catalase activity assay on mouse heart homogenates and cell lysates

Catalase protects cells from the accumulation of H_2O_2 by converting it into water and oxygen (Michiels et al., 1994). H_2O_2 is a major ROS and is a product of aerobic metabolism in the heart (Boveris and Chance, 1973). Catalase activity was measured based on the formation of a yellow complex due to the reaction between molybdate and H_2O_2. The solutions needed for the catalase assay are listed in Table 17 and the components of the three blank solutions are listed in Table 18. The color change after the catalase reaction is shown in Figure 3.

Table 17. The solutions needed for the catalase assay

Function	**Component**
Substrate	65 µM H_2O_2 in phosphate-buffered saline (PBS)
Stop solution and color indicator	32.4 mM ammonium molybdate in PBS
Sample solution	For tissue: the tissue and lysis buffer ratio is 1:50 (w/w) For cells: 300 µL of cell lysis solution was added to each well of a six-well plate

Table 18. The composite of the blank solutions

Blanks	**Component**
Blank 1	1.0 ml substrate, 1 ml molybdate, 50 µl sample solution
Blank 2	1.0 ml substrate, 1 ml molybdate, 50 µl lysis buffer
Blank 3	1.0 ml PBS, 1.0 ml molybdate, 50 µl lysis buffer

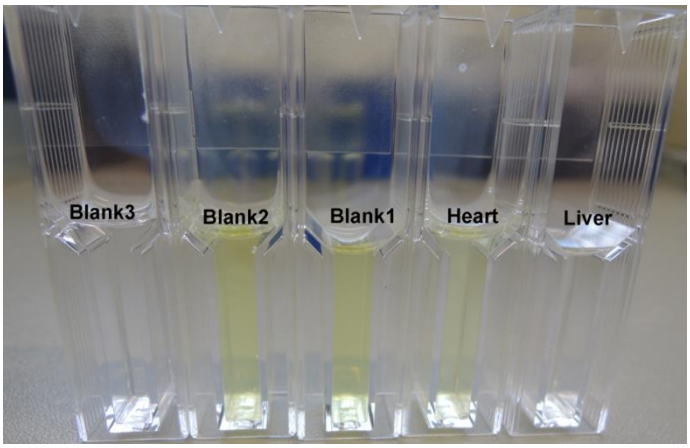

Fig.3. Measurements of catalase activity in heart tissue homogenates. From left to right the samples are blank 3, blank 2, blank 1, heart and liver. Blank 3 is the sample without the H_2O_2 substrate, revealing the colorless molybdate solution. In Blanks 2 and 1, the H_2O_2 reacted with molybdate to form a yellow complex. The heart homogenate reacted with the H_2O_2, but the surplus reacted with molybdate to form a weaker yellow color. The liver homogenate reacted with all of the H_2O_2 leaving no surplus, and was used as a positive control in these experiments.

The catalase assay was carried out as previously described (Goth, 1991) with some modifications. Briefly, tissue pieces and cells were homogenized in cell lysis buffer (25 mM Tris-HCl, 1 mM EDTA, 1 mM DTT, 250 mM sucrose, pH 7.8) at the ratio shown in Table 17. We prepared 40 ml of reaction substrate containing 65 µM H_2O_2 and 40 ml of stop solution containing 32.4 mM ammonium molybdate. We then mixed 50 µl of homogenate with 1.0 ml of the substrate and incubated for 3 min at 37°C. The enzymatic reaction was stopped by adding 1.0 ml of ammonium molybdate solution, and the absorbance at 405 nm was measured. The H_2O_2 solution was always freshly made before each measurement. The catalase activity was calculated using the following formula:

$$\text{Catalase activity (kU/L)} = (A_{Sample} - A_{Blank\text{-}1}) / (A_{Blank\text{-}2} - A_{Blank\text{-}3}) \times 271$$

3.5.6. Fluorimetric hydrogen peroxide assay

H_2O_2 levels were measured using the Amplite Fluorimetric Hydrogen Peroxide Assay Kit (AAT Bioquest). Briefly, cells cultured in six-well plates were washed with PBS at different time points after treatment and then collected in cell lysis solution. In each well, 50 µl of the H_2O_2 reaction mixture was added (red peroxidase substrate and horseradish peroxidase from the kit). Then the H_2O_2 standard solution, blank control samples, and test samples were added, making a final assay volume of 100 µl per well.

The plates were incubated at room temperature for 15 min, protected from the light. The increase in fluorescence was monitored with a fluorescence plate reader at $\lambda_{Excitation}/\lambda_{Emission}$ = (540 ± 10)/(590 ± 10) nm.

3.5.7. Methylthiazole tetrazolium (MTT) assay

The MTT colorimetric assay (Sigma-Aldrich) is used to determine the viable cell number in proliferation and cytotoxicity studies. This assay is based on the cleavage of the yellow tetrazolium salt MTT by mitochondrial dehydrogenases to form a soluble blue formazan product. The amount of formazan produced is directly proportional to the number of living cells (Sylvester, 2011). In this study, the effect of treatments on the viability of HL-1 cardiomyocytes was evaluated using the MTT assay as previously described (Vijayan et al., 2011) with slight modifications. Briefly, after treatment with 0.5% ethanol and *Pex14* siRNA for 48 h, cells were washed and incubated with 0.5 mg/ml MTT in cell culture medium for 3 h. The formazan crystals in viable metabolic cells were dissolved in isopropanol and the absorbance was measured at 570 nm. The percentage of viable cells was calculated using the following formula:

$$\%\text{viable cells} = \text{A570 of treated cell} / \text{A570 of non-treated cells} \times 100$$

3.5.8. Trypan blue exclusion test

The viability and number of HL-1 cardiomyocytes was assessed using the trypan blue exclusion test, which is based on the principle that viable cells have intact membranes that prevent the uptake of the dye, whereas dead cells have broken membranes which allow staining (Strober, 2015). The cell suspension (0.5 ml) was incubated with 0.1 ml trypan blue solution (0.5% w/v in PBS) for 5 min at room temperature. Afterwards, viable cells with clear cytoplasm and dead cells with blue cytoplasm were counted using a Neubauer Cell Counting Chamber (Brand GMBH, Wertheim, Germany) by counting four fields with 16 squares each. The numbers of living and dead cells were used to calculate the cell viability, as well as the total number of cells using the formula shown below.

$$\%\text{ viable cells} = [1.00 - (\text{Number of blue cells} \div \text{Number of total cells})] \times 100$$

3.6. Molecular biological and morphological experiments on mouse tissue and cells

3.6.1. Molecular biological experiments for gene expression analysis

The reverse transcription polymerase chain reaction (RT-PCR) is a highly sensitive and specific method to detect and quantify rare transcripts (Marone et al., 2001). The RT-PCR procedure includes RNA extraction, reverse transcription, PCR amplification and quantitative analysis (Marone et al., 2001).

3.6.1.1. RNA isolation from heart tissue and HL-1 cells and reverse transcription to generate cDNA

Total RNA was isolated from (1) HL-1 cells (passage 51–60), (2) newborn and adult whole hearts, and (3) the left atrium, right atrium, left ventricle and right ventricle, using RNAzol RT (Sigma-Aldrich) and the isolation protocol of the manufacturer. The heart samples were taken from wild-type (*Pex11α*$^{+/+}$), *Pex11α*$^{+/-}$ and *Pex11α*$^{-/-}$ mice.

3.6.1.1.1. Isolation of total RNA from mouse heart tissue

Mice were killed by cervical dislocation and the hearts were rapidly excised and stored in liquid nitrogen. For mRNA isolation, frozen tissue samples were transferred to RNAzol RT solution supplemented with 10% v/v glycerol (1 ml per up to 100 mg of tissue), and quickly homogenized in an Ultra Turrax T25 basic homogenizer for 30 s on ice. All further steps were carried out according to the RNAzol RT protocol.

3.6.1.1.2. Isolation of total RNA from HL-1 cells

HL-1 cells were harvested directly from the cell culture dish. After removing the medium, RNAzol RT solution supplemented with 10% v/v glycerol was added directly to each well (at least 1 ml of RNAzol RT per 10 cm^2 according to the RNAzol RT protocol), before scraping the cells into collection tubes. The cells were lysed by pipetting, and subsequent steps were carried out according to the RNAzol RT protocol.

3.6.1.1.3. Quality control and cDNA synthesis

The isolated total RNA was dissolved in RNase-free water and stored at −80°C. The quantity was determined by measuring the absorbance ratio at 260 and 280 nm using a Bio-Rad spectrophotometer. DNase I was added to to remove trace of genomic DNA by mixing 1 µg of RNA sample with 10× DNase I reaction buffer, 1 U/µl DNase I (Amp Grade) and DEPC-treated water to 10 µl, then incubating for 15 min at room temperature. The DNase I was then inactivated by adding 1 µl 25 mM EDTA and heating at 65°C for 10 min. The purified total RNA (1-2 µg) was then reverse transcribed to produce first-strand cDNA using Superscript II reverse transcriptase (Invitrogen) according to the manufacturer's protocol.

3.6.1.2. RNA analysis by semi-quantitative RT-PCR

Semi-quantitative PCR was carried out in a total reaction volume of 25 µl containing 0.1 µg cDNA and the primers listed in Table 19. The reaction mixture was heated to 95°C for 10 min, followed by 30–35 cycles of denaturation at 95°C for 30 s, annealing at the appropriate primer-specific annealing temperature (Table 19) for 30 s, and extension at 72°C for 60 s. The products were separated by agarose gel electrophoresis and bands were quantified using the Bio-Rad Gel Doc 2000 system.

All primers used for this study were laboratory stocks in the working group of Prof. Baumgart-Vogt.

Table 19. The RT-PCR primers used in this study.

Genes	NCBI reference of genes	Forward primers (5′→3′)	Reverse primers (5′→3′)	T_m (°C)	Product (bp)
Pex5	NM_001277805.1	GAGTGAAGAAGCAGTGGCTGCATAC	GGACAGAGACAGCTCATCCCTACAA	62	508
Pex6	NM_145488.1	AGTGTAAAGGGACCGGAGCTCATC	TCTAGCCCTTCCTCTAGGTCTCGAA	60	515
Pex7	NM_001161825.1	GTGAAGACCACAGGAGTACGGATTG	CCGTGAGACAAACAGGGTCATAGA	62	409
Pex13	NM_023651.4	GACCACGTAGTTGCAAGAGCAGAGT	CTGAGGCAGCTTGTGTGTTCTACTG	65	565
Pex14	NM_019781.2	CCAGACAGTGACTCAGGTGCAGA	TGGTGCCAGGTGGTCAAGATACT	62	982
Gnpat	NM_010322.3	TGAGGACGTGCAAGCCTTTG	TCCAGAAGCTGACGGGTGAA	62	759
Acox1	NM_015729.3	CTGAACAAGACAGAGGTCCACGAA	TGTAAGGGCCACACACTCACATCT	63	565
Aldp	NM_007435.2	GAGGGAGGTTGGGAGGCAGT	GGTGGGAGCTGGGGATAAGG	65	465
Acox3	NM_030721.2	GCCAAAGCTGATGGTGAGCTCTAT	AGGGGTGGCATCTATGTCTTTCAG	62	813
Pmp2	NM_008993.2	TCCTAAAGCTCTACCCGGTGCTC	AGGTGTCCACATCCTCCAGTTCA	63	395
Pmp24	NM_021534.3	ACCCCTCCAAGTAACACAGTCCAA	CATACAAGCTTGACACGTGCTGTG	62	577
Pmp34	NM_011399.3	GGGTCAAAGGTCAGCGTTCTTCT	ACTTCCCAGGGTCCTGTTTTCTG	62	461
Pmp35	NM_001163305.2	GATGGGGAGGATCAGGTGAAAAC	CCAAGGAGGCGTTCTGTCAAAGT	62	611
Abcd3	NM_008991.2	CTGGGCGTGAAATGACTAGATTGG	AGCTGCACATTGTCCAAGTACTCC	62	523
Abcd4	NM_001286759.1	GCTGCACAGAATGGAGTTGA	CAAAGCTCTTCAGGGTGGAG	62	296
Pparα	NM_011144.6	AGACCGTCACGGAGCTCACA	GGCCTGCCATCTCAGGAAAG	68	584
Pparβ	NM_011145.3	CACCGAGTTCGCCAAGAACA	AGAGCCCGCAGAATGGTGTC	60	363

Pparγ	NM_001127330.1	TCCGTAGAAGCCGTGCAAGA	CACCTTGGCGAACAGCTGAG	62	441
Gapdh	NM_008084	CACCATGGAGAAGGCCGGGG	GACGGACACATTGGGGGTAG	62	418
28S rRNA	NR_003278.1	CCTTCGATGTCGGCTCTTCCTAT	GGCGTTCAGTCATAATCCCACAG	62	254
β-actin	NM_007393.5	GTGGGCCGCTCTAGGCACCAA	CTCTTTGATGTCACGCACGATTTC	65	540

3.6.1.3. RNA analysis by real-time quantitative PCR

Real-time quantitative PCR (qRT-PCR) involves the addition of a fluorescent label to the PCR product allowing the quantity to be measured in real time. We used SYBR green, which can bind to double-stranded DNA or label sequence-specific DNA primers or cDNA probes (Ponchel et al., 2003). The computer transformed the signal detected by the sensor to the threshold cycle (Ct) value, which is proportional to the initial amount of cDNA (Ponchel et al., 2003). The primers were synthesized by Eurofins MWG Operon. A 20-µl qRT-PCR reaction mixture was prepared as follows (Table 20).

Table 20. The qRT-PCR components.

Component	**Volume**
cDNA template	1 µl
Maxima SYBR Green/ Fluorescein qPCR Master Mix (2 ×)	10 µl
Forward primer	0.3 µM
Reverse primer	0.3 µM
Water, nuclease-free	To 20 µl

Each qRT-PCR was performed in duplicate using an iCycler iQ System according to the manufacturer's protocol (Bio-Rad). Heating to 95°C for 8 min was followed by 45 cycles of denaturation at 95°C for 20 s, annealing at the appropriate primer-specific temperature (Table 21) for 30 s, and extension at 72°C for 30 s. Before each experiment, melt curves and primer efficiencies were determined for each primer pair to confirm the specificity of the PCR product using cDNA from the control group. The qRT-PCR data were normalized against the *Gapdh* and 28*S* rRNA housekeeping genes and were presented as relative expression levels using the ΔΔCt method (Yuan et al., 2006).

Table 21. The qRT-PCR primers used in this study.

Gene	NCBI reference	Forward primers (5′→3′)	Reverse primers (5′→3′)	Product (bp)
Cat	NM_009804.2	GGAGGCGGGAACCCAATAG	GTGTGCCATCTCGTCAGTGAA	102
Abcd1	NM_007435.1	ACAGTGCCATCCGCTACCTA	ATGAGCTACTAGACGGCTTCG	65
Acox1	NM_015729.3	CCGCCACCTTCAATCCAGAG	CAAGTTCTCGATTTCTCGACGG	86
Acox2	NM_001161667.1	ACGGTCCTGAACGCATTTATG	TTGGCCCCATTTAGCAATCTG	125
Acox3	NM_030721.2	CTGTTTTGCTCTCACCGAACT	TCGAAATCCGGGGAATGTAAGAT	89
Pex5	NM_001277805.1	AATGCAACTCTTGTATCCCGAG	GGCGAAAGTTTGACTGTTCAATC	91
Pex7	NM_001161825.1	GACAGGTGCGGTTGACTGTA	GCGTGGAACGGTGAAAAT	150
Pex11α	NM_011068.1	ACTGGCCGTAAATGGTTCAGA	CGGTTGAGGTTGGCTAATGTC	118
Pex11β	NM_0011069	CGCCTATTGATGGAACAAGAGACT	TCCAGGTCCCACAGTTTCTACTC	106
Pex11γ	NM_026951.2	GACTCTGCTTGGTGGTGGA	GCTCCGCAGCTTCTGTCTAA	111
Pex14	NM_019781.2	GCCACCACATCAACCAACTG	GTCTCCGATTCAAAAGAAGTCCT	97
Pparα	NM_011144.6	AGACCCTCGGGGAACTTAGA	CAGAGCGCTAAGCTGTGATG	123
Pparβ	NM_011145.3	GCAGCCTCAACATGGAATGTC	GAGCTTCATGCGGATTGTCC	116
Pparγ	NM_001127330.1	TTTTCAAGGGTGCCAGTTTC	CATGGACACCATACTTGAGCA	128
Sod1	NM_011434.1	GACCTGGGCAATGTGACTGCTG	GCACCAGTGTACGGCCAATGATG	108
α-Mhc	NM_001164171.1	TGTGGTGCCTCGTTCCA	TTTCGGAGGTACTGGGCTG	128
β-Mhc	NM_080728.2	ATGTGCCGGACCTTGGAAG	CCTCGGGTTAGCTGAGAGATCA	170
Nppa	NM_008725.3	TCGTCTTGGCCTTTTGGCT	TCCAGGTGGTCTAGCAGGTTCT	106

Nppb	NM_008726.5	AAGTCCTAGCCAGTCTCCAGA	GAGCTGTCTCTGGGCCATTTC	91
Nppc	NM_010933.5	CAGAAAAAGGGTGACAAGACTCC	ATCCCAGACCGCTCATGGA	229
Pdi	NM_028944.3	GTACCGTTTGAGACCTCCTGTC	CAACGAGTAGTCGTCCACTTCA	270
Calreticulin	NM_007591.3	AGTTTTGCTGTACTGGGCCT	GCTTCTCTGCAGCCTTGGTA	139
Col1a	NM_007742.4	GTGTGATGGGATTCCCTGGACCTA	CCTGAGCTCCAGCTTCTCCATCTT	126
Col3a	NM_009930.2	ACCCCCTGGTCCACAAGGATTA	ACGTTCTCCAGGTGCACCAGAAT	151
28S rRNA	NR_003278.1	AAAGCGGGTGGTAAACTCCA	GGTTTCACGCCCTCTTGAAC	118
Gapdh	NM_008084	TGGCAAAGTGGAGATTGTTGCC	AAGATGGTGATGGGCTTCCCG	156

3.6.2. Biochemical experiments for protein abundance analysis

Sodium dodecylsulfate polyacrylamide gel electrophoresis (SDS-PAGE) and Western blotting are still widely used to separate and identity proteins based on molecular weight. After the transfer of the separated proteins to a membrane, the specific proteins are visualized using labeled antibodies (Yang and Mahmood, 2012).

3.6.2.1. Preparation of heart tissue homogenates

Heart tissue stored in liquid nitrogen was added to lysis solution (25 mM Tris-HCl, 1 mM EDTA, 1 mM DTT, 250 mM sucrose, pH 7.8) containing 10% protease inhibitor mix M (SERVA, Heidelberg, Germany), and homogenized using an Ultra Turrax T25 basic homogenizer for 30 s on ice. The homogenates were transfered in Eppendorf tubes and centrifuged at 1,000 *g* for 10 min at 4°C. The supernatants were stored at –20°C.

3.6.2.2. Preparation of whole cell lysates

Cells in six-well plates were washed twice with PBS and 300 µl of cell lysis buffer (25 mM Tris-HCl, 1 mM EDTA, 1 mM DTT, 250 mM sucrose, pH 7.8) containing 10% protease inhibitor mix M was added to each well. Cells were scraped thoroughly using a rubber scraper and lysed by pipetting before collection in Eppendorf tubes. After incubation on ice for 30 min with brief vortexting every 10 min, the samples were centrifuged at 1,000 *g* for 10 min at 4°C and the supernatants were collected and stored at –20°C.

3.6.2.3. SDS-PAGE and Western blot

Polyacrylamide gels containing SDS were prepared as shown in Table 22. The solutions used for western blot are listed in Table 23. The protein concentration of each sample was measured using the Bradford Assay with bovine serum albumin (BSA) as the standard (Bradford, 1976). SDS-PAGE was carried out using Bio-Rad electrophoresis apparatus. Homogenates of each sample were separated on a 12% polyacrylamide gel with 5 µl color-stained precision markers as size references. Protein transfer onto polyvinylidene difluoride (PVDF) membranes (Millipore, Schwalbach,

Germany) was carried out in a Bio-Rad tank. The membranes were blocked for 1 h at room temperature in blocking solution comprising 10% fat-free milk powder (Carl Roth, Karlsruhe, Germany) in Tris-buffered saline with Tween-20 (TBST). Primary antibodies were diluted in blocking solution and the membrane was incubated with antibody solution overnight at 4°C on a rotor shaker (Table 14). After washing with TBST (3 × 10 min), membranes were incubated for 2 h with secondary antibodies. Bands were visualized using the Immunostar-AP detection kit (Bio-Rad) and exposed to BioMax MR films (Kodak, Stuttgart, Germany). Blots were stripped using stripping buffer (Table 23) at 60°C for 60 min and redetected with other primary antibodies or control markers.

Table 22. Preparation of 1.5-mm 12% polyacrylamide gels containing SDS

Buffer A	0.4% SDS 1.5 M Tris-HCl, adjusted to pH 8.8
Buffer B	0.4% SDS, 0.5 M Tris-HCl, adjusted to pH 6.8
Separating gel (12%)	2 ml ddH_2O, 10 ml buffer A, 8 ml 30% acrylamide,15 µl TEMED, 130 µl 10% APS
Stacking gel	5 ml ddH2O, 5 ml buffer B, 1.25 ml 30% acrylamide, 15 µl TEMED, 130 µl 10% APS
10× loading buffer	3.55 ml ddH2O, 1.25 ml 0.5 M Tris-HCl (pH 6.8), 2.5 ml 50% (w/v) glycerol, 2.0 ml 10% (w/v) SDS, 0.05% bromophenol blue, with 50 µl β-mercaptoethanol added before use

Table 23. Composition of solutions used for western blots

10×Electrophoresis buffer	250 mM Tris, 2 M glycine, 1% SDS
20× Transfer buffer	NuPAGE transfer buffer (Invitrogen, Heidelberg, Germany)
10× TBS	0.1 M Tris, 0.15 M NaCl in ddH_2O, adjusted to pH 8.0
10% Blocking buffer	10 g fat free milk powder in 100 ml 1× TBST
1× Washing buffer (TBST)	10 mM Tris/HCl, 0.15 M NaCl, 0.05% Tween-20, pH 8.0
Stripping buffer	62.5 mM Tris (pH 6.8), 0.2% SDS, 0.01% β-mercaptoethanol in ddH_2O

3.6.3. Morphological methods

3.6.3.1. Embedding of mouse heart tissue into paraffin

Mice were anesthetized with 1.5% isoflurane and killed by cervical dislocation. The hearts of wild-type and *Pex11α* knockout mice were fixed by perfusion via the left ventricle with 4% Paraformaldehyde (PFA) in PBS (pH 7.4). The hearts were dissected and stored overnight in the same fixative solution (Table 24). Fixed hearts were embedded into paraffin (Paraplast Plus, St. Louis, MO) using a Leica TP1020 embedding machine (3× 70%, 80%, 90% and 100% ethanol, each step for 90 min; 2× 100% xylene each step for 90 min; 2× paraffin each step for 120 min).

3.6.3.2. Hematoxylin and eosin staining of heart tissue

Hematoxylin and eosin (H&E) staining is a routine histological staining method which we used for primary structural analysis and to evaluate the morphology of heart tissue. Hearts from wild-type and *Pex11α* knockout mice were immersion-fixed overnight in 4% PFA and embedded in paraffin as above, and 5 µm sections were prepared and incubated at 60°C overnight in a slide holder. The sections were deparaffinized and rehydrated by immersing in 100% xylene (3× 10 min), followed by 2 min each in 99%, 96%, 80%, 70% and 50% ethanol, and 2 min deionized H_2O. The slides were then stained for 10 min at room temperature with hematoxylin (lot GHS3, Sigma-Aldrich), rinsed for 10 min under tap water to allow the blue stain to develop, and then immersed in eosin Y solution (lot MKBV9915v, Sigma-Aldrich) for 30 s. The samples were then dehydrated in 50%, 70%, 80% and 96% ethanol for 1 min each, then 2 min in 99% ethanol before mounting in DePeX (SERVA Electrophoresis GmbH) and drying overnight under a fume hood.

3.6.3.3. Immunofluorescence staining of mouse hearts and HL-1 cells

3.6.3.3.1. Immunofluorescence staining of mouse heart tissue

The solutions used for immunofluorescence staining of heart tissue are listed in Table 24. We prepared 2-µm sections using a Leica SM 2000 R rotation microtome. Sections deparaffinized and rehydrated as described above were digested with trypsin for 15 min at 37°C to expose epitopes, blocked with 4% BSA for 1 h, and incubated with specific primary antibodies overnight at 4°C (Table 24). On the following day, the

sections were incubated with fluorophore-conjugated secondary antibodies (Table 14). Nuclei were counterstained with 2 µM TO-PRO-3 iodide for 10 min at room temperature (Thermo Fisher Scientific). The sections were analyzed by confocal laser scanning microscopy (CLSM) using a Leica TCS SP2 instrument.

Table 24. Solutions used for immunofluorescence staining of heart tissue

Fixative solution	4% PFA in 1× PBS (150 mM NaCl, 13.1 mM K_2HPO_4 , 5 mM KH_2PO_4), pH 7.4
10× PBS	1.5 M NaCl, 131 mM K_2HPO_4, 50 mM KH_2PO_4, pH 7.4
Trypsin (0.1%)	0.1 g trypsin in 100 ml PBS, freshly prepared
TEG buffer	5 mM EGTA, 0.1 M Tris, pH 9.0
Blocking buffer (4% PBSA + 0.05% Tween-20)	8 g BSA and 100 µl Tween-20 dissolved in PBS to a final volume of 200 ml
Dilution buffer (1% PBSA + 0.05% Tween-20)	2 g BSA and 100 µl of Tween-20 dissolved in PBS to a final volume of 200 ml

3.6.3.3.2 Immunofluorescence staining of HL-1 cells

Cardiomyocytes grown on fibronectin-coated coverslips were rinsed with PBS (pH 7.4) and fixed with 4% PFA in PBS for 20 min at room temperature. After fixation, cells were washed three times with PBS and incubated for 10 min in PBS containing 1% glycine, then 10 min in PBS containing 1% glycine and 0.1% Triton X-100 for permeabilization. After washing with PBS, cells were incubated for 30 min in PBS containing 1% BSA and 0.05% Tween-20. The coverslips were then incubated with primary antibodies overnight at 4°C in a moist chamber, followed by washing with PBS (3 × 5 min) and incubation with secondary antibodies for 1 h at room temperature. Nuclei were counterstained with 2 µM TO-PRO-3 iodide (Vijayan et al., 2011). The solutions used for immunofluorescence staining of HL-1 cells are listed in Table 25.

Table 25. Solutions for immunofluorescence staining of HL-1 cells

Fixative solution	4% PFA in PBS (150 mM NaCl, 13.1 mM K_2HPO_4 , 5 mM KH_2PO_4), pH 7.4
Glycine (1%)	1 g Glycine in 100 ml PBS
Glycine (1%) + Triton X-100 (0.3%)	1 g Glycine in 100 ml PBS and 0.3 ml Triton X-100
Blocking buffer: 1% PBSA + 0.05% Tween-20	2 g BSA in 200 ml PBS and 100 µl Tween-20
Mowiol 4-88 solution	Add 16.7 % Mowiol 4-88 (w/v) into 80 ml of PBS then stir overnight to mix the solution, add additional 40 ml of glycerol, stir again overnight. Centrifuge at 15,000 U/min for 1h and take off the supernatant next day and store at -20°C for further use.
Anti-fading agent (2.5%)	2.5 g N-propyl-gallate in 50 ml PBS and 50 ml glycerol
Mounting medium	Mowiol 4-88 mixed with anti-fading agent at a ratio of 3:1

3.7. Statistical analysis

Statistical analysis was carried out using GraphPad Prism v6.0 (Table 15). We used an unpaired Student's t-test for comparisons between two values with one variant, and analysis of variance (ANOVA) for multi-group values with one variant, to evaluate the difference between and within experimental groups. Numerical data were presented as the mean ± standard deviation (SD). The data were visualized as bar diagrams, in which each column represents the mean value for three independent replicates for each group. The error bars represent the SD within each experimental group. The significance of the differences between the groups were indicated with the following symbols: *($P \leq 0.05$), **($P \leq 0.01$) and ***($P \leq 0.001$).

4. Results

4.1. Distribution of peroxisomes in the normal heart

Little is known about the distribution and functionality of peroxisomes in the heart. There has been no systematic morphological analysis of peroxisomes in heart tissues or cardiomyocytes, and peroxisomal gene expression in the heart has not been examined in detail. However, such investigations could provide us with relevant information about the role of peroxisomes in the pathogenesis of heart diseases, and the impact of peroxisomal gene defects on heart functions. To address this knowledge gap, we first investigated the expression of genes encoding peroxisomal proteins in the heart and liver using *in silico* data, and we studied the distribution of peroxisomes in the heart tissues of adult wild-type mice by immunofluorescence microcopy.

4.1.1. *In silico* expression levels of genes encoding peroxisomal biogenesis regulators, metabolic transporters, and enzymes in the heart and liver

Expressed sequence tags (ESTs) are short, single-pass sequences of 200–500 bp, which can be used to characterize the transcripts expressed in specific tissues (Okubo et al., 1992). Data derived from EST sequencing in different tissues are stored in dbEST, and are extracted into UniGene. EST counts for each entry can therefore be used to estimate the relative expression levels of different genes in various tissues and organs calculated as a transcripts per million (TPM) value, which indicates the abundance of the corresponding mRNA (Wagner et al., 2012).

The liver has the highest content of peroxisomes among mammalian organs (Islinger et al., 2010) and is therefore suitable as a positive control to evaluate peroxisome-related gene expression and protein content in other organs. By comparing the TPM values in the UniGene library, we were able to compare the expression levels of all the genes listed in Fig. 4 in the mouse liver and heart. We found that the TPM values for *Acox1*, *Acox2*, *Cat*, *Pparα* and *Pparγ* were higher in the liver than the heart, whereas the opposite profile was observed for *Acox3*, *Pex13*, *thiolase*, *Gnpat* and *Pparβ*. This suggests there are differences in the metabolic activities of heart and liver peroxisomes.

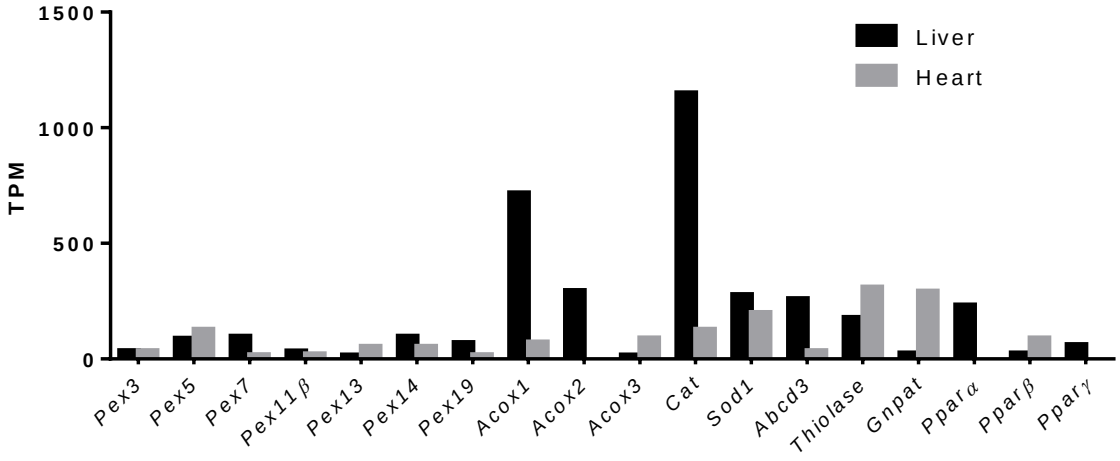

Fig. 4. Transcript per million (TPM) values of genes encoding peroxisomal proteins in the mouse liver and heart. The TPM values were acquired from the UniGene database. Gene abbreviations: *Pex*: peroxin; *Acox*: peroxisomal acyl-coenzyme A oxidase; *Cat*: catalase; *Sod*: superoxide dismutase; *Abcd*: ATP binding cassette subfamily D; *thiolase*: 3-ketoacyl-CoA-thiolase; *Gnpat*: glyceronephosphate O-acyltransferase; *PPAR*: peroxisome proliferator-activated receptor.

4.1.2. Genes encoding peroxisomal proteins are differentially expressed at the mRNA level in mouse ventricles and atria

The data mining revealed that many peroxisome-related genes are expressed in the heart and that cardiomyocyte peroxisomes possess a specialized proteome that differs metabolically from liver peroxisomes. We therefore compared the expression of peroxisomal genes in different parts of the heart.

The mRNA expression levels were determined by semi-quantitative RT-PCR in the left and right atria and ventricles of 10-week-old C57BL/J mice (Fig. 5). First, we determined the expression of three housekeeping genes (*Gapdh*, *28S rRNA* and *β-actin*) in the four compartments to ensure a stable reference gene was available. *Gapdh* and *28S rRNA* were more stably expressed in the different compartments than *β-actin* (Figure 5D) and we therefore retained *Gapdh* and *28S rRNA* as housekeeping genes for PCR normalization. The semi-quantitative RT-PCR data revealed that most of the important genes encoding peroxisomal biogenesis proteins, membrane transporters and β-oxidation enzymes are expressed in the mouse heart, confirming the *in silico* findings. Interestingly, *Pex5* and *Pex6* were uniformly expressed in different compartments whereas *Pex7* and *Pex13* were expressed at higher levels in the

ventricles than the atria. The *Acox1*, *Acox3*, *Gnpat*, *Aldp*/*Abcd1* and *Cat* genes showed heterogeneous expression levels among the four compartments but were generally expressed more strongly in the ventricles than the atria. *Abcd4/Pmp69, Abcd3/Pmp70, Pmp24* and *Pmp35* were uniformly expressed.

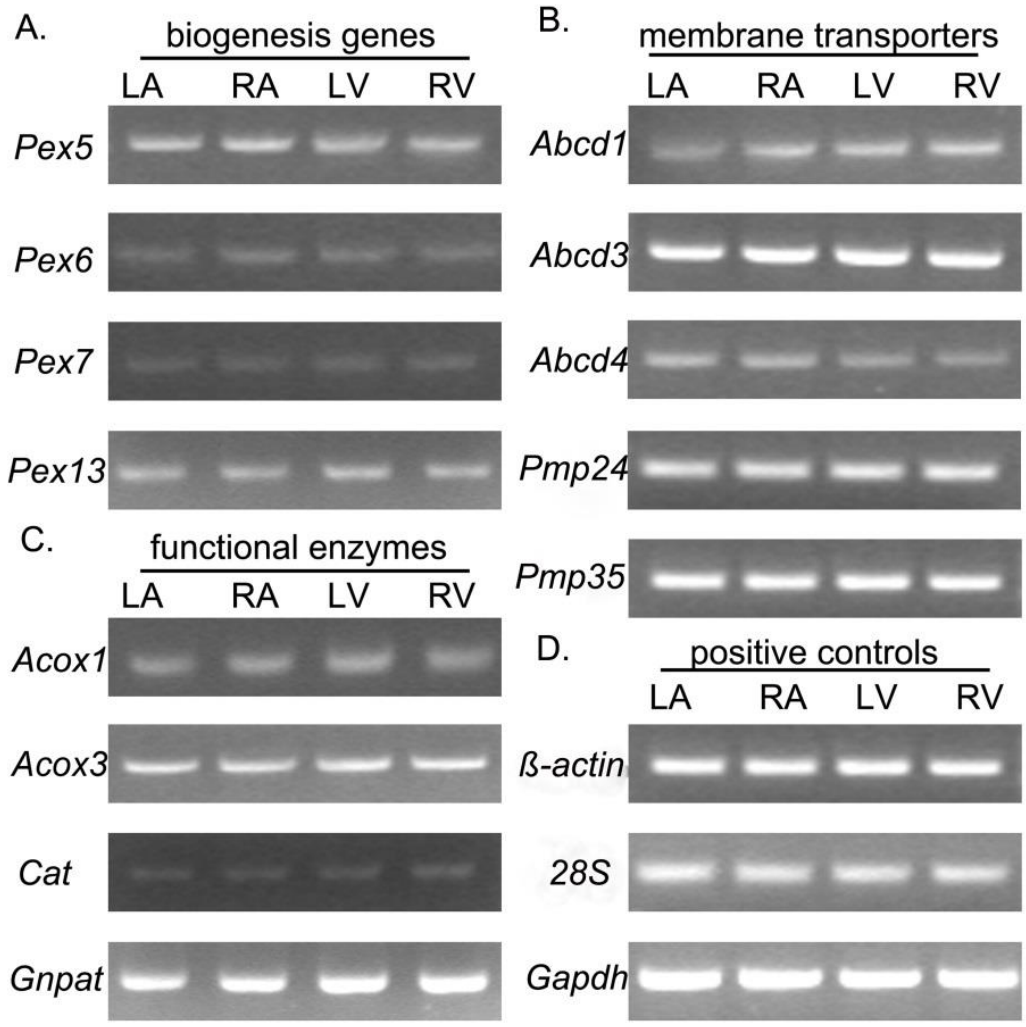

Fig. 5. Genes encoding peroxisomal proteins are differentially expressed in mouse heart tissues. Total RNA from different parts of the heart was analyzed by semi-quantitative RT-PCR to determine relative expression levels: (a) biogenesis genes, (b) peroxisomal membrane transporters (c) peroxisomal enzymes; (d) housekeeping genes (positive controls). Abbreviations: LA left atrium; RA right atrium; LV left ventricle; RV right ventricle; *Pex* peroxin; *Acox* peroxisomal acyl-coenzyme A oxidase; *Cat* catalase; *Abcd* ATP binding cassette subfamily D; *Gnpat*: glyceronephosphate O-acyltransferase; *Pmp*: peroxisomal membrane protein; *28S* 28S rRNA.

[Some of these data have been published as Figure 3 in Colasante, Chen, Ahlemeyer and Baumgart-Vogt, 2015]

The semi-quantitative PCR results indicated that most of the genes encoding peroxisomal proteins are differentially expressed among the compartments of the mouse heart. We therefore carried out qRT-PCR experiments to confirm these findings and generate quantitative expression profiles (Fig. 6). We found that *Cat*, *Pex11* (*Pex11α, Pex11β* and *Pex11γ*), *Pex14*, *Sod1*, *Acox1*, *Pparα* and *Pparγ* were expressed at significantly higher levels in the left ventricle than in other parts of the heart, whereas *Pparβ* and the *Abcd1* were most strongly expressed in the left atrium.

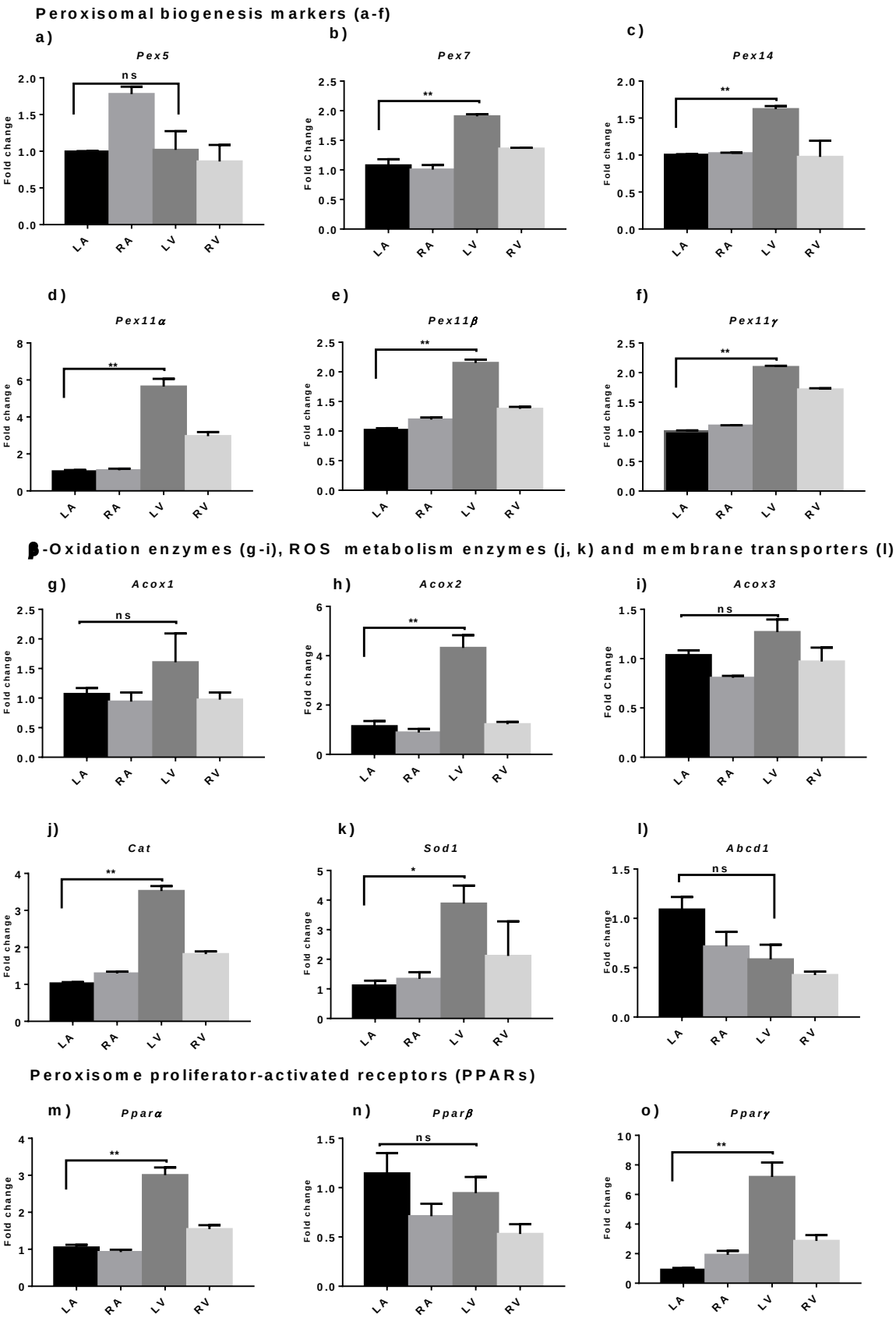
Peroxisomal biogenesis markers (a-f)
a)
Pex5
ns
b)
Pex7
**
c)
Pex14
**
d)
Pex11α
**
e)
Pex11β
**
f)
Pex11γ
**
β-Oxidation enzymes (g-i), ROS metabolism enzymes (j, k) and membrane transporters (l)
g)
Acox1
ns
h)
Acox2
**
i)
Acox3
ns
j)
Cat
**
k)
Sod1
*
l)
Abcd1
ns
Peroxisome proliferator-activated receptors (PPARs)
m)
Pparα
**
n)
Pparβ
ns
o)
Pparγ
**
Fold change
Fold Change
LA
RA
LV
RV

Fig. 6. Quantitative real-time PCR analysis showing that some peroxisome-related genes are differentially expressed in mouse heart tissues. Total RNA from different heart compartments was analyzed to profile the expression of genes encoding peroxisomal biogenesis proteins, metabolic enzymes, membrane transporters and PPARs, with *28S rRNA* as an internal standard to normalize the amount of mRNA. The columns show the mean ± SD for three experiments in each group, the mRNA expression of the left atrium (LA) was set to 1. Student's t test was used to compare the LA value with each of the other compartments. **[Some of these data have been published as Figure 3 in Colasante, Chen, Ahlemeyer and Baumgart-Vogt, 2015]**

4.1.3. The abundance of peroxisomal marker proteins differs among the four heart compartments

The mRNA values reported above revealed the differential expression of genes encoding peroxisomal proteins among the four heart compartments, but differences at the mRNA level are not always translatable to changes in protein abundance. In order to determine the abundance of peroxisomal proteins directly, western blot analysis was carried out using specific antibodies against catalase, PEX13p and PEX14p. The results confirmed that catalase, PEX13p and PEX14p were indeed more abundant in the ventricles than in the atria (Fig. 7).

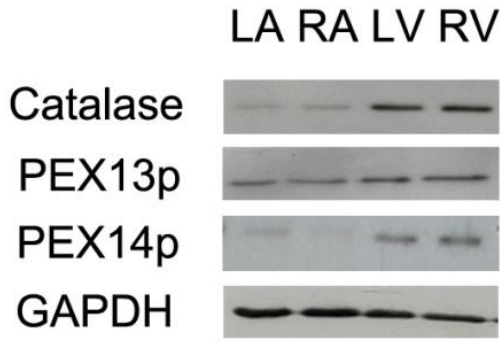

Fig. 7. Catalase, PEX13p and PEX14p are more abundant in the ventricles than the atria. Comparative western blots of different heart compartments revealed differences in the levels of CAT, PEX13p and PEX14p. LA: left atrium, RA: right atrium, LV: left ventricle, RV: right ventricle **[Published as Figure 3 in Colasante, Chen, Ahlemeyer and Baumgart-Vogt, 2015]**

Immunofluorescence analysis of formalin-fixed paraffin-embedded (FFPE) mouse heart tissue sections using antibodies against CAT, PEX14p and ABCD3 indicated that the abundance of these three proteins was higher in the ventricles than the atria (Fig. 8). This experiment also showed that the ventricles contain significantly higher numbers of peroxisomes.

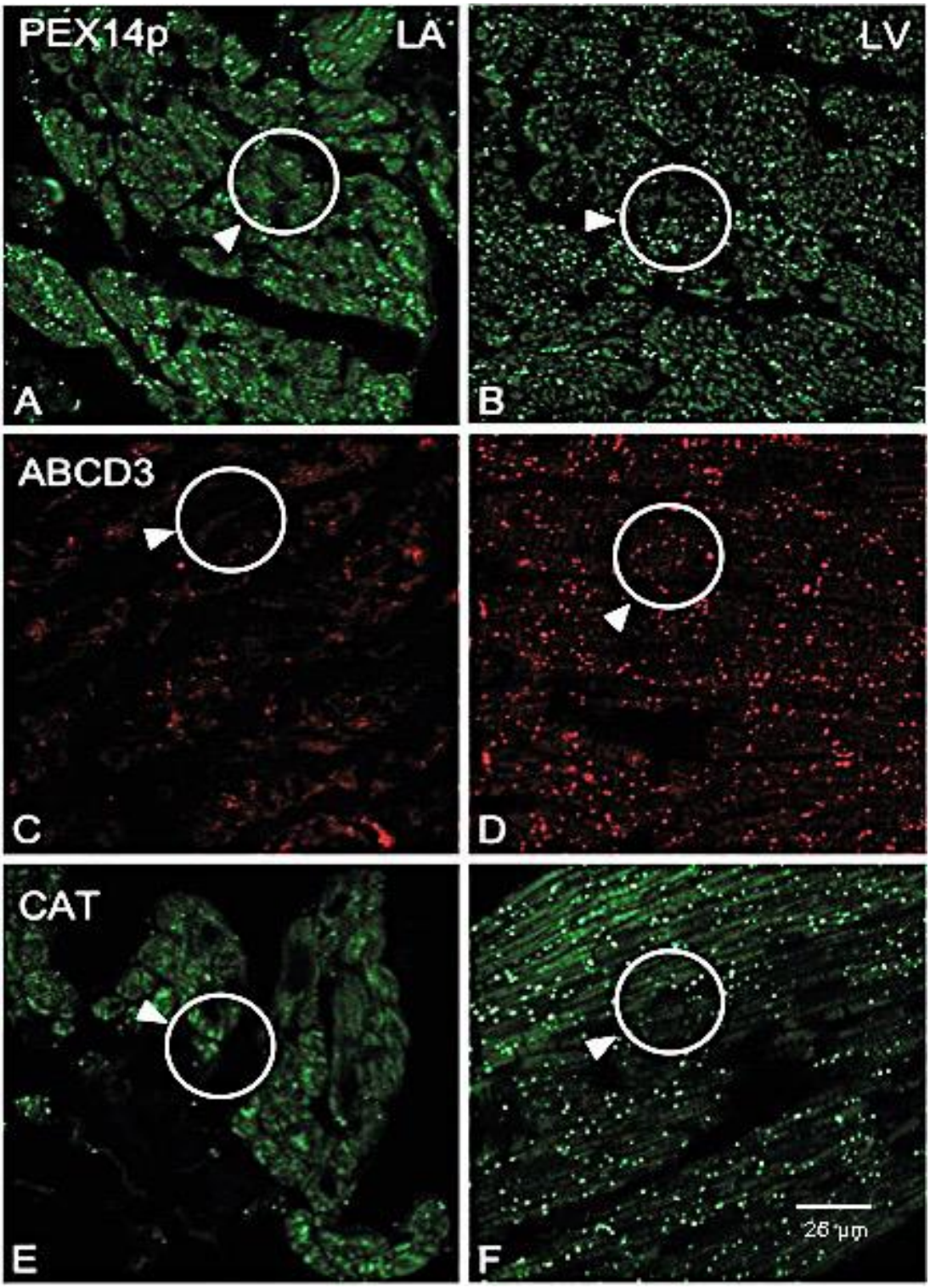

Fig. 8. Differences in the abundance of PEX14p, ABCD3 and CAT between the left ventricle and left atrium of the mouse heart. Immunofluorescence analysis of PEX14p, ABCD3 and CAT protein expression in the left atrium (LA) and left ventricle (LV) was carried out after fixing mouse hearts in 4% PFA. Scale bar: 25 µm. Primary antibody dilutions: PEX14p (1:4000), ABCD3 (1:1000), CAT (1:2000). **[Published as Figure 3 in Colasante, Chen, Ahlemeyer and Baumgart-Vogt, 2015]**

4.2. Developmental profile of peroxisome gene and protein expression

There is limited information available about the dynamic behavior of peroxisome genes and proteins during mouse development, but our initial data mining (Section 4.1) provided evidence that peroxisomal gene expression changes during heart development in the mouse. A better understanding of such developmental changes could provide new insight to the role of peroxisomes in heart protection. We therefore analyzed the developmental profiles of genes encoding peroxisomal proteins and the proteins themselves in newborn and adult mice.

First, we compared the hearts of 2-day-old and 8-week-old mice by semi-quantitative RT-PCR, revealing that *Pmp2* and *Pex6* are expressed at higher levels in the adult than in newborn animals, whereas the other genes are expressed at the same level regardless of age (Fig. 9).

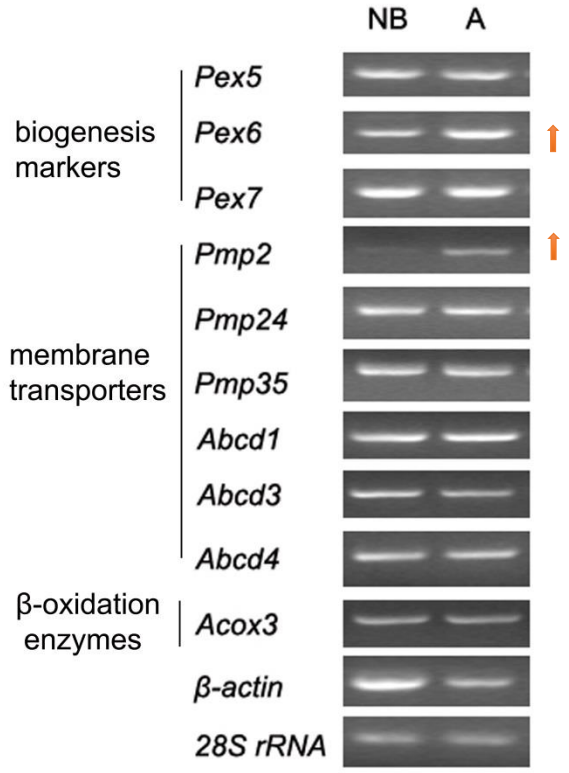

Fig. 9. Semi-quantitative RT-PCR analysis of peroxisome-related and housekeeping gene expression in newborn (NB) and adult (A) mouse hearts. We analyzed the expression of peroxisomal biogenesis markers (*Pex5*, *Pex6* and *Pex7*) and genes encoding membrane transporters (*Pmp2*, *Pmp24, Pmp35, Abcd1, Abcd3* and *Abcd4*) and enzymes (*Acox1*). The housekeeping gene *β-actin* was not suitable as a loading control, so *28S rRNA* was used instead.

Next, we carried out qRT-PCR to determine the quantitative gene expression profiles of six peroxisomal genes. The expression levels of *α-Mhc* and *β-Mhc*, encoding the ventricular α-myosin and β-myosin heavy chains, are regulated by hormones and show opposing developmental profiles (Lompre et al., 1984). Accordingly, these genes are often used as markers for heart maturity, disease and stress, and we therefore used them as positive controls. As anticipated, the *α-Mhc* mRNA level was 2.2-fold higher

in the adult heart compared to the newborn heart, whereas *β-Mhc* mRNA levels were significantly higher in the newborn heart than the adult heart (Fig. 10A,B). Interestingly, *Cat*, *Pex11α* and *Acox1* were expressed at much higher levels in the adult heart than the newborn heart, whereas *Sod1* showed the opposite profile, and *Abcd3* and *Pex14* showed no significant differences regardless of age (Fig. 10C-H). This indicates that the genes encoding peroxisomal proteins are regulated individually and not in concert as the heart ages.

Cardiac markers (A and B)

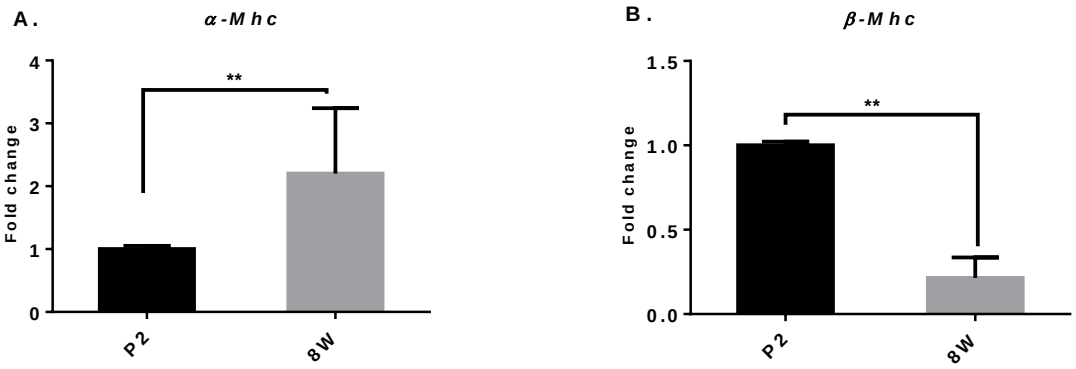

Peroxisomal biogenesis genes (C and D)

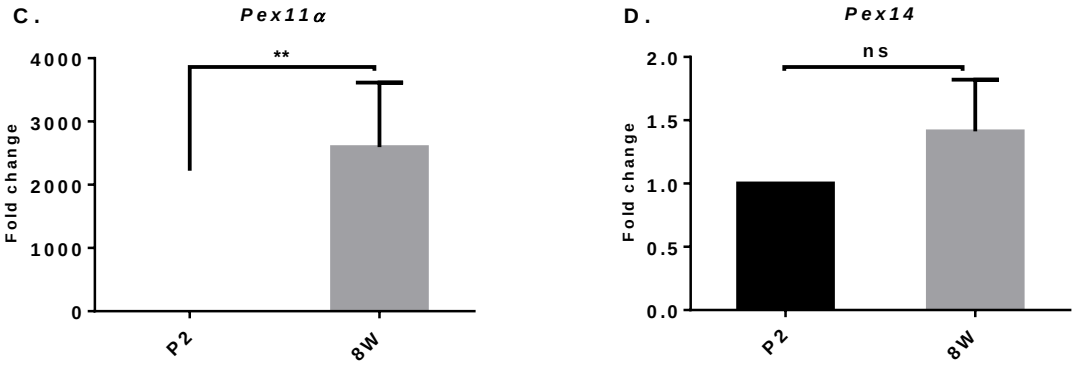

ROS metabolism (E and F)

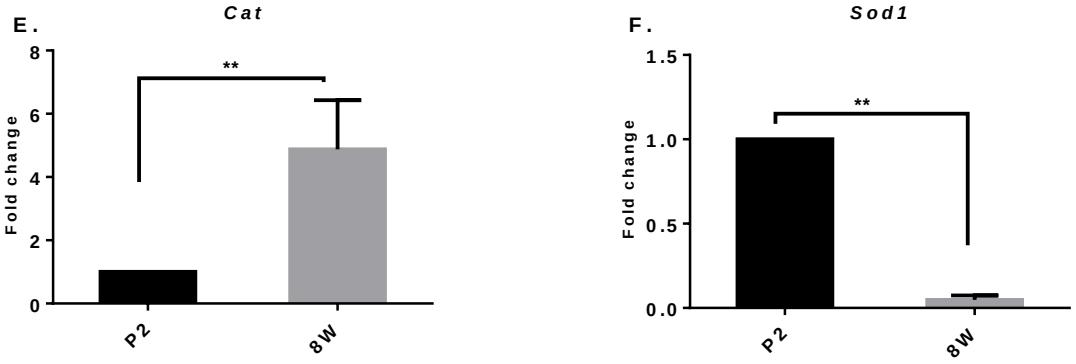

β-Oxidation enzyme (G) and peroxisomal membrane transporter (H)

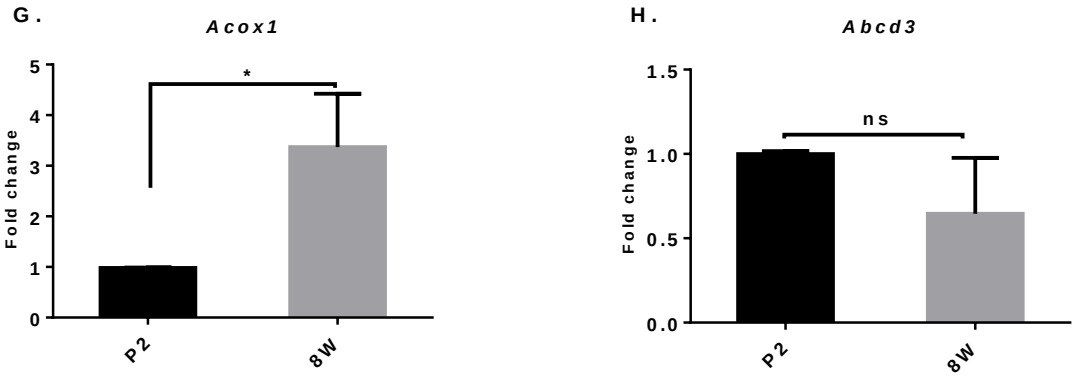

Fig. 10. Analysis of *α-Mhc, β-Mhc, Cat*, *Pex14*, *Pex11α, Abcd3* and *Acox1* expression in the newborn and adult heart by qRT-PCR. Total RNA was isolated from 2-day-old (P2) and 8-week-old (8W) mouse hearts, and *28S rRNA* was used as an internal standard. The columns represent the mean ± SE of four experiments in each group. The expression level at P2 was set to 1, and Student's t-test for unpaired values was used to compare the relative levels in the adult and newborn hearts.

Next, the abundance of selected peroxisomal proteins was analyzed by western blot, revealing differences between the newborn and adult mouse in the abundance of catalase and PEX14p (Fig. 11). Catalase was much more abundant in the adult heart, whereas PEX14p was more abundant in the newborn heart.

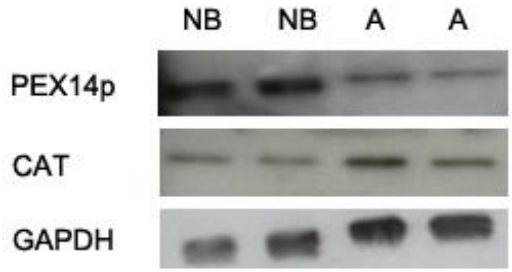

Fig. 11. Abundance of the peroxisome biogenesis protein PEX14p and the enzyme catalase as the heart ages. Western blot analysis of PEX14p and catalase in newborn (NB) and adult (A) whole heart homogenates, based on 15 µg total protein loaded in each lane. The membrane was probed using anti-PEX14p, anti-Cat and anti-GAPDH antibodies.

4.3. *Pex11α* and *Pex14* expression in ischemia-reperfusion hearts

It is unclear whether peroxisomes, and in particular the peroxisome-related genes and proteins discussed above, play a role in the hypoxia injury induced by heart attack. We therefore investigated the expression of these genes and proteins in the ischemia-reperfusion rat model, a powerful tool for the study of heart function at the molecular level and an enduring model for ischemia-reperfusion injury.

The following experiments were carried out in collaboration with Professor Böning (Department of Cardiovascular Surgery, University Hospital Giessen and Marburg, Campus Giessen, Giessen, Germany), who kindly provided the rat samples. The rat heart ischemia-reperfusion model used in this study involved two steps: (1) ischemia for 90 min induced by aortic clamping, and (2) subsequent reperfusion for 90 min. The heart was exposed to intervention for less than 4 h before storage at –80°C.

Quantitative real-time PCR was carried out using cDNA isolated from the ischemia-reperfusion heart and an untreated control to determine the expression mRNAs for the 2 peroxin proteins of PEX11α and PEX14, thus providing evidence for the effect of ischemia-reperfusion injury on peroxisome biogenesis. Interestingly, *Pex11α* expression was significantly downregulated in the ischemia-reperfusion heart compared to the control group, whereas there was no difference in *Pex14* expression (Fig. 12).

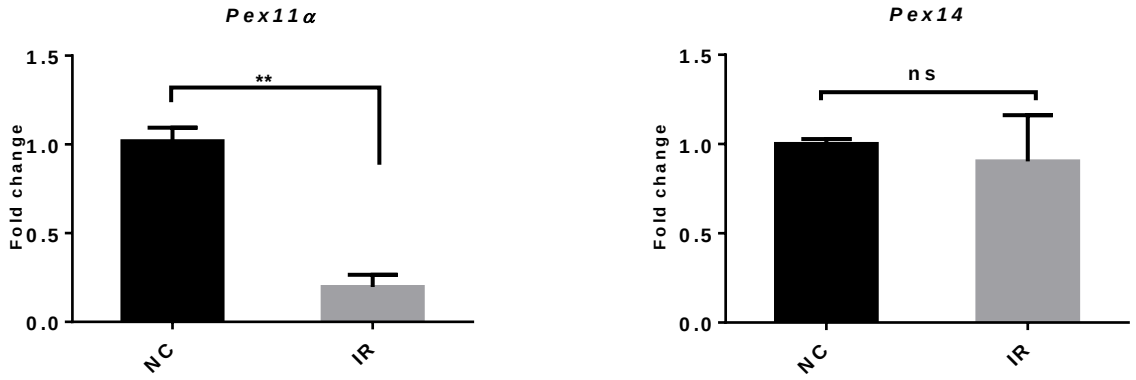

Fig. 12. *Pex11α* and *Pex14* expression in ischemia-reperfusion (IR) hearts and normal control (NC) hearts. Left ventricular tissue was kindly provided by Prof. Böning. Total RNA was isolated and 2 µg was used to prepare cDNA for qRT-PCR analysis of *Pex11α* and *Pex14* expression, with *28S rRNA* as an internal standard to normalize the amount of mRNA. The columns represent the mean ± SE for three experiments in each group. The expression level in the control hearts was set to 1, and Student's t-test for unpaired values was used to determine the relative expression levels in the ischemia-reperfusion hearts.

To confirm the relevance of the gene expression levels, we measured the abundance of PEX14p in the same experimental model. Antibodies that differentiate between the three isoforms of PEX11 are not yet available, so we were unable to confirm the qRT-PCR results for *Pex11α* at the protein level. Interestingly, the western blot data for PEX14p contradicted the qRT-PCR results and revealed that the protein was more abundant in the left ventricle of the ischemia-reperfusion hearts than the controls, whereas PEX3p was more abundant in the control hearts than the ischemia-reperfusion model (Fig. 13). ABCD3 and catalase showed no significant difference in abundance between the two groups (Fig. 13).

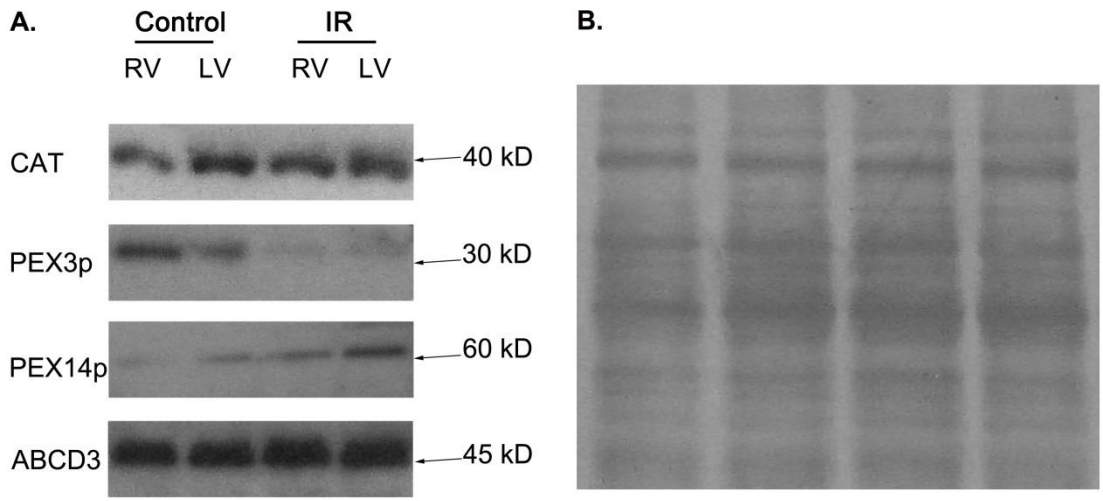

Fig. 13. Abundance of peroxisome-related proteins in ischemia-reperfusion (IR) rat hearts and normal controls. A. Total protein homogenates were prepared from the left and right ventricular heart tissue of control rats and an ischemia-reperfusion group. Anti-CAT, anti-PEX13p, anti-PEX14p and anti-ABCD3 antibodies were used to detect the proteins by western blotting. B. Coomassie Brilliant Blue staining was used to ensure equal gel loading.

4.4. Peroxisomal characteristics in the hearts of *Pex11α* knockout mice

The strong downregulation of *Pex11α* gene expression in the ischemia-reperfusion model indicated that ischemia-reperfusion injury may affect peroxisome biogenesis and fission by reducing the levels of PEX11α. We therefore tested the *Pex11α* general knockout mouse model (X. Li, Baumgart, et al., 2002) to investigate whether the loss of this protein influences the functionality of the heart. The development and partial characterization of the *Pex11α* knockout mouse has been described (Li et al., 2002).

4.4.1. The phenotype of the *Pex11α* knockout mouse line

As previously reported, the *Pex11α* knockout mouse line showed no major observable differences in phenotype compared to wild-type mice (Li et al., 2002).

4.4.2. Body and heart weight of the *Pex11α* knockout mice

We measured the total body weight and heart weight of age-matched (8–10 weeks) *Pex11α* knockout and wild-type mice, revealing no differences in either parameter (Fig. 14). This suggested the absence of a macroscopic phenotype in the hearts of the *Pex11α* knockout mice.

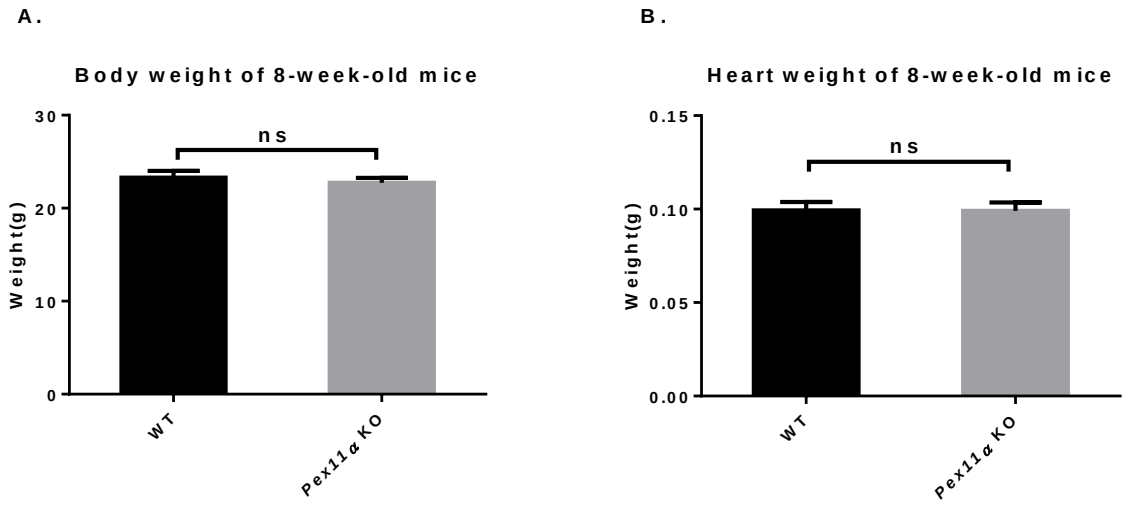

Fig. 14. Total body weight and heart weight of the *Pex11α* knockout mice and wild-type mice. The body weight **(A)** and heart weight **(B)** of *Pex11α* knockout mice and wild-type mice were recorded at the same age (8 weeks). The columns represent the mean ± SE for five mice in each experimental group. Student's t-test for unpaired values was used to compare the values from each group.

4.4.3. H&E staining of wild-type and *Pex11α* knockout mouse heart tissue

To determine whether the absence of the *Pex11α* gene affected the ultrastructure of the cardiomyocytes, paraffin-embedded sections of wild-type and *Pex11α* knockout hearts were compared by histological staining with H&E. There were no obvious differences in cellular morphology or structure between the two groups (Fig. 15).

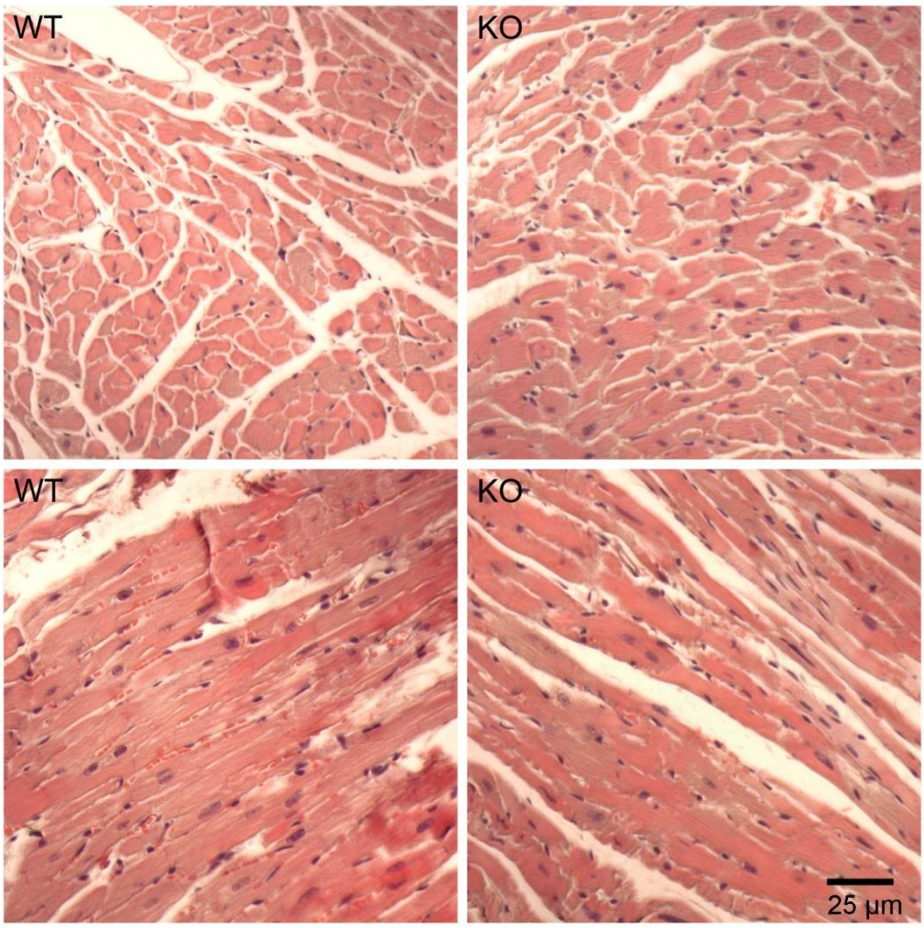

Fig. 15. Morphological comparison of wild-type (WT) and *Pex11α* knockout (KO) mouse heart tissues. H&E staining of PFPE heart tissue revealed no differences in histology. Images were captured using a Leica DMRD fluorescence microscope equipped with a Leica DC 480 camera. Scale bar: 25 µm.

4.4.4. Abolishing *Pex11α* expression induces genes encoding peroxisome-related proteins and PPARs in the mouse heart

To investigate whether the *Pex11α* knockout induced changes in peroxisome-related gene expression, qRT-PCR was used to compare the hearts from wild-type and *Pex11α* knockout mice. This experiment confirmed the absence of *Pex11α* mRNA in the knockout mice (Fig. 16A). Interestingly, whereas *Pex11γ* was expressed at the same level in both lines, *Pex11β* was significantly induced in the *Pex11α* knockout mice. *Pex7* and *Acox1* were also induced in the *Pex11α* knockout line, whereas *Pex5*, *Cat*, *Acox2* and *Acox3* showed no significant differences. Furthermore, the loss of *Pex11α* also resulted in a slight but non-significant increase in *Pparβ* expression (1.6-fold, $P>0.05$) and a significant increase in *Pparγ* expression (2.9-fold, $P< 0.01$), suggesting a peroxisome-based PPAR-feedback loop (Fig. 16J-L).

Peroxisomal biogenesis genes of the *Pex11α* family

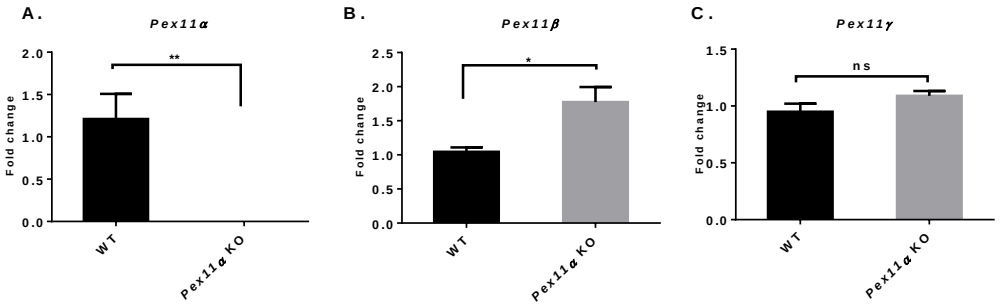

Peroxisomal biogenesis genes for PTS1 (*Pex5*) and PTS2 (*Pex7*) receptors (D and E) and ROS metabolism enzyme catalase (F)

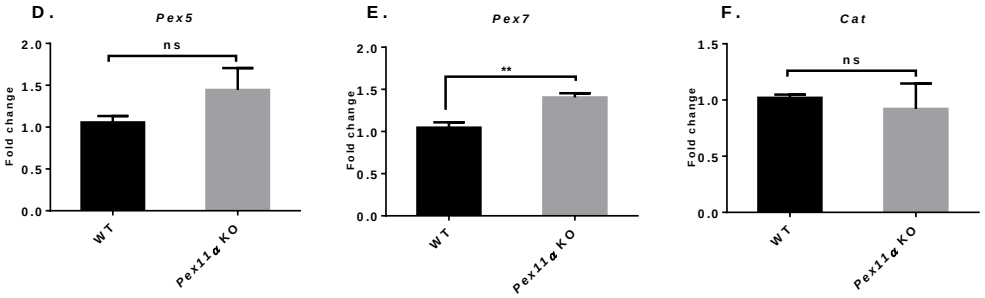

Fatty acid β-oxidation emzymes (G-I)

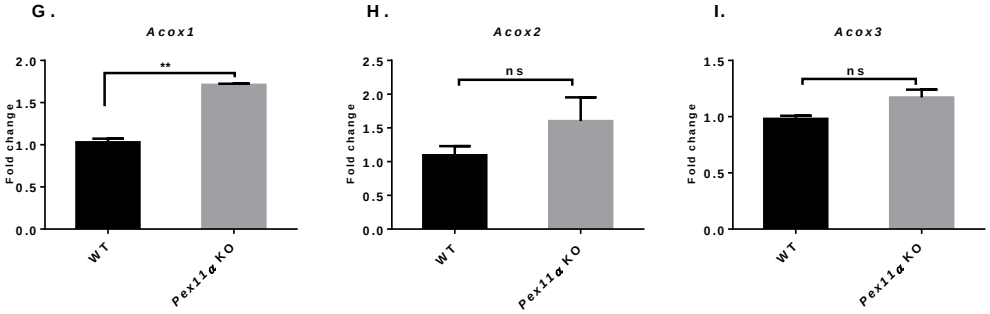

Peroxisome proliferator-activated receptors (J-L)

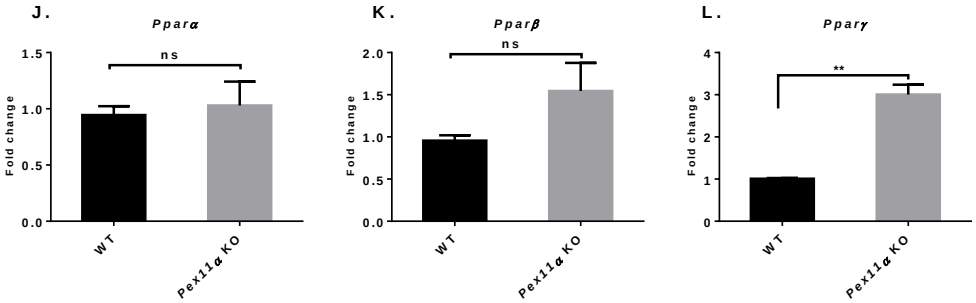

Fig. 16. The knockout of *Pex11α* increases the expression of certain peroxisome-related genes and PPARs in the mouse heart. Total RNA was isolated from the left ventricle of wild-type (WT) and *Pex11α* knockout (KO) mice for the analysis of peroxisome- related and PPAR genes. The columns represent the mean ± SE of three mice in each experimental group. Student's t-test for unpaired values was used to compare the *Pex11α* knockout mice with the corresponding wild-type group.

4.4.5. *Pex11α* knockout animals display abnormal peroxisome morphology

Immunofluorescence staining of mouse hearts showed that the morphology of the peroxisomes in the *Pex11α* knockout line is abnormal. Both the size and the number of peroxisomes increased in the knockout mice compared to wild-type controls. The peroxisomes in the *Pex11α* knockout hearts were much bigger, irregular in shape, and some adopted an unusual ring-like structure (Fig. 17).

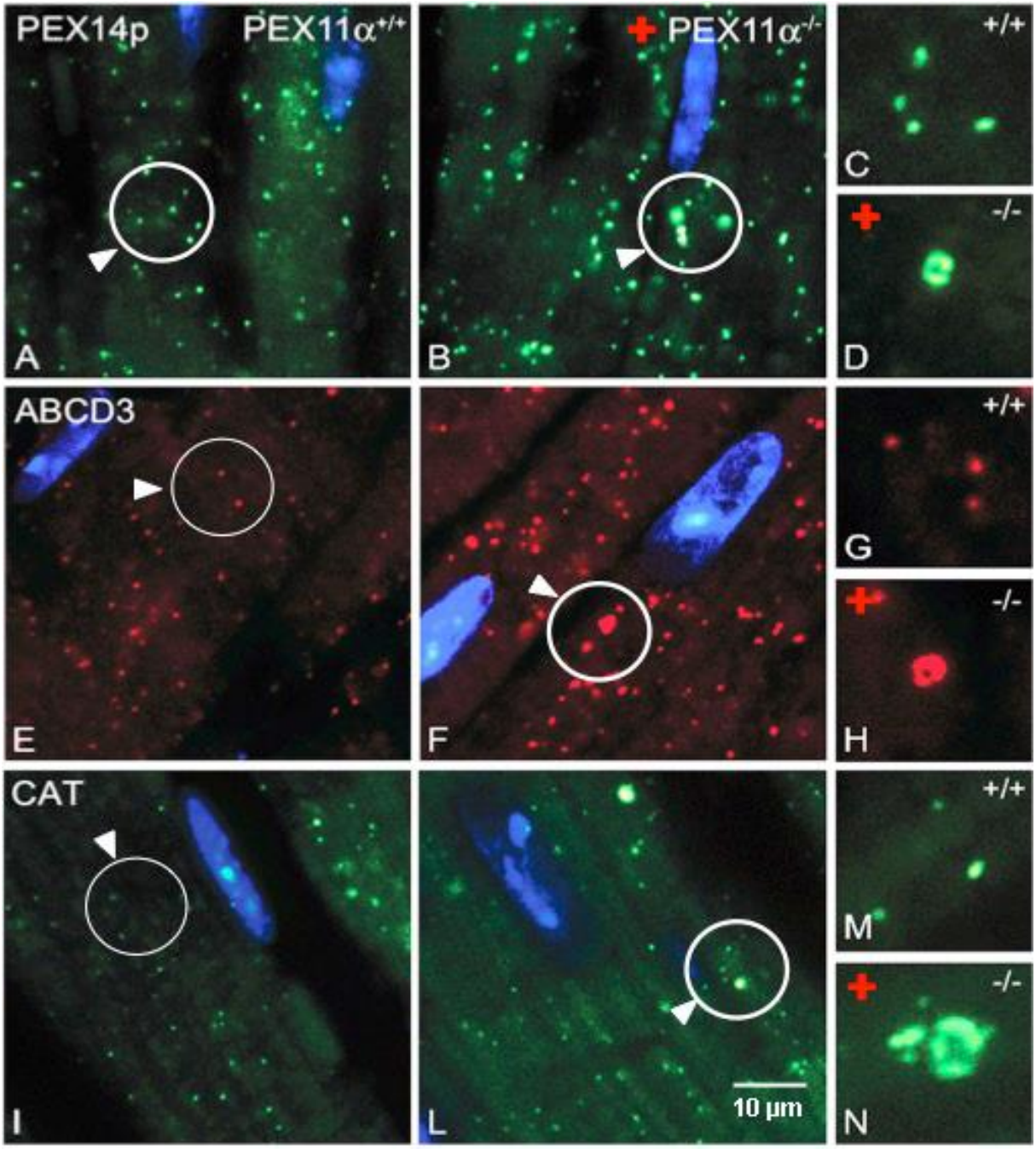

Fig. 17. Immunofluorescence staining of wild-type and *Pex11α* knockout mouse hearts using antibodies against PEX14p, ABCD3 and CAT. Mouse heart tissue was fixed in 4% PFA and embedded in paraffin before 2-µm sections were prepared for immunofluorescence staining. The primary antibodies were diluted as follows: PEX14p (1:4000), ABCD3 (1:1000), CAT (1:2000). **[Published as Fig. 4 in Colasante, Chen, Ahlemeyer and Baumgart-Vogt, 2015]**

4.4.6. Effect of *Pex11α* knockout on the abundance of peroxisomal proteins

Next we determined the abundance of selected peroxisomal proteins by western blot in the *Pex11α* knockout and wild-type lines, revealing the presence of higher levels of catalase and PEX14p in the hearts of *Pex11α* knockout mice (Fig. 18).

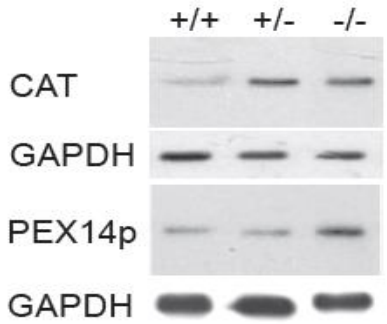

Fig. 18. Abundance of catalase and PEX14p in *Pex11α* knockout and wild-type mouse hearts. Western blot analysis was used to compare the abundance of peroxisomal proteins in the homogenates of hearts from wild-type, homozygous *Pex11α* knockout and heterozygous mice. **[Published as Fig. 4 in Colasante, Chen, Ahlemeyer and Baumgart-Vogt, 2015]**

4.4.7. Catalase activity in the *Pex11α* knockout heart homogenates

We observed no difference in *Cat* expression between the hearts of *Pex11α* knockout and wild-type mice, but the protein was more abundant in the knockout line. We therefore carried out a catalase assay to confirm that the protein abundance corresponded to higher enzymatic activity in the *Pex11α* knockout mouse. Due to the limited number of animals, it was not possible to carry out statistical analysis of the results. However, we observed a clear increase in catalase activity in the knockout line (Fig. 19).

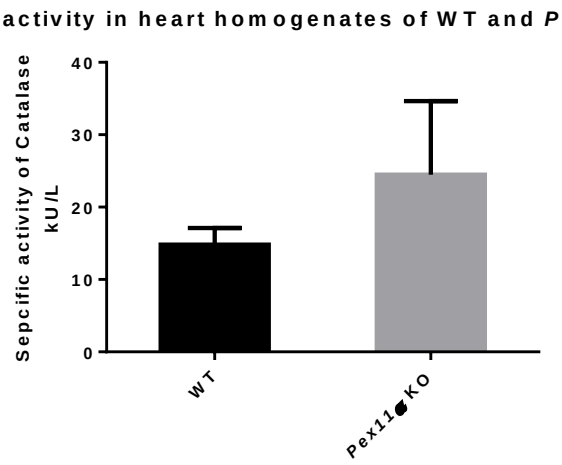

Fig. 19. The specific activity of catalase in the hearts of *Pex11α* knockout and wild-type mice. Left ventricular tissue homogenates from three wild-type (WT) mice and three *Pex11α* knockout (KO) mice were used to measure catalase activity (kU/L). Four of the six mice in these experiments were 8-week-old male mice and the other two were 11-week-old female mice. The results therefore cannot be analyzed statistically and are shown in descriptive form only.

4.4.8. Cardiac-specific genes are modulated in the *Pex11α* knockout line

Quantitative RT-PCR revealed the disrupted expression of many typical cardiac marker genes. For example, *α-Mhc* (predominant in the normal adult heart) and *β-Mhc* (predominant in the neonatal heart) were both expressed at much lower levels in the *Pex11α* knockout line. Furthermore, *Nppc* (encoding CNP) was downregulated in the *Pex11α* knockout line but *Nppb* (encoding BNP) was upregulated and *Nppa* (encoding ANP) was unaffected. The endoplasmic reticulum markers *PDI* and *Calreticulin* showed no differences in expression in the hearts of the wild-type and knockout mice, and similar results were observed for the extracellular matrix and pro-fibrotic markers *Col1a* and *Col3a* (Fig. 20).

Cardiac specific markers (A-E)

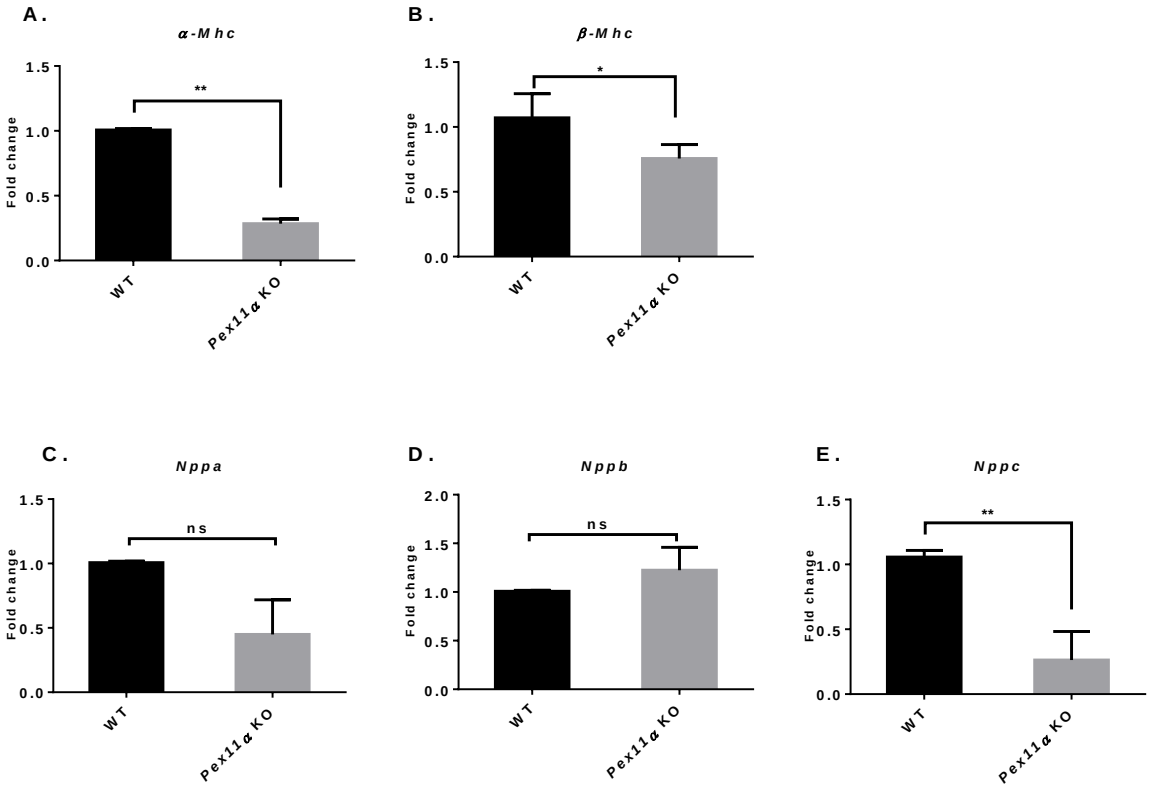

Endoplasmic reticulum markers (F and G)

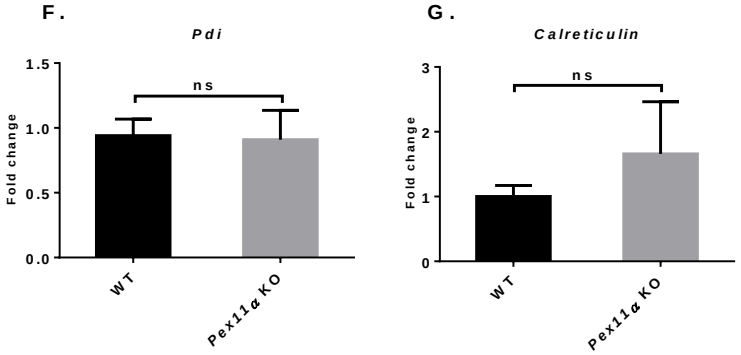

Extracellular matrix markers (H and I)

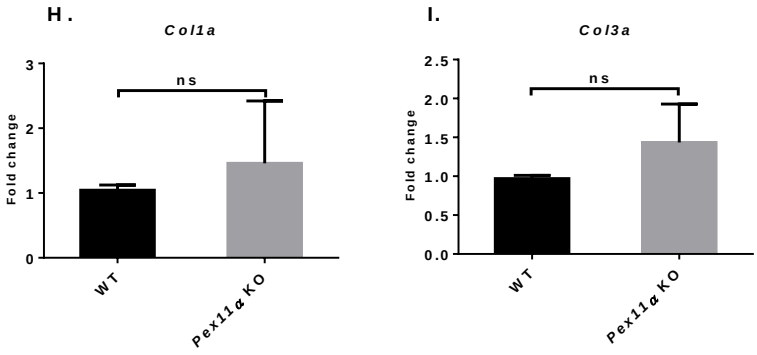

Fig. 20. Modulation of cardiac-specific genes in the hearts of *Pex11α* knockout mice. Total RNA was isolated from the hearts of wild-type (WT) and *Pex11α* knockout (KO) mice for the qRT-PCR analysis of cardiac-specific genes, using *28S rRNA* as an internal control. The columns represent the mean ± SE for three mice in each experimental group. Student's t-test for unpaired values was used to compare the *Pex11α* mice with the corresponding wild-type control group.

4.4.9. Mitochondria are affected by oxidative stress in the *Pex11α* knockout line

The loss of peroxisomal biogenesis proteins induces severe oxidative stress in many cell types due to the primary loss of peroxisomal function and the secondary effect on mitochondria (Baumgart et al., 2001). SOD2 is often used to monitor the upregulation of antioxidant enzymes in cells with peroxisomal deficiency, so we compared the abundance of this protein in the hearts of wild-type and *Pex11α* knockout mice. We found that SOD2 was more abundant in the *Pex11α* knockout line, confirming the elevation of oxidative stress in the heart mitochondria (Fig. 21).

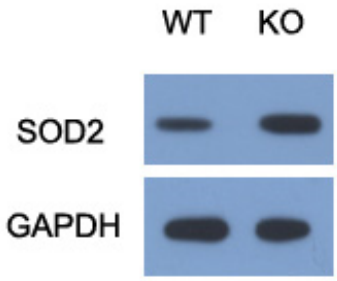

Fig. 21. SOD2 protein is more abundant in the hearts of *Pex11α* knockout mice than wild-type controls. Cleared homogenates prepared from the left ventricles of wild-type (WT) and *Pex11α* knockout (KO) mice were compared by loading 15 µg total protein in each lane and staining the gels using antibodies specific for SOD2 and thereafter GAPDH.

4.4.10. Shortening capacity of *Pex11α* knockout cardiomyocytes

The modulation of cardiac markers in the *Pex11α* knockout line suggested there may be an impact on the physiological function of isolated cardiomyocytes. We therefore measured the cell shorting capacity of isolated cardiomyocytes from each line, revealing no significant differences in cell shortening parameters. We subjected the cardiomyocytes to stress by treating them with the catalase inhibitor 3-amino-1,2,4-triazole (3-AT), which inhibited the cell shortening capabilities equally in both groups ($P < 0.01$, Fig. 22A). However, the percentage of cell shortening in the *Pex11α*

knockout cardiomyocytes after 3-AT treatment was significantly larger than that of the wild-type cardiomyocytes (Fig. 22B-D).

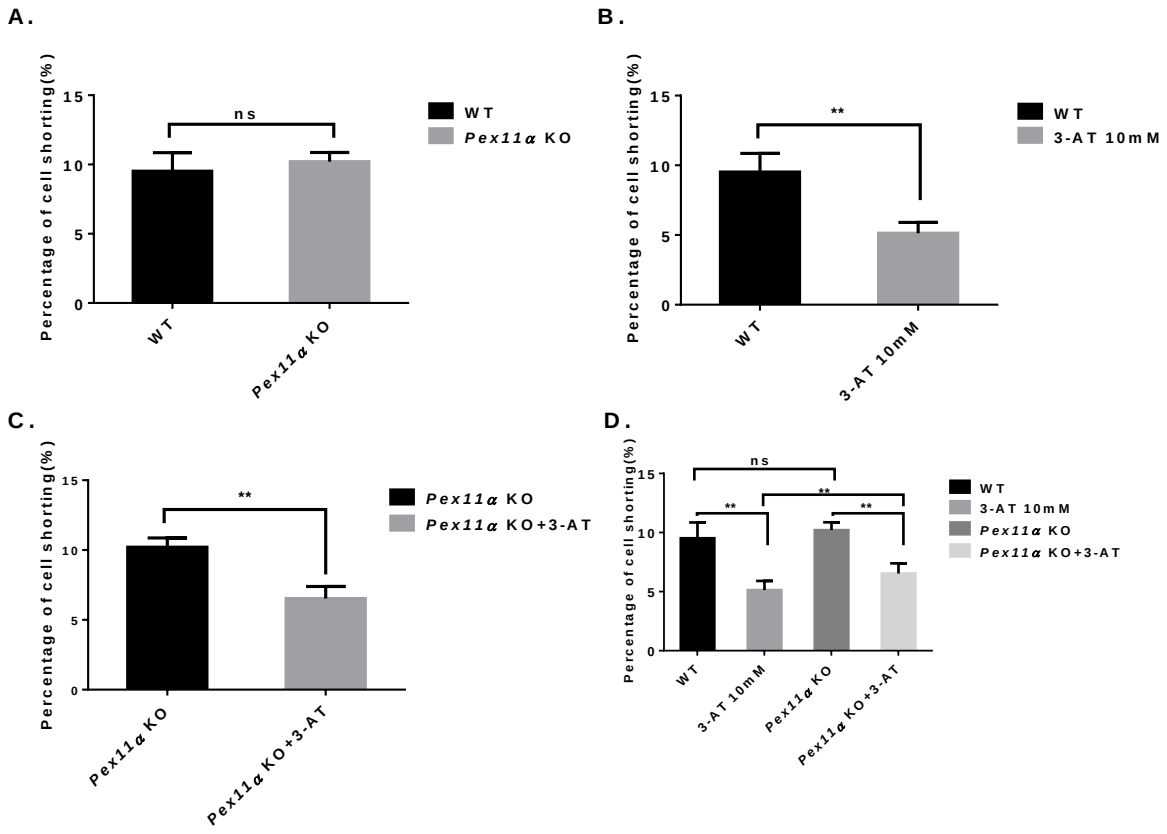

Fig. 22. The cell shortening performance of wild-type and *Pex11α* knockout mouse cardiomyocytes. Primary cardiomyocytes were isolated from the ventricles of wild-type (WT) and *Pex11α* knockout (KO) mice, and cell shortening was measured. The columns represent the mean ± SE for four mice in each experimental group. Student's t-test for unpaired values was used to compare the values recorded for *Pex11α* cardiomyocytes with the corresponding wild-type control group, or the treatment group with the non-treatment group.

4.4.11. H&E staining and cardiomyocyte counting in wild-type and *Pex11α* knockout heart tissues following ischemia-reperfusion injury

The results summarized above indicated no significant difference in the morphology of wild-type and *Pex11α* knockout hearts under normal conditions. We therefore examined the same parameters following ischemia-reperfusion injury, and found that a significantly larger number of cells in the *Pex11α* knockout hearts suffered injury-induced damage compared to wild-type hearts ($P<0.01$, Fig. 23).

A.

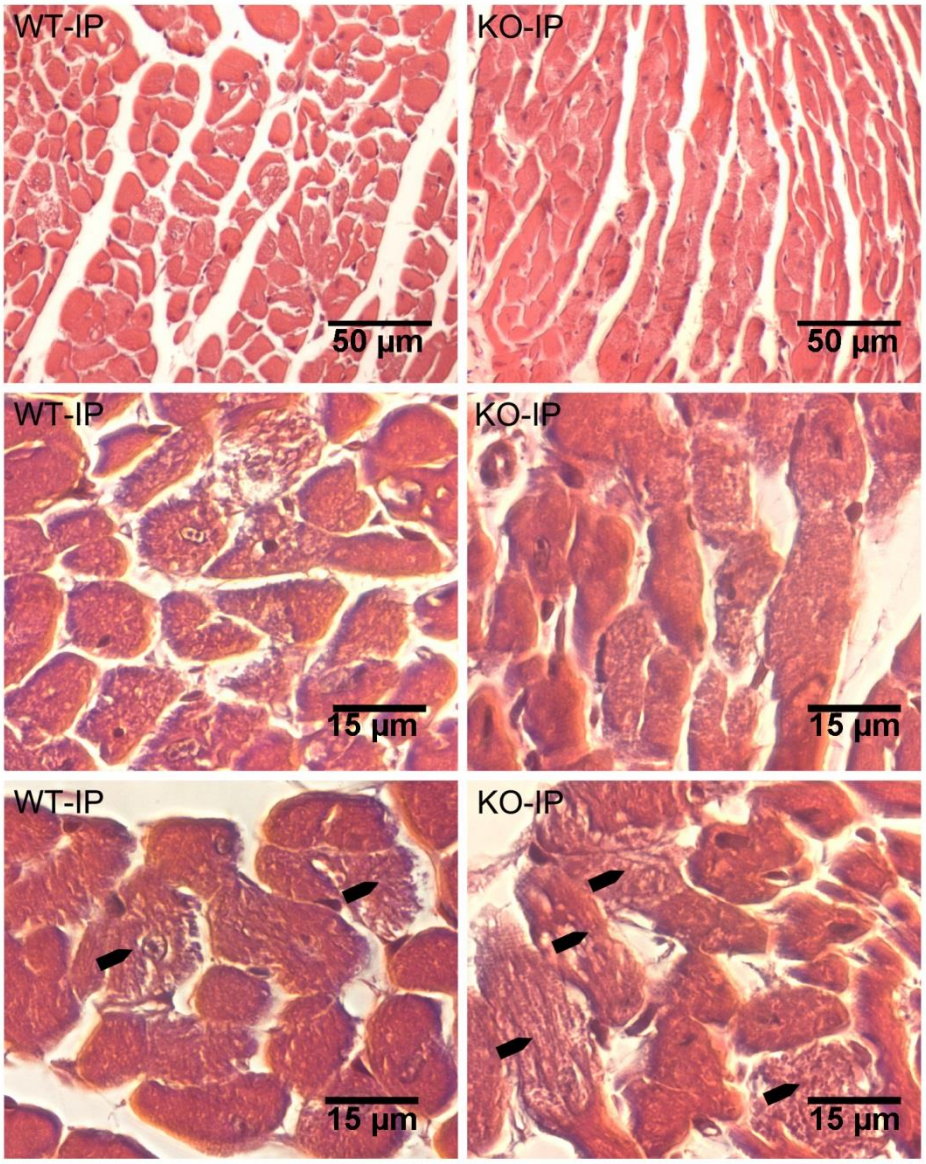
WT-IP
KO-IP
50 µm
50 µm
WT-IP
KO-IP
15 µm
15 µm
WT-IP
KO-IP
15 µm
15 µm

B.

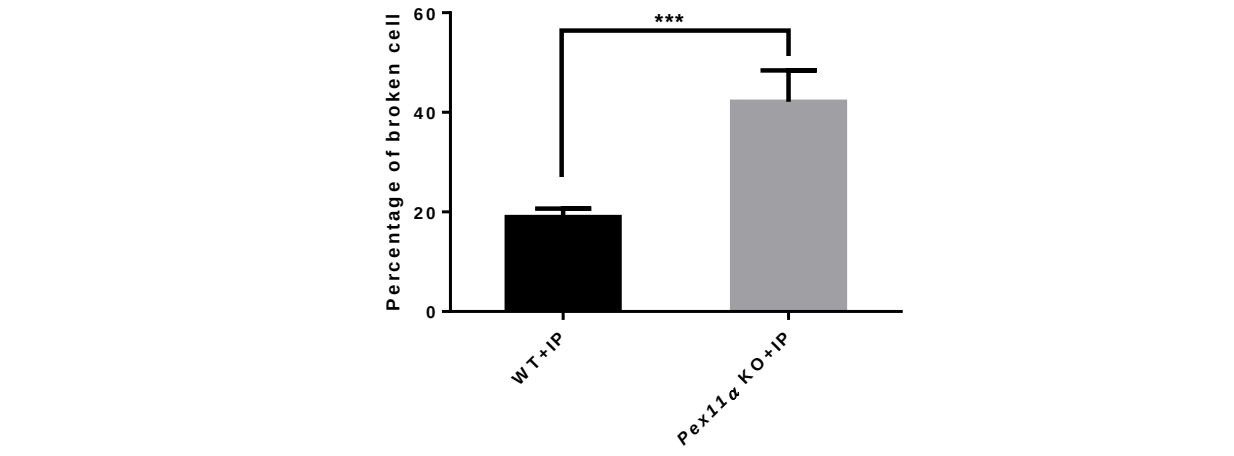
Percentage of broken cardiomyocytes after Ischemia Reperfusion in each slides
Percentage of broken cell
60
40
20
0
***
WT+IP
Pex11α KO+IP

Fig. 23. Figure legend on page 76

Fig. 23. H&E staining (A) and cell counting (B) of cardiomyocytes in the hearts of wild-type and *Pex11α* knockout mice after ischemia-reperfusion injury. Heart tissue was fixed in 4% PFA and embedded in paraffin, and 5-µm sections were stained with H&E. All cells in each slide were counted, and broken cells were noted. All together 500 hundred cells were used for each group. The columns represent the mean ± SE for four mice in each experimental group. Student's t-test for unpaired values was used to compare the values from *Pex11α* mice with the corresponding wild-type control group (Scale bar: 50 µm and 15 µm).

4.5. HL-1 cells as a model to study functional cardiac alterations induced by peroxisomal dysfunction

To reduce the number of animal experiments, the model cell line HL-1 was used to analyze the effects of peroxisomal alterations on cardiomyocyte functions and signaling pathways.

4.5.1. HL-1 cells grew best in flasks coated with 0.1% gelatin

Before commencing detailed experiments, we established the optimal growth conditions for HL-1 cells on coated coverslips. HL-1 cells grow rapidly using the precise conditions and medium described by the Claycomb group. All culture flasks must be coated before cell seeding, and we tested several different materials and coating methods. We found that cells grew better on a plastic surface than on glass coverslips, and that 0.1% gelatin and fibronectin in gelatin were both suitable for coating, with neither showing toxicity or negative effect on cellular morphology.

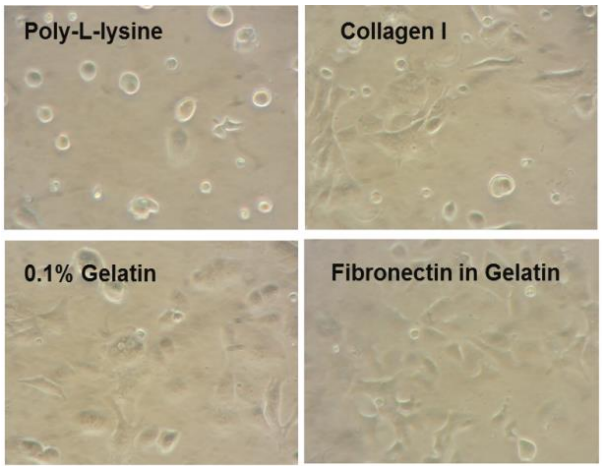

Fig. 24. Morphology of HL-1 cells growing on coated surfaces. HL-1 cells were cultured in six-well plates treated with different coating materials overnight (ploy-L-lysine, collagen I, 0.1% gelatin, and fibronectin in gelatin). Cells were observed by light microscopy 48 h after seeding.

4.5.2. Most peroxisome-related genes are expressed in HL-1 cardiomyocytes

The establishment of the HL-1 cell line was followed by many physiological and molecular studies (Nguyen et al., 1999; White et al., 2004; Wondergem et al., 2012). As a tumor cell line, it is still a matter of debate whether HL-1 cells possess the characteristics of *in vivo* atrial cardiomyocytes. Therefore, we investigated whether peroxisomal genes were expressed at sufficient levels for analysis by comparing them with the source tissue (mouse left atrium). Although we confirmed the expression of all the peroxisomal genes in HL-1 cells, the levels differed from mouse left atrium tissue. *Cat* and *Abcd1* were expressed at a lower level in the HL-1 cells than in the mouse left atrium, whereas *Sod1* and *Pex14* showed the opposite profile. The *Pex11* family was also expressed in the HL-1 cells. *Pex11α* expression was lower in the cells than in vivo, whereas *Pex11β* was expressed at similar levels in both, and *Pex11γ* was strongly elevated in the cells. Interestingly, the largest discrepancy was found in the PPAR family: *Pparα* and *Pparγ* were hardly expressed in HL-1 cells, whereas *Pparβ* was expressed at approximately the same level in the HL-1 cells and the mouse atrium tissue (Fig. 25).

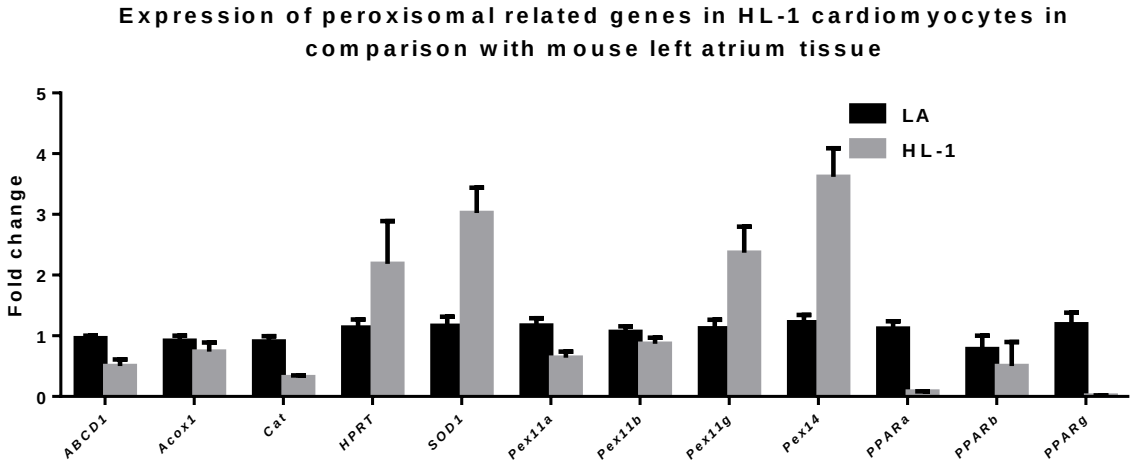

Fig. 25. Comparative expression of genes encoding peroxisomal proteins and PPARs in the HL-1 cell line and left atrium of the mouse heart. Total RNA was isolated from HL-1 cells and left atrium tissue for qRT-PCR analysis using primers for peroxisomal markers and PPARs, with *28S rRNA* as an internal control. The columns represent the mean ± SE for three mice in each experimental group. Student's t-test for unpaired values was used to compare the values for HL-1 cells with the atrial tissue.

4.5.3. Potential methods to induce catalase: ethanol treatment and catalase overexpression

Alcohol consumption is a risk factor in many heart diseases (Djoussé et al., 2008). Catalase is induced in rats fed on an ethanol-rich diet (Fahimi et al., 1979). However, the mechanism by which alcohol influences the heart remains unclear and its response is not well understood. To investigate the protective function of peroxisomes under stress conditions, we treated HL-1 cells with 0.5% ethanol for 72 h, revealing a 4.5-fold increase in *Cat* mRNA levels (see Fig. 26A) and also an increase in the abundance of catalase protein (Fig. 26B). We also observed a 2.3-fold increaser in catalase activity in the ethanol-treated group ($P<0.05$, Fig 26C).

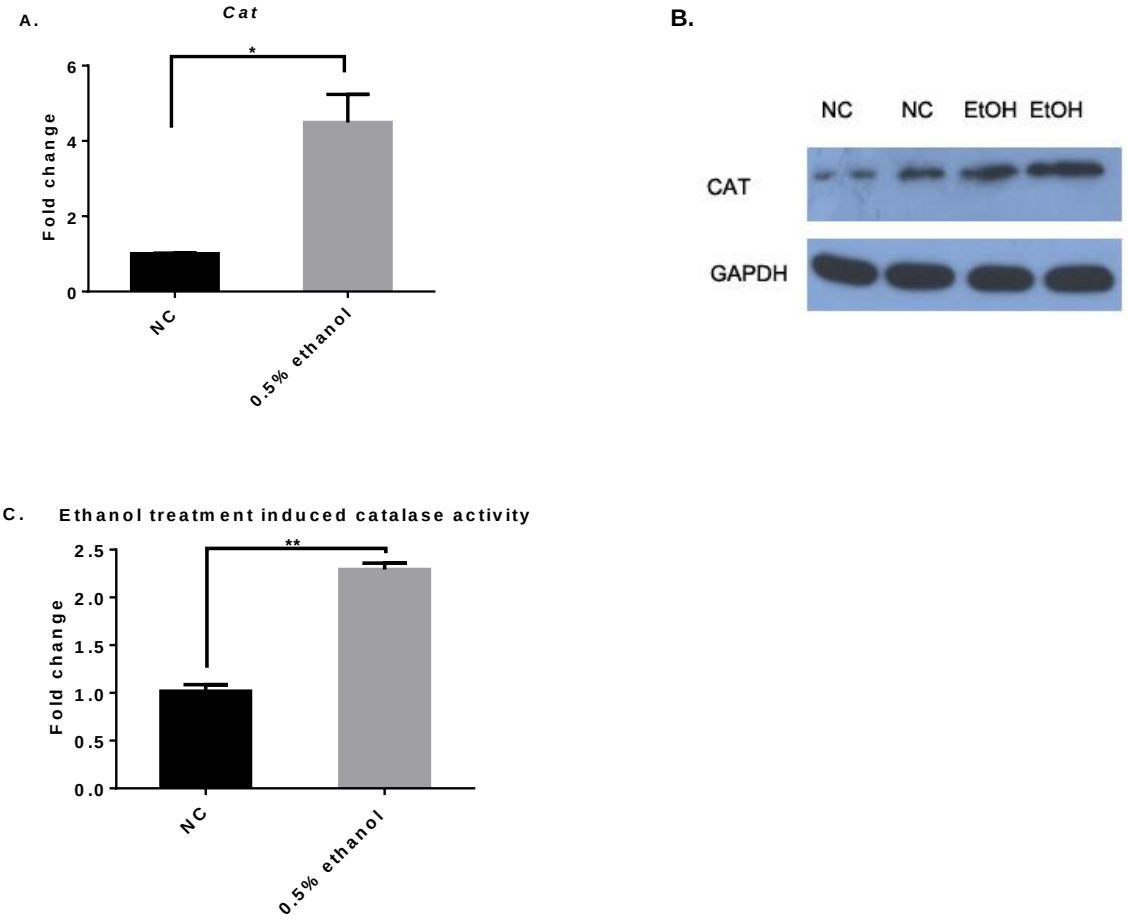

Fig. 26. The induction of catalase by ethanol. *Cat* mRNA levels (A), the abundance of catalase protein (B), and catalase activity (C) were higher in HL-1 cells treated with 0.5% ethanol. HL-1 cells were cultured in six-well plates pretreated with fibronectin in gelatin overnight. When they had reached 50% confluence, the cells were treated with 0.5% ethanol for 72 h. Total RNA was isolated for qRT-PCR analysis using *Cat* gene-specific primers and *28S rRNA* as an internal control. Western blots and catalase activity assays were carried out using total cell homogenates. The columns represent the mean ± SE for three experiments in each group. The *Cat* mRNA level in the control group was set to 1, and Student's t-test for unpaired values was used to compare the ethanol-treatment group with the control group.

4.5.4. The effect of *Pex14* knockdown on HL-1 cells

4.5.4.1. Establishment of the *Pex14* siRNA knockdown model

HL-1 cells are difficult to transfect and various transfection reagents were tested with little success (data not shown) until Lipofectamine 3000 reagent was used, resulting in satisfactory performance and reproducibility. At the mRNA level, we achieved a knockdown efficiency of ~90% (i.e., 10% of normal *Pex14* mRNA levels) after 6 days, corresponding to a dramatic decrease in PEX14p protein abundance (Fig. 27).

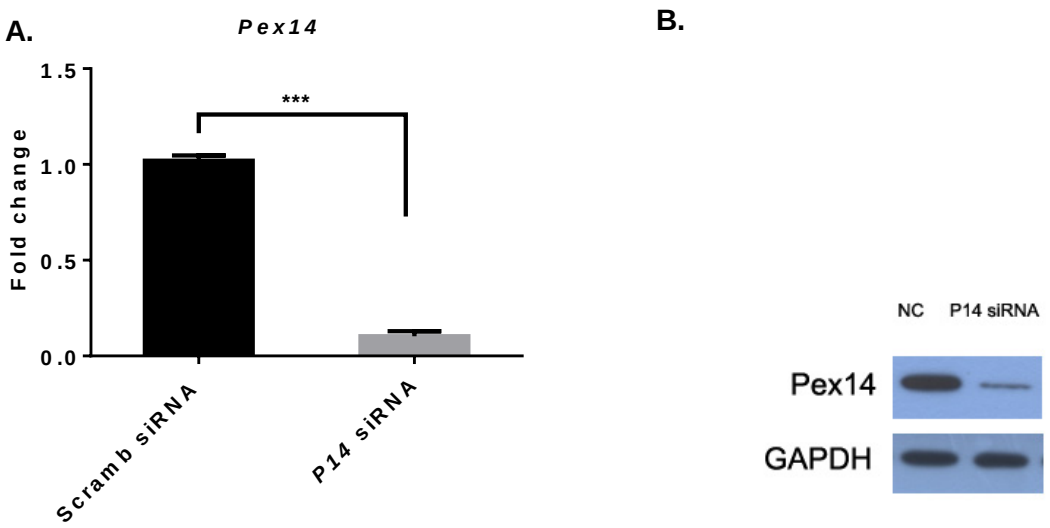

Fig. 27. The expression of *Pex14* mRNA and PEX14p was significantly diminished in HL-1 cells transfected with *Pex14* siRNA. HL-1 cells were cultured in six-well plates coated with fibronectin and gelatin at starting concentrations of 1.5–2 × 10^5 per well. Attachment was observed 4–6 h after seeding, and the cells were then transfected by adding 10 µl of Lipofectamine 3000 reagent and 150 pmol of *Pex14* siRNA into each well. After 6 days, cells were harvested and total RNA was isolated for PCR, and total protein was isolated for western blot analysis. The columns represent the mean ± SE for three experiments in each group. The average value for the control group was set to 1, and Student's t-test for unpaired values was used to compare the knockdown cells (treated with *Pex14* siRNA) to the control group (treated with Scramble siRNA).

4.5.4.2. *Pex14* siRNA knockdown induces catalase but does not affect the mitochondrial marker SOD2 in HL-1 cardiomyocytes

Knockdown of the peroxisomal biogenesis protein PEX14 disrupts peroxisomal matrix protein import, which leads to severe oxidative stress in many cell types due to primary peroxisomal and secondary mitochondrial dysfunction (Baumgart et al., 2001; Ahlemeyer et al., 2012). Catalase and SOD2 are often used to monitor the upregulation

of antioxidant enzymes in cells with peroxisomal deficiency. Accordingly, we found that *Cat* was upregulated 2.4-fold in the *Pex14* knockdown group ($P < 0.05$) and the catalase protein was also more abundant in these cells, as confirmed by western blot. There was no difference between the knockdown and control cells in terms of the mitochondrial marker SOD2 or cell viability as determined by the MTT assay, which partly reflects mitochondrial function (Fig. 28).

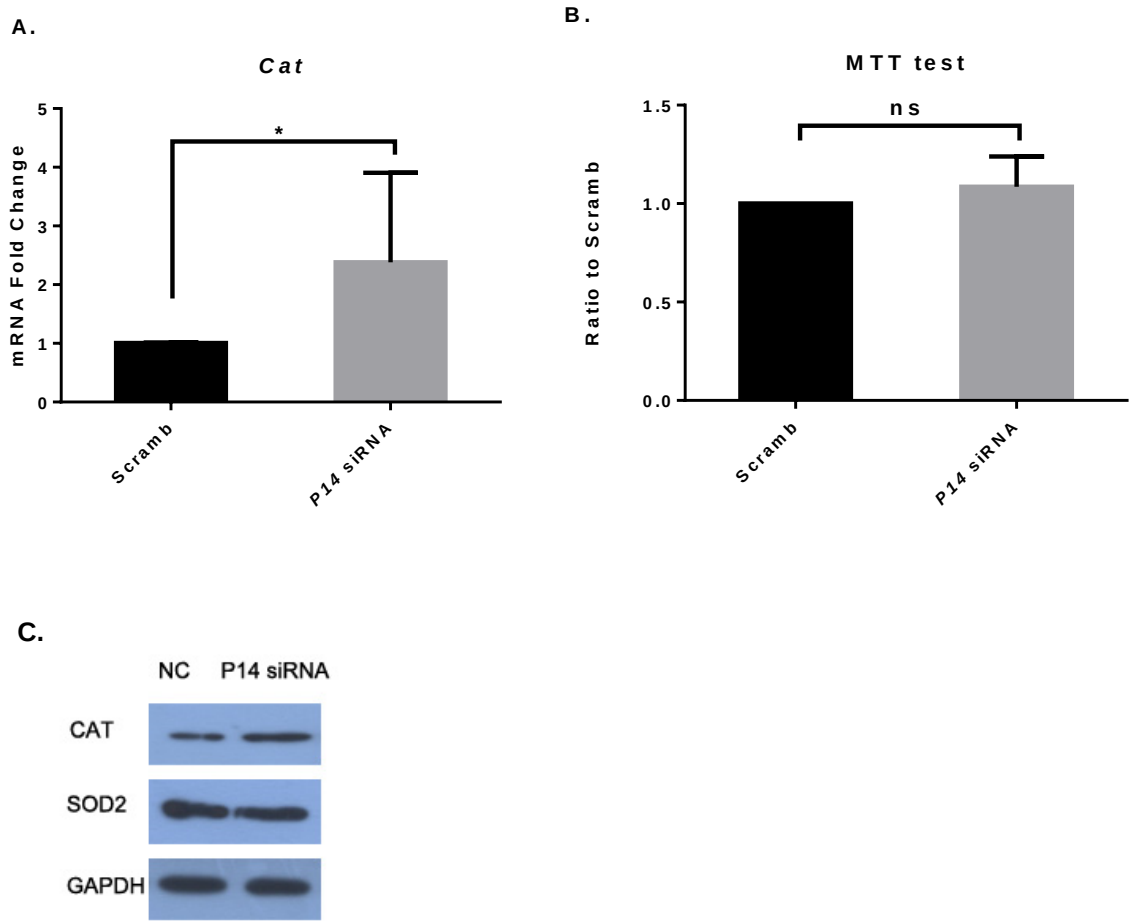

Fig. 28. The effect of *Pex14* siRNA knockdown on catalase and mitochondrial markers in HL-1 cardiomyocytes. *Pex14* siRNA knockdown induces Cat gene expression (A) and increases the abundance of catalase protein (B) but does not affect the mitochondrial marker SOD2 (B) or cell viability (C). After 6 days of exposure to *Pex14* siRNA, total RNA and total protein were isolated from HL-1 cells for RT-PCR and western blot analysis, respectively, or cells were directly used in the MTT assay. The columns in A and C represent the mean ± SE for three experiments in each group. The average value of the control group was set to 1, and Student's t-test for unpaired values was used to compare the knockdown cells (treated with *Pex14* siRNA) to the control group (treated with Scramble siRNA).

4.5.4.3. *Pex14* siRNA knockdown modulates the expression of cardiac markers

The effect of *Pex14* knockdown in HL-1 cardiomyocytes has not been reported thus far, so it was important to determine the expression profiles of cardiac markers. We observed the downregulation of *Nppa* and the upregulation of *Nppb* (although the sample numbers were not sufficient to test statistical significance) and the expression profile of *Nppc* did not change. Interestingly, *α-Mhc* (predominant in the adult heart) was strongly suppressed (83.3-fold) in the *Pex14* knockdown cells, whereas *β-Mhc* (which inhibits cardiomyocyte contractile function) was upregulated 1.8 fold (Fig. 29).

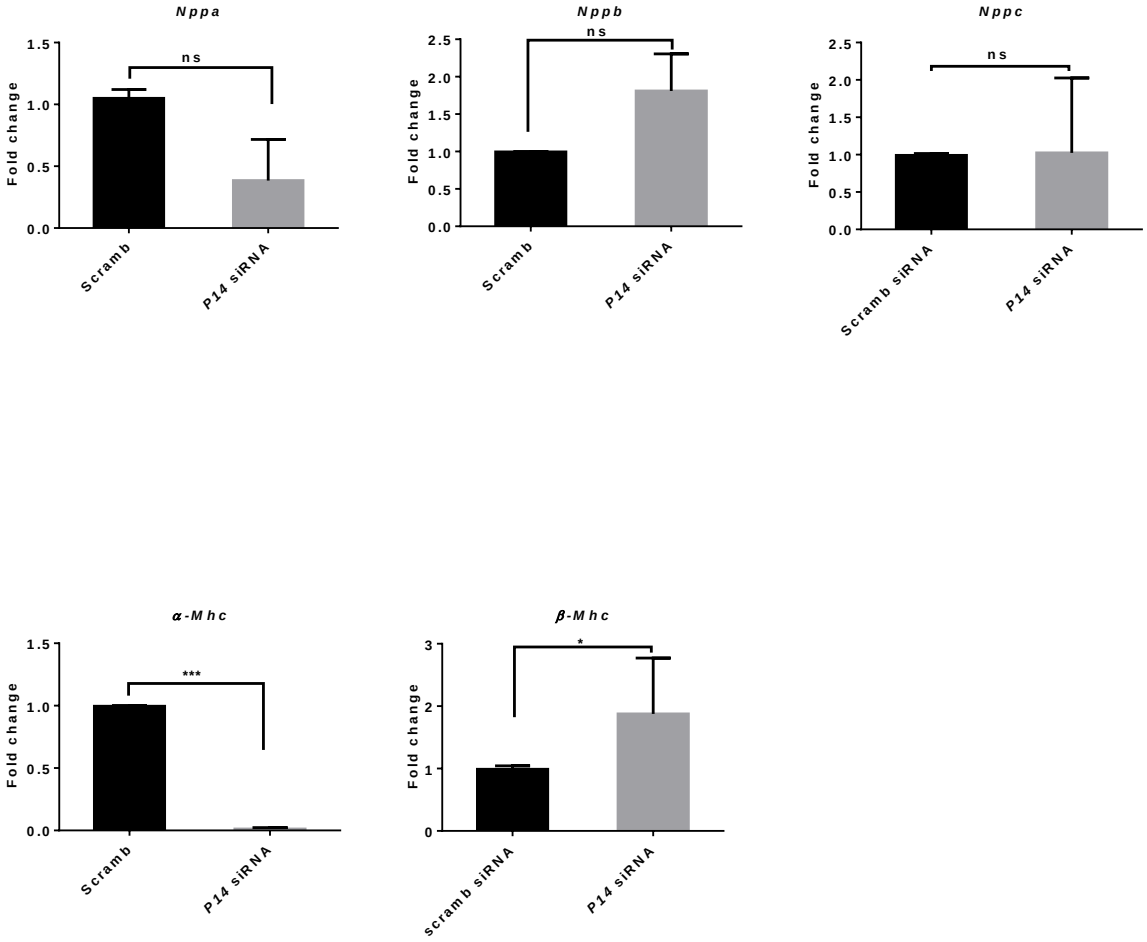

Fig. 29. Cardiac markers are modulated in *Pex14* knockdown HL-1 cells. After 6 days of exposure to *Pex14* siRNA, total RNA was isolated from HL-1 cells for the analysis of *Nppa*, *Nppb*, *Nppc, α-Mhc* and *β-Mhc* expression by RT-PCR. The columns represent the mean ± SE for three experiments in each group. The average value of the control group was set to 1, and Student's t-test for unpaired values was used to compare the knockdown cells (treated with *Pex14* siRNA) to the control group (treated with Scramble siRNA).

4.5.4.4. *Pex14* siRNA knockdown inhibits HL-1 cell proliferation

The total number of HL-1 cells and the proportion of dead cells were determined after transfection with *Pex14* siRNA to investigate the effect of *Pex14* knockdown on cell proliferation. Following the *Pex14* siRNA treatment, the total cell number was lower than the Scramble siRNA control group, but the proportion of dead cells was higher (Fig. 30).

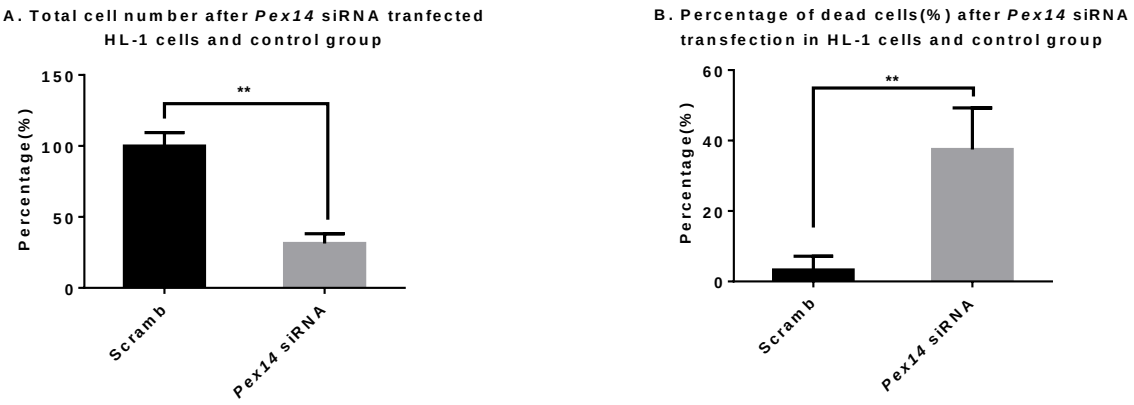

Fig. 30. *Pex14* siRNA knockdown inhibits the proliferation and viability of HL-1 cells. After 6 days of exposure to *Pex14* siRNA, cells were harvested and stained with trypan blue. The total cell number in each group was determined, and the proportion of dead cells was calculated. The columns represent the mean ± SE for three experiments in each group. The average total cell number of the control group was set to 1, and Student's t-test for unpaired values was used to compare the knockdown cells (treated with *Pex14* siRNA) to the control group (treated with Scramble siRNA).

5. Discussion

5.1. Overview of the thesis

The scientific literature provides little information about the role of peroxisomes in the heart. We therefore studied the characteristics of peroxisomes in cardiomyocytes to gain insight into their metabolic role, and particularly the effect of peroxisome dysfunction in cultured HL-1 cardiomyocytes and whole heart tissues. We observed the heterogeneous distribution of peroxisomes in different heart tissues as well as variations in peroxisomal enzyme composition, with the greatest abundance of peroxisomes in the left ventricle. Peroxisome-related gene expression and protein abundance changed during heart development. The analysis of *Pex11α* knockout mice and *Pex14* knockdown cardiomyocytes indicated that peroxisomal dysfunction affected the expression of typical cardiac marker genes, suggesting that peroxisomal metabolic activity is necessary to maintain cardiac homeostasis and protect cardiac functions.

5.2. Part I: Functional characterization of peroxisomes in the mouse heart

5.2.1. The expression of genes encoding peroxisomal proteins in the mouse heart

The protective role of peroxisomes in the heart is well established (Fahimi et al., 1979). The antioxidant activity of catalase, an abundant peroxisomal enzyme, explains part of this protective effect, but the full nature of the protective activity and its regulation are not clearly understood.

The *in silico* analysis of EST data allowed us to compare the expression of peroxisome-related genes in the heart and liver. However, the *in silico* comparison of EST data can only provide an approximate expression profile because the indicated values are mostly based on sequencing data from single animals. The values do not provide accurate expression levels in each organ, but at least show whether a gene is expressed or not and give some rough indication of relative expression levels in different tissues (Nagaraj et al., 2007). The data retrieved by database mining revealed that many important peroxisomal genes are expressed at detectable levels in the mouse heart. The liver has the highest content of peroxisomes among mammalian organs (Baumgart, 1997; Völkl et al., 1999), so the differential expression of

peroxisomal genes between the heart and liver offered a reflection of their specialized metabolic functions. Our results, showing that the *Cat* gene encoding catalase is expressed more strongly in the liver than the heart, support earlier studies reporting that the catalase activity per gram of heart tissue is about 2% of liver catalase activity in rats and mice (Y. Chen et al., 1994; Doroshow et al., 1980).

The metabolic activity of the liver generates abundant ROS (Jaeschke and Ramachandran, 2011) and therefore requires large amounts of catalase to degrade these harmful molecules and to protect the hepatocytes (DeJong et al., 2007). The liver is also the main organ for detoxification and oxidative management (Dunning et al., 2013). Importantly, the liver metabolizes diverse fatty acids, and this process takes place in both mitochondria and peroxisomes. However, the spectrum of fatty acids that peroxisomes can degrade is much wider than the capabilities of the mitochondria, including LCFAs, VLCFAs, methyl branched chain fatty acids, prostaglandins, polyunsaturated fatty acids (PUFAs), leukotrienes and toxic lipid intermediates (Colasante et al., 2015). In contrast, the heart uses fatty acids mainly for the production of energy via mitochondrial β-oxidation. This is reflected by the results of our *in silico* analysis, which showed that genes involved in fatty acid transportation (*Abcd3*) and peroxisomal β-oxidation (*Acox-1* and *Acox-2*) are more strongly expressed in the liver than the heart.

Interestingly, the *Gnpat* gene encoding glyceronephosphate O-acyltransferase, which is essential for the initiation of ether phospholipid (plasmalogen) biosynthesis in peroxisomes (Wanders and Waterham, 2006), was more strongly expressed in the heart than the liver. Plasmalogens are membrane-localized antioxidants that prevent lipid peroxidation. They are highly enriched in the heart and are necessary to maintain functional cellular membranes (Braverman et al., 2012; Lessig and Fuchs, 2009).

In conclusion, the difference between metabolic functions in the heart and liver is reflected by the expression profiles of genes encoding peroxisome-related proteins.

5.2.2. Selection of housekeeping genes and protein loading controls for the analysis of heart tissue

An appropriate internal standard is necessary for the quantitative analysis of PCR and western blot data. Common RNA internal standards include glyceraldehyde-3-

phosphate dehydrogenase (GAPDH), β-actin and 28*S* rRNA because their expression levels are relatively constant under different experimental conditions (Zhong and Simons, 1999). We tested several internal controls to determine their suitability and found some interesting differences in expression that narrowed our selection.

GAPDH, a key enzyme which catalyzes the sixth step in the glycolysis pathway, is expressed at high levels in mouse and human skeletal and heart muscle (Piechaczyk et al., 1984). It is often used as a protein loading control for western blots and as an internal control for RT-PCR. Because glycolysis readily responds to environmental changes and intracellular metabolic demands, it was unclear whether GAPDH would be suitable as a control for the analysis of the heart, which is greatly affected by metabolic fluctuations. However, we found that *Gapdh* mRNA and GAPDH protein levels remained stable, allowing its use as a marker for the comparison of peroxisome related mRNA and protein levels in different parts of the heart. In fetal and adult mouse hearts, GAPDH was more stable than the other internal controls, including β-actin.

The 18*S* and 28*S* ribosomal RNAs make up 80% of a total RNA sample and are unlikely to fluctuate under conditions that affect the expression of mRNAs (deLeeuw et al., 1989). Under hypoxic conditions, 28*S* rRNA was a reliable internal control for the comparative analysis of transcription (Zhong et al., 1999). Accordingly, we also found that 28*S* rRNA was suitable as an internal control, although it can only be used for the analysis of RNA samples and GAPDH was required for proteins.

Actin and tubulin are also widely used as loading controls for western blots and PCR analysis, but many studies have reported differential expression in animal tissues and cultured cells (Eaton et al., 2013; Suzuki et al., 2011; Wishart et al., 2008). Similarly, we observed the unequal distribution of β-actin in different parts of the heart and at different developmental stages, so this marker was not used in our experiments.

5.2.3. Genes related to peroxisome biogenesis and metabolism are differentially expressed in the four heart chambers

The heart is a muscular organ with four chambers: two atria and two ventricles (Zimmerman, 1966). The ventricles have thicker walls than the atria and the cardiomyocyte organization is also compartment-specific, reflecting their different functions (Simek et al., 1995). These functional differences are reflected in the gene

expression and metabolic activity of each chamber, although these aspects have not been characterized in detail (Barth et al., 2005).

Previous studies of peroxisomes in the heart were restricted to the left ventricle, using catalase as the only marker (Hand, 1974; Herzog et al., 1974; Oberley et al., 1990). The experiments presented herein are the first to use peroxisome-related markers to demonstrate significant differences in peroxisome-related gene expression, peroxisomal protein abundance and peroxisome number in the four heart chambers. PCR, western blot and immunofluorescence analysis provided concordant data showing that peroxisome-related mRNAs and proteins are more abundant in the ventricles than the atria, and that the left ventricle (which has the highest workload) is particularly enriched for peroxisomal enzymes and mRNAs.

In summary, these observations provide the first evidence that the functional and anatomical differences between the atria and ventricles are reflected by the expression of peroxisome-related genes and the abundance of peroxisomal proteins. Within the heart, peroxisomal activity appears to be modulated to adjust to the various metabolic requirements and workloads of the four heart chambers.

5.2.4. Developmental profiles of peroxisomal gene expression

5.2.4.1. Energy conversion and ROS metabolism during heart development

The substrates for metabolism and energy generation in the heart change substantially during the transition from fetal to postnatal development (Carley et al., 2014). The fetal heart utilizes mainly carbohydrates as the primary energy source (Wittels and Bressler, 1965) whereas LCFAs are the principal metabolic fuel of the adult heart (Carlsten et al., 1961; Shipp, 1964). After birth, there is a rapid switch from carbohydrate to fatty acid utilization.

The newborn heart is more susceptible to oxidative stress and ischemia-reperfusion injury than the adult heart (Cabigas et al., 2012). One important reason for ischemia-reperfusion injury is the noxious effects of ROS (Kalogeris et al., 2014). The accumulation of ROS leads to apoptosis, inflammation and changes in the profile of contractile proteins in the heart (Cabigas et al., 2012).

Despite the link between fatty acid and ROS metabolism in peroxisomes, there is little information available about the function of these organelles during postnatal

development in the heart. Therefore, we compared peroxisome-related gene expression in the hearts of newborn and adult mice to identify peroxisomal proteins that change in abundance during heart development.

5.2.4.2. Potential protective function of peroxisomes during heart maturation

Peroxisomes are involved in the maturation of many organs. Earlier studies conducted by the Baumgart-Vogt group have shown that hepatoblastoma and osteoblast differentiation is accompanied by an increase in the expression of peroxisome-related genes and the abundance of the corresponding proteins (Qian et al., 2015; Stier et al., 1998). Our results indicate that heart development may also involve the proliferation of peroxisomes to establish the β-oxidation pathway and antioxidant activity. We found that the peroxisomal biogenesis markers *Pex6* and *Pex11α*, the membrane transporter gene *Pmp2*, and genes related to the β-oxidation pathway (*AcoxI*) and the detoxification of ROS (C*at*), were more strongly expressed in the hearts of adult mice than newborns. This may reflect the higher stress levels experienced by the adult heart, including the abundance of ROS. There was a striking 1000-fold increase in *Pex11α* expression between the newborn and adult hearts. However, due to the lack of specific antibodies, it was not possible to detect the PEX11α protein to determine whether this difference is also reflected at the protein level. Because *Pex11α* is a key gene involved in peroxisome proliferation (Li, Baumgart, et al., 2002), the high levels of *Pex11α* mRNA are likely to reflect the requirement for rapid peroxisome proliferation to increase the number of peroxisomes in the adult heart.

5.3. Part II: HL-1 cells as a model to study peroxisomal function

5.3.1. The HL-1 cell line is a promising model to study heart peroxisomes

The HL-1 cardiomyocyte line is derived from the mouse left atrium and can be serially passaged while maintaining a differentiated phenotype (Claycomb et al., 1998). Earlier results showed that HL-1 mRNA and miRNA expression profiles were comparable to those of human and mouse hearts, suggesting HL-1 cardiomyocytes are suitable as a model for cardiomyocytes *in vivo* (Schlesinger et al., 2011).

HL-1 cells have not previously been used to investigate the function of heart peroxisomes so we initially characterized the expression of peroxisome-related genes

and the abundance of the corresponding proteins in HL-1 cells, compared to the mouse left atrium. Although many peroxisome-related genes were expressed in HL-1 cells, expression levels were not always comparable to the mouse left atrium.

Despite these differences, the cells still represent a good model for the investigation of peroxisomal functions in the heart because (1) all common peroxisomal marker genes are stably expressed, (2) HL-1 cells are the closest cell line to primary cardiomyocytes in terms of morphological phenotype (compared to H9C2 cells), and (3) the cells can easily be transfected with plasmids or siRNA for molecular analysis.

5.3.2. HL-1 cells for the analysis of peroxisome dysfunction *in vitro*

5.3.2.1. Establishment of transfection conditions for *Pex14* knockdown

After establishing the HL-1 cell line in our laboratory and assessing the expression of the main peroxisome-related genes, we used RNA interference (RNAi) to knock down *Pex14* gene expression and thus determine the effect on cell viability and the expression of peroxisomal, mitochondrial and cardiac markers.

Pex14 is required for peroxisomal biogenesis, and mutations in this gene are associated with three known clinical case studies (Huybrechts et al., 2008; Komatsuzaki et al., 2015; Shimozawa et al., 2004). Symptoms of PEX14 deficiency include severe hypotonia, failure to thrive, psychomotor retardation, liver dysfunction, and sensorineural hearing impairment (Komatsuzaki et al., 2015). Biochemical analysis indicated elevated levels of VLCFAs and low levels of serum plasmalogens in the patients (Komatsuzaki et al., 2015). The loss of *Pex14* in HL-1 cells inhibits growth and proliferation, mimicking severe Zellweger syndrome phenotypes (Maxwell et al., 2003). The intracellular role of PEX14 in peroxisomal biogenesis has been studied in detail. PEX14 is required as a docking factor in the peroxisomal membrane to allow the import of matrix proteins (Neuhaus et al., 2014) and it also serves as a membrane anchor for microtubules, and is therefore required for peroxisome motility (Bharti et al., 2011). Recently, PEX14 was identified as an optimal marker for the characterization of peroxisomes in different cell types, tissues and species in morphological studies (Grant et al., 2013).

The rapid growth of HL-1 cells reduces the transfection efficiency, but this can be addressed by starting with a low number of cells in the transfection experiments. We

found that cell densities of 1.5–2×10^5 per 9.6 cm^2 well gave the best transfection results (over 90% mRNA knockdown and protein knockdown). A drawback of using such low initial cell numbers was that longer post-transfection culture periods were needed to produce a sufficient number of cells for mRNA and protein analysis. However, the *Pex14* knockdown was stable until at least 6 days post-transfection, so we were able to investigate mRNA levels after 48–72 h and protein levels after 6–7 days.

5.3.2.2. Consequences of the loss of *Pex14* in HL-1 cells

The knockdown of *Pex14* inhibits cell proliferation and therefore we recovered fewer cardiomyocytes after transfection compared to the control sample (transfected with an inactive siRNA). The quantity of *Cat* mRNA was higher in the *Pex14* knockdown cells, which is also seen in *Pex* gene knockout models (our unpublished data). *Cat* expression is probably induced to compensate for the higher level of ROS generated in cells deficient for *Pex14*. Unfortunately, because only a few cells were available after transfection, it was not possible to measure the abundance of catalase protein or catalase enzyme activity directly. However, we speculate that the induction of *Cat* expression results in higher catalase activity in the cytoplasm of *Pex14* knockdown cells because the enzyme would not be imported into the peroxisome correctly. Gene expression studies also revealed the radical downregulation of *α-Mhc* and a moderate upregulation of *β-Mhc* in the *Pex14* knockdown cells. The downregulation of *α-Mhc* expression was previously reported in human hypertrophic hearts (Miyata et al., 2000; Reiser et al., 2001). The upregulation of *β-Mhc* in heart tissue is detrimental because it inhibits the contractile function of cardiomyocytes (Sugiura et al., 1992). Therefore, we speculate that the *Pex14* knockdown, which blocks the import of peroxisomal matrix proteins, significantly inhibits the function of peroxisomes in HL-1 cells, with consequential effects on fatty acid metabolism and oxidative stress management that might cause hypertrophic-like changes and impaired contractile function.

We also analyzed mitochondrial markers and mitochondrial function in the *Pex14* knockdown cells, given the functional overlap and interaction between these two organelles in terms of fatty acid metabolism and oxidative stress management. The abundance of the mitochondrial marker SOD2, an enzyme involved in mitochondrial ROS scavenging, and the ability of mitochondrial succinate dehydrogenase to reduce the tetrazolium dye (MTT assay), were unaffected by the loss of *Pex14*. These results

indicate that mitochondria are not affected by the knockdown of *Pex14*. However, to confirm this hypothesis, it would be necessary to investigate other parameters such as mitochondrial membrane potential and morphology.

5.3.3. HL-1 cells to study the induction/repression of peroxisome proliferation in vitro

HL-1 cells have been subjected to various treatments in order to simulate specific diseases (Andersen et al., 2009; Cormier-Regard et al., 1998; Nguyen and Claycomb, 1999; Wondergem et al., 2012). Similarly, we treated HL-1 cells with a PPARβ agonist to induce the expression of peroxisome-related genes, confirming that PPARβ agonists can induce PPAR expression in mouse cardiomyocytes. The activation of PPARβ by GW501516 reduced glucose utilization in skeletal muscle cells by switching mitochondrial substrate preference from carbohydrates to lipids (Brunmair et al., 2006). However, the effects of PPAR agonists on the heart are controversial. For example, the PPARγ agonist rosiglitazone is cardioprotective during ischemia-reperfusion (Morrison et al., 2011), but in patients with type 2 diabetes the long-term use of rosiglitazone increases the risk of cardiac events (Morrison et al., 2011). These controversial results suggest that the administration of PPAR agonists and antagonists should be evaluated carefully, allowing the selection of suitable candidates.

Long-term cardiomyocyte-specific PPARβ/δ deficiency in mice leads to the depression of myocardial fatty acid oxidation, bioenergetics, and premature death with lipotoxic cardiomyopathy (Wang et al., 2010). PPARβ/δ can also induce myogenesis by modulating myostatin activity (Bonala et al., 2012). The treatment of HL-1 cells with the PPARβ agonist upregulated *Cat* and *Pex14* expression. PPARα, PPARγ and RXR agonists can upregulate *Cat* mRNA and catalase protein expression in primary rat astrocytes (Khoo et al., 2013). However, we observed no change in the level of catalase in western blots following the treatment of HL-1 cells with PPARα and PPARγ agonists (data not shown). This may reflect the much lower basal *Pparα* and *Pparγ* expression in HL-1 cells compared to mouse atrial tissue, indicating that this cell line might be not suitable for the study of PPARα and PPARγ treatments. Catalase overexpression in HL-1 cells has also been established in our laboratory (unpublished data), offering a powerful tool to study the beneficial effects of catalase overexpression in the future.

5.4. Part III: Alterations of peroxisomal markers, cardiac markers and function in *Pex11α* knockout animals

5.4.1. *Pex11α* and its function in peroxisome proliferation

The PEX11 protein family consists of three members: PEX11α, PEX11β and PEX11γ (Li, Baumgart, et al., 2002). PEX11 proteins share several common features: they are small, very basic, and contain putative transmembrane regions, and are the most abundant peroxins in the peroxisomal membrane (Erdmann and Blobel, 1996; Tusnády and Simon, 2001). PEX11 proteins are required for peroxisome growth and division (Koch et al., 2010; Orth et al., 2007) and are believed to participate in the elongation step of peroxisome proliferation. *Pex11α* and *Pex11β* knockout models have been generated in cooperation with Prof. Baumgart-Vogt to analyze the function of the *Pex11* genes *in vivo* (Li, Baumgart, et al., 2002; Li and Gould, 2002).

Pex11β knockout mice display many of the pathological characteristics of Zellweger syndrome and provide an excellent model for the study of peroxisomal dysfunction (Li and Gould, 2002). However, constitutive *Pex11β* knockout mice do not survive long after birth, which makes it impossible to study the function of *Pex11β* in the adult heart. In contrast*, Pex11α* knockout mice have a normal macroscopic phenotype and lifespan, making it possible to investigate adult heart functions in these animals. No severe peroxisomal proliferation defects were observed in the livers of *Pex11α* knockout mice treated with peroxisome proliferators, but the size of the peroxisomes was abnormal (Li, Baumgart, et al., 2002). Furthermore, there were no significant effects on the peroxisomal α-oxidation or β-oxidation of fatty acids or ether-lipid synthesis in the hepatocytes of these animals. Although the loss of *Pex11α* did not affect the lifespan and macroscopic phenotype of mice under normal conditions, mice challenged with a high-fat diet displayed a higher body weight than wild-type mice, a greater number of tubule-interstitial lesions in the kidneys, and elevated levels of liver triglycerides and plasma free fatty acids (Weng et al., 2013). *Pex11α* overexpression also induced peroxisome proliferation in cultured mouse and human cells (Koch et al., 2010; Li, Baumgart, et al., 2002). Finally, PEX11α is the main factor responsible for peroxisomal division in fungi and is required for normal growth, whereas the loss of PEX11β and PEX11γ has no effect on fungal growth (Lee et al., 2015).

5.4.2. *Pex11α* knockout mice without an obvious macroscopic phenotype show many alterations at the molecular, morphological and functional levels

Our results showed that both *Pex11α* and *Pparγ* are expressed at higher levels in the left ventricle than other heart compartments, which suggests that the corresponding proteins play a central role in this part of the heart. We also found that *Pex11α* was upregulated after ischemia-reperfusion injury in rat hearts. We therefore investigated the effect of the *Pex11α* knockout on the functionality of the mouse heart.

We observed a clear *Pex11α* knockout phenotype at the molecular level despite the minimal macroscopic effects. When *Pex11α* was disrupted the other two members of the *Pex11* family (*Pex11β* and *Pex11γ*) were upregulated, indicating a compensatory effect in which the other PEX11 isoforms take over at least a part of the function of *Pex11α.* The overexpression of PEX11β in human cells can induce peroxisomal proliferation. Moreover, the three PPAR genes (*Pparα, Pparβ* and *Pparγ*) were induced in the hearts of the *Pex11α* knockout mice, with *Pparγ* expressed at the highest level.

Endogenous ligands of the PPAR nuclear receptor family include prostaglandins and leukotrienes, which are fatty acids and derivatives of lipid metabolism (Huss and Kelly, 2004; Vanden Heuvel, 2004; Xu et al., 1999). Many of the known PPAR ligands are substrates for peroxisomal β-oxidation and cannot be oxidized inside mitochondria (Colasante et al., 2015). For this reason, the loss of peroxisomal activity might cause either the accumulation of these derivatives (e.g. eicosanoids) or their depletion (e.g. PUFAs), triggering the dysregulation of the PPAR system and in turn the energy and ROS metabolism of the cell. Our results demonstrated that even a mild peroxisomal biogenesis defect as caused by the loss of *Pex11α* can induce changes in the expression of PPARs. We therefore propose that peroxisomes are directly involved in the modulation of the intracellular levels of PPAR ligands and act as sensors of cellular lipid homeostasis. When this system is perturbed by the inhibition of peroxisomal biogenesis or peroxisomal β-oxidation (e.g. by inflammation or aging), or by continuously overloading the β-oxidation pathway with LCFAs, lipid homeostasis is disrupted, leading to progressive cardiac dysfunction.

Nppa and *Nppc* (encoding the cardiac markers ANP and CNP) were downregulated in the hearts of *Pex11α* knockout mice, whereas *Nppb* (encoding BNP) was induced. Because an increase of BNP is clinically related to right-heart failure (Seeger et al.,

2013), it is also possible that the *Pex11α* deficiency plays a role in the functional maintenance of the right heart.

Mitochondrial changes have already been observed in various organs of peroxisomal disease models (Baumgart et al., 2001). Changes in the mitochondrial respiratory chain enzymes induce mitochondrial manganese superoxide dismutase, which indirectly suggests an increase in the production of ROS (Baumgart et al., 2001). SOD2 was upregulated in the hearts of *Pex11α* knockout mice, possibly indicating an increase in ROS levels caused by the peroxisomal defect. Mitochondrial changes were also observed in the livers of *Pex11α* knockout mice, where ring-shaped mitochondria surrounded lipid droplets, and mitochondrial proliferation was reported (Li, Baumgart, et al., 2002).

Despite the molecular changes noted above, the physiological function of isolated cardiomyocytes (assessed by measuring their cell shorting capacity) revealed no differences between the *Pex11α* knockout and wild-type mice. The reason for this observation is unclear, but we speculate that under control conditions the *Pex11α* phenotype is compensated by other PEX11 proteins. Indeed, when we challenged the *Pex11α* knockout heart using an ischemia-reperfusion model, we found that the heart tissue from the knockout mice suffered more damage than the control sample. Ischemic heart disease is one of the leading causes of morbidity and mortality worldwide (Forini et al., 2015). The protection of the ischemic myocardium is highly dependent on early reperfusion. However, inappropriate reperfusion also induces reperfusion injury which causes more damage to the heart tissue (Kalogeris et al., 2014). ROS are thought to play a critical role in ischemia-reperfusion injury. If the function of peroxisomes is inhibited by the loss of *Pex11α* activity, then it is likely that the defective peroxisomes left in the cardiomyocytes are unable to protect the cells from the oxidative stress caused by the ischemia-reperfusion injury. In conclusion, cardiac function is compromised by the *Pex11α* knockout, but the effect is only visible when the heart is exposed to stress.

5.5. Part IV: Perspectives

5.5.1. Catalase as an important protector of heart function

H_2O_2, a major ROS responsible for oxidative stress (Halliwell, 1999), is continuously generated by several superoxide dismutases, glucose oxidases and monoamine oxidases (Baud, 2004). The hydroxyl radicals derived from H_2O_2 can damage DNA, proteins, and membrane lipids (Halliwell et al., 1992). The two most important enzymes involved in H_2O_2 detoxification are glutathione peroxidase and catalase (Baud, 2004; Dringen and Hamprecht, 1997). Catalase is localized in the matrix of peroxisomes in most mammalian cells (Ballinger et al., 1994; Yokota and Fahimi, 1981; Zaar, 1992). In some species (sheep, monkey and guinea pig), catalase is also present in the cytosol of hepatocytes (Bulitta et al., 1996; Geerts et al., 1984; Roels, 1976; Roels et al., 1982; Yamamoto et al., 1988). In pathological conditions caused by peroxin deficiency, the incorrect targeting of catalase has been observed in the hepatocytes of patients (Baumgart et al., 2003; Kamei et al., 1993; Terlecky et al., 2006). The presence of catalase in the cytoplasm might protect the cells from further damage reflecting the metabolic changes caused by peroxisomal deficiency. The protective function of peroxisomal catalase in the heart was first reported almost 40 years ago (Fahimi et al., 1979).

There are few studies of peroxisomal catalase in the heart. Previous studies have shown that catalase is localized to the peroxisomes of cardiomyocytes (Herzog et al., 1974; Hicks and Fahimi, 1977; Yokota and Asayama, 1992). Compared to the liver, which has the greatest abundance of peroxisomes, catalase activity in the heart is very low (Chen et al., 1994; Doroshow et al., 1980). This explains the low resistance of the heart to pathological conditions such as ischemia-reperfusion injury (Chen et al., 1994). Hearts that overexpress catalase are protected from the toxicity of anticancer drugs like doxorubicin, which induce a burst of ROS that can damage cardiomyocytes (Kang et al., 1996). Similarly, mouse hearts that overexpress catalase are more resistant to ischemia-reperfusion injury (Li et al., 1997). Moreover, endotoxin pretreatment increases endogenous myocardial catalase activity and reduces the severity of ischemia-reperfusion injury in isolated rat hearts (Brown et al., 1989). Catalase also plays a major role in ethanol oxidation (Bradford et al., 1993). The cardiac-specific overexpression of catalase in mice rescues ventricular myocytes from ethanol-induced cardiac contractile defects (Zhang et al., 2003).

Here we found that the treatment of HL-1 cardiomyocytes with ethanol induces the expression of the *Cat* gene, which may protect the cells from ethanol-induced stress and damage. The protective mechanism of catalase is unclear. In newborn mice, the cardioprotective effects of catalase have been observed following the administration of the PPARγ agonist rosiglitazone (Chen et al., 2012). H_2O_2 significantly inhibited sarcomere shortening in newborn ventricular cells, but treatment with rosiglitazone induced *Cat* expression in the heart and restored normal shortening behavior. However, the protective effect was eliminated by the application of a PPARγ antagonist or by the direct inhibition of catalase (Chen et al., 2012).

5.5.2. Potential modulation of cardiomyocyte functions by peroxisomal calcium signaling

Ca^{2+} signaling plays a major role in excitation-contraction coupling and the contractile output of cardiomyocytes (Fearnley et al., 2011). It is also necessary for the modulation of corresponding short-term and long-term muscle cell adaptations (Wanders, 2004). The expression of the ventricular calcium-sensing receptor affects the contractile parameters of ventricular heart muscle cells and can modify the electromechanical coupling of cardiomyocytes (Schreckenberg et al., 2015).

Peroxisomes are also involved in calcium handling. Calcium blockers such as nicardipine, nifedipine and diltiazem suppress the activities of peroxisomal enzymes induced by clofibrate *in vivo*, including the peroxisomal fatty acyl-CoA oxidizing system and carnitine acetyltransferase (Watanabe and Suga, 1988). The first study of calcium levels in the lumen of peroxisomes reported a concentration of 52±5 nM, compared to 100 nM in the mitochondria and 1 mM in the endoplasmic reticulum, although the accuracy is disputed because the study was not carried out using living cells and the purity of isolated peroxisomes could not be proven (Raychaudhury et al., 2006). A later study based on living cells reported that peroxisomes contain 20–50 times as much Ca^{2+} as the cytosol, with concentrations up to 100 µM (Lasorsa et al., 2008). Interestingly, as Ca^{2+} levels increase in the cytoplasm, a corresponding increase occurs in peroxisomes accompanied by the activation of catalase (Costa et al., 2013). The mechanism of calcium transport through the peroxisomal membrane is not understood, although the membrane bristles with receptors that are responsible for the exchange of metabolic intermediates and ions (Wanders, 2004).

The involvement of peroxisomes in calcium handling suggests they could modulate the contractile function of cardiomyocytes by regulating calcium storage in the cytosol, and may prevent calcium overload in the heart leading to cardiomyocyte insufficiency.

5.5.3. Peroxisomes as markers of maturation and disease indicator

Our results show that the abundance of peroxisomal markers changes dynamically during heart development and is also affected by the disease state, as shown in the ischemia-reperfusion model. *Pex11α* expression increases by 1000-fold during heart development but is suppressed by ischemia-reperfusion injury. This gene could therefore provide a highly sensitive marker for changes in heart functions. Certain peroxisomal markers may be better indicators of such changes than the common cardiac markers *α-Mhc* and *β-Mhc*. To the best of our knowledge, the results reported herein provide the first evidence that peroxisomal markers are suitable indicators of cardiac functions. The next step would be to investigate the behavior of such markers in patients with diverse cardiac defects.

6. Summary

Peroxisomes are ubiquitous organelles hosting a wide range of essential metabolic enzymes involved in lipid metabolism and free radical detoxification. Therefore these organelles maintain homeostasis in the intracellular environment and protect against disease. The importance of normal peroxisomal function, and the link between dysfunction and disease development, is demonstrated by patients with Zellweger syndrome and corresponding mouse models. Due to the extremely short lifespan of Zellweger patients and the severe neurological phenotype, the cardiac symptoms are not reported as the cause of the mortality. However, in less severe peroxisome-related diseases, as seen in patients suffering from adult Refsum disease, the heart deficiency is clearly manifested.

In the work described in this thesis, initial data mining confirmed the expression of many peroxisomal genes in the heart, and we experimentally confirmed that peroxisomal gene expression differed between the heart and liver, with corresponding changes in protein abundance and enzyme activity. Furthermore, we found that the number of peroxisomes, and the gene and protein expression profiles, differed among the four chambers of the heart. The abundance of peroxisomal mRNAs and proteins was higher in the ventricles than the atria. Postnatal development and maturation of the heart was accompanied by marked changes in the abundance of peroxisomal markers, suggesting that such markers could be used to monitor cardiac development and maturation and possibly also to diagnose cardiac diseases. Accordingly, following ischemia-reperfusion, *Pex11α* gene expression was suppressed and the abundance of PEX14p increased, confirming that these markers are affected by ischemia-reperfusion injury.

Using a general *Pex11α* knockout mouse, we found that the loss of this gene induced a clear molecular phenotype involving the dysregulation of peroxisome-related genes as well as changes in mitochondrial and endoplasmic reticulum markers in the heart. However, no macroscopic phenotype was observed and there were no obvious changes in the morphology of cardiomyocytes under normal conditions. Interestingly, cardiomyocytes from the hearts of *Pex11α* knockout mice showed no impairment of contractile function under control conditions even though cardiac markers were

affected. However, the hearts of *Pex11α* knockout mice were less resistant to ischemia-reperfusion injury, suggesting that *Pex11α* and peroxisomes have a protective role during the ischemia-reperfusion process.

Finally, we established a knockdown model of peroxisome deficiency in HL-1 cells. These cells contain many peroxisomes with an appropriate enzyme composition. The knockdown of the peroxisomal biogenesis gene *Pex14* by RNAi caused the disruption of cardiac markers, the induction of mitochondrial markers and the inhibition of cell proliferation.

In conclusion, the data presented in this thesis demonstrate that the peroxisomal compartment is most abundant in the left ventricle and is closely associated with and supportive of normal heart functions. When peroxisomes are depleted or deficient in cardiomyocytes, there is a severe disruption of cardiomyocyte homeostasis. Protective and therapeutic strategies using peroxisome-related genes as targets may therefore help to prevent cardiac dysfunction caused, for example, by ischemia reperfusion injury, thus maintaining the healthy function of the heart.

7. Zusammenfassung

Peroxisomen sind ubiquitäre Zellorganellen, die ihre Hauptfunktion im Stoffwechsel von Lipid und reaktiven Sauerstoffspezies (ROS) ausführen. Peroxisomen spielen eine sehr wichtige Rolle in der Erhaltung der Lipidhomöostase innerhalb der Zelle und der Verhinderung von Krankheitsprozessen.

Die Wichtigkeit der normalen peroxisomalen Funktionen und deren wichtige Bedeutung bei ihrem Funktionsausfall werden in vielen Zellweger-Syndrom Patienten und Mausmodellen deutlich. Da Patienten mit Zellweger-Syndrom eine extrem kurze Lebenserwartung haben, wurden kardiologische Symptome der Patienten bisher nicht als Todesursache beobachtet und berichtet. Bei leichteren Phenotypen von peroxisomalen Erkrankungen, z.B. adulte Refsum-Symdrom-Patienten, sind jedoch klare Zeichen der kardialen Dysfunktion deutlich präsent.

Die am Anfang der Doktorarbeit durchgeführte Datenbanksuche bestätigte bereits die Expression vieler peroxisomaler Gene im Herzen von der C57BL/6J-Mäusen. Weiterhin, zeigten die Ergebnisse dieser Thesis, dass die peroxisomalen Enzymaktivitäten und Expressionen unterschiedlich waren zwischen Herz und Leber, und dass die Verteilung und Anzahl der Peroxisomen in Vorhöfen und Herzkammern voreinander abweichend waren. In den Herzkammern, war der Gehalt der peroxisomalen mRNAs und Proteine deutlich höher als in den Vorhöfen. Die postnatale Entwicklung und Reifung des Herzens wurde begleitet von einer deutlichen Veränderung der Peroxisomenmarker. In der Tat, könnten somit peroxisomale Gene als mögliche Krankheitsmarker geeignet sein. Nach Ischämie-Reperfusion des Herzens, wurde eine starke Reduzierung an *Pex11α* und eine Erhöhung des *Pex14* Gens beobachtet, was darauf hindeutet, dass Peroxisomen in Ischämie-Reperfusionsschäden involviert sein könnten.

Mit Hilfe eines *Pex11α* Gen-Knockout Mausmodells, das von unserer Arbeitsgruppe mit-etabliert wurde (Li, et al., 2002), wurde nachgewiesen, dass *Pex11α* Gendefekt im Herzen, nicht nur dramatische Störungen der peroxisomalen Gene verursachen konnten, sondern auch zur Veränderungen in Mitochondrien und von endoplasmischen Reticulum Markern führen konnten. Trotz des vorhandenen deutlichen molekularen Phänotyps, wurden unter normalen Bedingungen jedoch kein makroskopischer Phänotyp und keine Änderungen von morphologischen Parametern festgestellt. Obwohl die kardialen Marker in *Pex11α* Knockout Kardiomyozyten

verändert waren, wurde das Kontraktionsverhalten der Kardiomyozyten nicht beeinflusst. Dagegen, waren die Herzen von *Pex11α* knockout Mäusen nicht so resistent gegen Ischämie-Reperfusionsschäden, was darauf hindeutet, dass Peroxisomen und das *Pex11α* Gen eine wichtige Rolle bei der Protektion der Herzfunktion im Rahmen der Ischämie-Reperfusionsschädungsprozesse spielen könnten.

Zusätzlich wurden Zellkulturstudien an HL-1 Kardiomyozyten durchgeführt, die eine vergleichbare peroxisomale Gene Expression wie Kardiomyozyten im Mausvorhof aufweisen. Weiterhin wurde durch Transfektion von HL-1-Zellen mit *Pex14* siRNA ein knockdown Modell des *Pex14*-Gens zur Nachahmung eines Zellweger-Syndroms in Zellkultur etabliert. Zu den *Pex14*-defizierten Zellen konnten eine veränderte kardiale Markerexpression, erhöhte mitochondriale Marker sowie eine Hemmung der Proliferation der Zellen beobachtet werden.

In Rahmen der vorgelegte Doktorarbeit konnten folgende Erkenntnisse erzielt werden: Peroxisomen sind reichlich in der Linkskammer vorhandeln und unterstützten die normale Herzfunktion. Im Fall eines peroxisomales Gendefekts, kommt es zu Störungen der Homöostase des Herzens. Die prophylaktische oder therapeutische Peroxisominduktion könnte sich deshalb bei Herz-Kreislauf-Erkrankungen, z.B. Ischämie-Reperfusionsschäden, positiv auswirken.

8. Reference

Abel, E. D. (2004). Glucose transport in the heart. *Frontiers in Bioscience : A Journal and Virtual Library*, *9*, 201–15. Retrieved from http://www.ncbi.nlm.nih.gov/pubmed/14766360

Adams, M. D., Kelley, J. M., … Moreno, R. F. (1991). Complementary DNA sequencing: expressed sequence tags and human genome project. *Science (New York, N.Y.)*, *252*(5013), 1651–6. Retrieved from http://www.ncbi.nlm.nih.gov/pubmed/2047873

Aerni-Flessner, L., Abi-Jaoude, M., … Hruz, P. W. (2012). GLUT4, GLUT1, and GLUT8 are the dominant GLUT transcripts expressed in the murine left ventricle. *Cardiovascular Diabetology*, *11*(1), 63. https://doi.org/10.1186/1475-2840-11-63

Andersen, A.-D., Poulsen, K. A., … Pedersen, S. F. (2009). HL-1 mouse cardiomyocyte injury and death after simulated ischemia and reperfusion: roles of pH, Ca2+-independent phospholipase A2, and Na+/H+ exchange. *AJP: Cell Physiology*, *296*(5), C1227–C1242. https://doi.org/10.1152/ajpcell.00370.2008

Antonenkov, V. D., Grunau, S., … Hiltunen, J. K. (2010). Peroxisomes Are Oxidative Organelles. *Antioxidants & Redox Signaling*, *13*(4), 525–537. https://doi.org/10.1089/ars.2009.2996

Baes, M., Dewerchin, M., … Carmeliet, P. (2002). Generation ofPex5-loxP mice allowing the conditional elimination of peroxisomes. *Genesis*, *32*(2), 177–178. https://doi.org/10.1002/gene.10047

Baes, M., Gressens, P., … Mannaerts, G. P. (1997). A mouse model for Zellweger syndrome. *Nature Genetics*, *17*(1), 49–57. https://doi.org/10.1038/ng0997-49

Baes, M., and Van Veldhoven, P. P. (2012a). Mouse models for peroxisome biogenesis defects and ??-oxidation enzyme deficiencies. *Biochimica et Biophysica Acta - Molecular Basis of Disease*, *1822*(9), 1489–1500. https://doi.org/10.1016/j.bbadis.2012.03.003

Baes, M., and Van Veldhoven, P. P. (2012b). Mouse models for peroxisome biogenesis defects and β-oxidation enzyme deficiencies. *Biochimica et Biophysica Acta (BBA) - Molecular Basis of Disease*, *1822*(9), 1489–1500. https://doi.org/10.1016/j.bbadis.2012.03.003

Baker, A., Carrier, D. J., … Theodoulou, F. L. (2015). Peroxisomal ABC transporters: functions and mechanism. *Biochemical Society Transactions*, *43*(5), 959–65. https://doi.org/10.1042/BST20150127

Ballinger, C. A., Mendis-Handagama, C., … Kinkade, J. M. (1994). Changes in the localization of catalase during differentiation of neutrophilic granulocytes. *Blood*, *83*(9), 2654–68. Retrieved from http://www.ncbi.nlm.nih.gov/pubmed/8167345

Barak, Y., Liao, D., … Evans, R. M. (2002). Effects of peroxisome proliferator-activated receptor on placentation, adiposity, and colorectal cancer. *Proceedings of the National Academy of Sciences*, *99*(1), 303–308. https://doi.org/10.1073/pnas.012610299

Barak, Y., Nelson, M. C., … Evans, R. M. (1999). PPAR gamma is required for placental, cardiac, and adipose tissue development. *Molecular Cell*, *4*(4), 585–95. Retrieved from http://www.ncbi.nlm.nih.gov/pubmed/10549290

Baud, O. (2004). Glutathione Peroxidase-Catalase Cooperativity Is Required for Resistance to Hydrogen Peroxide by Mature Rat Oligodendrocytes. *Journal of Neuroscience*, *24*(7), 1531–1540. https://doi.org/10.1523/JNEUROSCI.3989-03.2004

Baumgart, E. (1997). Application of in situ hybridization, cytochemical and immunocytochemical techniques for the investigation of peroxisomes: A review including novel data. *Histochemistry and Cell Biology*, *108*(3), 185–210. https://doi.org/10.1007/s004180050160

Baumgart, E., Fahimi, H., … Grabenbauer, M. (2003). A review of morphological techniques for detection of peroxisomal (and mitochondrial) proteins and their corresponding mRNAs during ontogenesis in mice: Application to the PEX5-knockout mouse with Zellweger syndrome. *Microscopy Research and Technique*, *61*(2), 121–138. https://doi.org/10.1002/jemt.10322

Baumgart, E., Vanhorebeek, I., … Baes, M. (2001). Mitochondrial Alterations Caused by Defective Peroxisomal Biogenesis in a Mouse Model for Zellweger Syndrome (PEX5 Knockout Mouse). *The American Journal of Pathology*, *159*(4), 1477–1494. https://doi.org/10.1016/S0002-9440(10)62534-5

Baumgart, E., Volkl, A., … Fahimi, H. (1989). Biogenesis of peroxisomes: Immunocytochemical investigation of peroxisomal membrane proteins in

proliferating rat liver peroxisomes and in catalase-negative membrane loops. *Journal of Cell Biology*, *108*(6), 2221–2231.

Beach, A., Burstein, M. T., … Titorenko, V. I. (2012). Integration of peroxisomes into an endomembrane system that governs cellular aging. *Frontiers in Physiology*, *3*, 283. https://doi.org/10.3389/fphys.2012.00283

Beier, K., Völkl, A., and Fahimi, H. (1997). TNF-alpha downregulates the peroxisome proliferator activated receptor-alpha and the mRNAs encoding peroxisomal proteins in rat liver. *FEBS Letters*, *412*(2), 385–7. Retrieved from http://www.ncbi.nlm.nih.gov/pubmed/9256257

Benson, D., Cavanaugh, M., … Sayers, E. W. (2016). GenBank. *Nucleic Acids Research*. https://doi.org/10.1093/nar/gkw1070

Berger, J., and Gärtner, J. (2006). X-linked adrenoleukodystrophy: Clinical, biochemical and pathogenetic aspects. *Biochimica et Biophysica Acta (BBA) - Molecular Cell Research*, *1763*(12), 1721–1732. https://doi.org/10.1016/j.bbamcr.2006.07.010

Berger, J., and Moller, D. E. (2002). The Mechanisms of Action of PPARs. *Annual Review of Medicine*, *53*(1), 409–435. https://doi.org/10.1146/annurev.med.53.082901.104018

Bernhard, W., and Rouiller, C. (1956). Microbodies and the problem of mitochondrial regeneration in liver cells. *The Journal of Biophysical and Biochemical Cytology*, *2*(4 Suppl), 355–60.

Bharti, P., Schliebs, W., … Erdmann, R. (2011). PEX14 is required for microtubule-based peroxisome motility in human cells. *Journal of Cell Science*, *124*(10), 1759–1768. https://doi.org/10.1242/jcs.079368

Bienert, G. P., Schjoerring, J. K., and Jahn, T. P. (2006). Membrane transport of hydrogen peroxide. *Biochimica et Biophysica Acta (BBA) - Biomembranes*, *1758*(8), 994–1003. https://doi.org/10.1016/j.bbamem.2006.02.015

Bishop, S., and Altschuld, R. (1970). Increased glycolytic metabolism in cardiac hypertrophy and congestive failure. *American Journal of Physiology -- Legacy Content*, *218*(1).

Bjorkman, J., Tonks, I., … Crane, D. I. (2002). Conditional inactivation of the

peroxisome biogenesisPex13 gene by Cre-loxP excision. *Genesis*, *32*(2), 179–180. https://doi.org/10.1002/gene.10044

Boguski, M. S., Lowe, T. M. J., and Tolstoshev, C. M. (1993). dbEST — database for “expressed sequence tags.” *Nature Genetics*, *4*(4), 332–333. https://doi.org/10.1038/ng0893-332

Bonala, S., Lokireddy, S., … Kambadur, R. (2012). Peroxisome Proliferator-activated Receptor β/δ Induces Myogenesis by Modulating Myostatin Activity. *Journal of Biological Chemistry*, *287*(16), 12935–12951. https://doi.org/10.1074/jbc.M111.319145

Bonekamp, N. A., Sampaio, P., … Schrader, M. (2012). Transient Complex Interactions of Mammalian Peroxisomes Without Exchange of Matrix or Membrane Marker Proteins. *Traffic*, *13*(7), 960–978. https://doi.org/10.1111/j.1600-0854.2012.01356.x

Böning, A., Hagmüller, S., … Mühlfeld, C. (2014). Is Warm or Cold Calafiore Blood Cardioplegia Better? Hemodynamic, Metabolic, and Electron Microscopic Differences. *Thoracic and Cardiovascular Surgeon*, *62*(8), 683–689. https://doi.org/10.1055/s-0034-1383722

Boveris, A., and Chance, B. (1973). The mitochondrial generation of hydrogen peroxide. General properties and effect of hyperbaric oxygen. *Biochemical Journal*, *134*(3), 707–716. https://doi.org/10.1042/bj1340707

Bradford, B. U., Seed, C. B., … Thurman, R. G. (1993). Evidence that catalase is a major pathway of ethanol oxidation in vivo: dose-response studies in deer mice using methanol as a selective substrate. *Arch Biochem Biophys*. https://doi.org/10.1006/abbi.1993.1269

Braverman, N. E., D’Agostino, M. D., and MacLean, G. E. (2013). Peroxisome biogenesis disorders: Biological, clinical and pathophysiological perspectives. *Developmental Disabilities Research Reviews*, *17*(3), 187–196. https://doi.org/10.1002/ddrr.1113

Braverman, N. E., and Moser, A. B. (2012). Functions of plasmalogen lipids in health and disease. *Biochimica et Biophysica Acta (BBA) - Molecular Basis of Disease*, *1822*(9), 1442–1452. https://doi.org/10.1016/j.bbadis.2012.05.008

Breckenridge, R. (2014). Molecular Control of Cardiac Fetal/Neonatal Remodeling.

Journal of Cardiovascular Development and Disease, *1*(1), 29–36. https://doi.org/10.3390/jcdd1010029

Brown, J. M., Grosso, M. A., … Repine, J. E. (1989). Endotoxin pretreatment increases endogenous myocardial catalase activity and decreases ischemia-reperfusion injury of isolated rat hearts. *Proceedings of the National Academy of Sciences of the United States of America*, *86*(7), 2516–20. Retrieved from http://www.ncbi.nlm.nih.gov/pubmed/2648406

Brunmair, B., Staniek, K., … Fürnsinn, C. (2006). Activation of PPAR-δ in isolated rat skeletal muscle switches fuel preference from glucose to fatty acids. *Diabetologia*, *49*(11), 2713–2722. https://doi.org/10.1007/s00125-006-0357-6

Bulitta, C., Ganea, C., … Völkl, A. (1996). Cytoplasmic and peroxisomal catalases of the guinea pig liver: evidence for two distinct proteins. *Biochimica et Biophysica Acta*, *1293*(1), 55–62. Retrieved from http://www.ncbi.nlm.nih.gov/pubmed/8652628

Burkart, E. M., Sambandam, N., … Kelly, D. P. (2007). Nuclear receptors PPARbeta/delta and PPARalpha direct distinct metabolic regulatory programs in the mouse heart. *The Journal of Clinical Investigation*, *117*(12), 3930–9. https://doi.org/10.1172/JCI32578

Burnett, J. C., Kao, P. C., … Reeder, G. S. (1986). Atrial natriuretic peptide elevation in congestive heart failure in the human. *Science (New York, N.Y.)*, *231*(4742), 1145–7. Retrieved from http://www.ncbi.nlm.nih.gov/pubmed/2935937

Cabigas, E. B., Ding, G., … Davis, M. E. (2012). Age- and chamber-specific differences in oxidative stress after ischemic injury. *Pediatric Cardiology*, *33*(2), 322–31. https://doi.org/10.1007/s00246-011-0137-z

Carley, A. N., Taegtmeyer, H., and Lewandowski, E. D. (2014). Matrix Revisited: Mechanisms Linking Energy Substrate Metabolism to the Function of the Heart. *Circulation Research*, *114*(4), 717–729. https://doi.org/10.1161/CIRCRESAHA.114.301863

Carlsten, A., Hallgren, B., … Myrén, I. (1961). Myocardial metabolism of glucose, lactic acid, amino acids and fatty acids in healthy human individuals at rest and at different work loads. *Scandinavian Journal of Clinical and Laboratory Investigation*, *13*, 418–28. Retrieved from

http://www.ncbi.nlm.nih.gov/pubmed/13876667

Chang, C. C., South, S., … Gould, S. J. (1999). Metabolic control of peroxisome abundance. *Journal of Cell Science*, 1579–90. Retrieved from http://www.ncbi.nlm.nih.gov/pubmed/10212151

Chen, T., Jin, X., … Ding, G. (2012). Cardioprotection from oxidative stress in the newborn heart by activation of PPAR gamma is mediated by catalase. *Free Radical Biology and Medicine*, *53*(2), 208–215. https://doi.org/10.1016/j.freeradbiomed.2012.05.014

Chen, Y., Saari, J., and Kang, Y. (1994). Weak antioxidant defenses make the heart a target for damage in copper-deficient rats. *Free Radical Biology & Medicine*, *17*(6), 529–36. Retrieved from http://www.ncbi.nlm.nih.gov/pubmed/7867969

Cheng, L., Ding, G., … Yang, Q. (2004). Cardiomyocyte-restricted peroxisome proliferator-activated receptor-δ deletion perturbs myocardial fatty acid oxidation and leads to cardiomyopathy. *Nature Medicine*, *10*(11), 1245–1250. https://doi.org/10.1038/nm1116

Claycomb, W. C., Lanson, N. A., … Izzo, N. J. (1998). HL-1 cells: a cardiac muscle cell line that contracts and retains phenotypic characteristics of the adult cardiomyocyte. *Proceedings of the National Academy of Sciences of the United States of America*, *95*(6), 2979–84. Retrieved from http://www.ncbi.nlm.nih.gov/pubmed/9501201

Colasante, C., Chen, J., … Baumgart-Vogt, E. (2015). Peroxisomes in cardiomyocytes and the peroxisome / peroxisome proliferator-activated receptor-loop. *Thrombosis and Haemostasis*, *113*, 452–463. https://doi.org/10.1160/TH14-06-0497

Cormier-Regard, S., Nguyen, S. V, and Claycomb, W. C. (1998). Adrenomedullin gene expression is developmentally regulated and induced by hypoxia in rat ventricular cardiac myocytes. *The Journal of Biological Chemistry*, *273*(28), 17787–92. Retrieved from http://www.ncbi.nlm.nih.gov/pubmed/9651380

Costa, A., Drago, I., … Pozzan, T. (2013). Peroxisome Ca2+ Homeostasis in Animal and Plant Cells (pp. 111–133). https://doi.org/10.1007/978-94-007-6889-5_7

Daley, W. P., Peters, S. B., and Larsen, M. (2008). Extracellular matrix dynamics in development and regenerative medicine. *Journal of Cell Science*, *121*(3), 255–

264. https://doi.org/10.1242/jcs.006064

Dammai, V., Subramani, S., … Lazarow, P. . (2001). The human peroxisomal targeting signal receptor, Pex5p, is translocated into the peroxisomal matrix and recycled to the cytosol. *Cell*, *105*(2), 187–96. https://doi.org/10.1016/S0092-8674(01)00310-5

De Craemer, D., Vamecq, J., … Van den Branden, C. (1994). Peroxisomes in liver, heart, and kidney of mice fed a commercial fish oil preparation: original data and review on peroxisomal changes induced by high-fat diets. *Journal of Lipid Research*, *35*(7), 1241–50. Retrieved from http://www.ncbi.nlm.nih.gov/pubmed/7964185

De Duve, C., and Baudhuin, P. (1966). Peroxisomes (microbodies and related particles). *Physiological Reviews*, *46*(2), 323–357.

DeJong, R. J., Miller, L. M., … Barillas-Mury, C. (2007). Reactive oxygen species detoxification by catalase is a major determinant of fecundity in the mosquito Anopheles gambiae. *Proceedings of the National Academy of Sciences*, *104*(7), 2121–2126. https://doi.org/10.1073/pnas.0608407104

Del Río, L. A., and López-Huertas, E. (2016). ROS Generation in Peroxisomes and its Role in Cell Signaling. *Plant & Cell Physiology*, *181600*(April), pcw076. https://doi.org/10.1093/pcp/pcw076

Demarquoy, J., and Le Borgne, F. (2015). Crosstalk between mitochondria and peroxisomes. *World Journal of Biological Chemistry*, *6*(4), 301–9. https://doi.org/10.4331/wjbc.v6.i4.301

Desvergne, B., and Wahli, W. (1999). Peroxisome Proliferator-Activated Receptors: Nuclear Control of Metabolism [1]. *Endocrine Reviews*, *20*(5), 649–688. https://doi.org/10.1210/edrv.20.5.0380

Dirkx, R., Vanhorebeek, I., … Baes, M. (2005). Absence of peroxisomes in mouse hepatocytes causes mitochondrial and ER abnormalities. *Hepatology*, *41*(4), 868–878. https://doi.org/10.1002/hep.20628

Dixit, E., Boulant, S., … Kagan, J. C. (2010). Peroxisomes Are Signaling Platforms for Antiviral Innate Immunity. *Cell*, *141*(4), 668–681. https://doi.org/10.1016/j.cell.2010.04.018

Djouadi, F., Weinheimer, C. J., … Kelly, D. P. (1998). A gender-related defect in lipid metabolism and glucose homeostasis in peroxisome proliferator- activated receptor alpha- deficient mice. *The Journal of Clinical Investigation*, *102*(6), 1083–91. https://doi.org/10.1172/JCI3949

Dodt, G., and Gould, S. J. (1996). Multiple PEX genes are required for proper subcellular distribution and stability of Pex5p, the PTS1 receptor: evidence that PTS1 protein import is mediated by a cycling receptor. *The Journal of Cell Biology*, *135*(6 Pt 2), 1763–74. Retrieved from http://www.ncbi.nlm.nih.gov/pubmed/8991089

Doenst, T., Nguyen, T. D., and Abel, E. D. (2013). Cardiac metabolism in heart failure: Implications beyond atp production. *Circulation Research*, *113*(6), 709–724. https://doi.org/10.1161/CIRCRESAHA.113.300376

Doroshow, J. H., Locker, G. Y., and Myers, C. E. (1980). Enzymatic Defenses of the Mouse Heart Against Reactive Oxygen Metabolites. *Journal of Clinical Investigation*, *65*(1), 128–135. https://doi.org/10.1172/JCI109642

Dreyer, C., Krey, G., … Wahli, W. (1992). Control of the peroxisomal beta-oxidation pathway by a novel family of nuclear hormone receptors. *Cell*, *68*(5), 879–87. Retrieved from http://www.ncbi.nlm.nih.gov/pubmed/1312391

Dringen, R., and Hamprecht, B. (1997). Involvement of glutathione peroxidase and catalase in the disposal of exogenous hydrogen peroxide by cultured astroglial cells. *Brain Research*, *759*(1), 67–75. https://doi.org/10.1016/S0006-8993(97)00233-3

Dunning, S., ur Rehman, A., … Moshage, H. (2013). Glutathione and antioxidant enzymes serve complementary roles in protecting activated hepatic stellate cells against hydrogen peroxide-induced cell death. *Biochimica et Biophysica Acta (BBA) - Molecular Basis of Disease*, *1832*(12), 2027–2034. https://doi.org/10.1016/j.bbadis.2013.07.008

Eaton, S. L., Roche, S. L., … Pde, T. C. (2013). Total Protein Analysis as a Reliable Loading Control for Quantitative Fluorescent Western Blotting. *PLoS ONE*, *8*(8), e72457. https://doi.org/10.1371/journal.pone.0072457

Erdmann, R., and Blobel, G. (1996). Identification of Pex13p a peroxisomal membrane receptor for the PTS1 recognition factor. *The Journal of Cell Biology*,

135(1), 111–21. Retrieved from http://www.ncbi.nlm.nih.gov/pubmed/8858167

Fahimi, H. (1969). Cytochemical localization of peroxidatic activity of catalase in rat hepatic microbodies (peroxisomes). *Journal of Cell Biology*, *43*(2), 275–288. https://doi.org/10.1083/jcb.43.2.275

Fahimi, H., and Baumgart, E. (1999). Current Cytochemical Techniques for the Investigation of Peroxisomes: A Review. *Journal of Histochemistry & Cytochemistry*, *47*(10), 1219–1232. https://doi.org/10.1177/002215549904701001

Fahimi, H., Kino, M., … Abelman, W. H. (1979). Increased myocardial catalase in rats fed ethanol. *The American Journal of Pathology*, *96*(2), 373–90. Retrieved from http://www.ncbi.nlm.nih.gov/pubmed/474705

Fan, D., Takawale, A., … Kassiri, Z. (2012). Cardiac fibroblasts, fibrosis and extracellular matrix remodeling in heart disease. *Fibrogenesis & Tissue Repair*, *5*(1), 15. https://doi.org/10.1186/1755-1536-5-15

Faust, P. L., and Hatten, M. E. (1997). Targeted deletion of the PEX2 peroxisome assembly gene in mice provides a model for Zellweger syndrome, a human neuronal migration disorder. *The Journal of Cell Biology*, *139*(5), 1293–305. Retrieved from http://www.ncbi.nlm.nih.gov/pubmed/9382874

Fearnley, C. J., Roderick, H. L., and Bootman, M. D. (2011). Calcium Signaling in Cardiac Myocytes. *Cold Spring Harbor Perspectives in Biology*, *3*(11), a004242–a004242. https://doi.org/10.1101/cshperspect.a004242

Finck, B. N. (2007). The PPAR regulatory system in cardiac physiology and disease. *Cardiovascular Research*, *73*(2), 269–277. https://doi.org/10.1016/j.cardiores.2006.08.023

Fisher, A. (2009). Redox Signaling Across Cell Membranes. *Antioxidants & Redox Signaling*, *11*(6), 1349–1356. https://doi.org/10.1089/ars.2008.2378

Fisher, D., Heymann, M., and Rudolph, A. (1980). Myocardial oxygen and carbohydrate consumption in fetal lambs in utero and in adult sheep. *The American Journal of Physiology*, *238*(3), H399-405. Retrieved from http://www.ncbi.nlm.nih.gov/pubmed/7369385

Forini, F., Nicolini, G., and Iervasi, G. (2015). Mitochondria as Key Targets of

Cardioprotection in Cardiac Ischemic Disease: Role of Thyroid Hormone Triiodothyronine. *International Journal of Molecular Sciences*, *16*(3), 6312–6336. https://doi.org/10.3390/ijms16036312

Fransen, M., Nordgren, M., … Apanasets, O. (2012). Role of peroxisomes in ROS/RNS-metabolism: Implications for human disease. *Biochimica et Biophysica Acta (BBA) - Molecular Basis of Disease*, *1822*(9), 1363–1373. https://doi.org/10.1016/j.bbadis.2011.12.001

Fujiki, Y., Okumoto, K., … Tamura, S. (2014). Peroxisome biogenesis in mammalian cells. *Frontiers in Physiology*, *5 AUG*(August), 1–8. https://doi.org/10.3389/fphys.2014.00307

Geerts, A., De Prest, B., and Roels, F. (1984). On the topology of the catalase biosynthesis and -degradation in the guinea pig liver. A cytochemical study. *Histochemistry*, *80*(4), 339–45. Retrieved from http://www.ncbi.nlm.nih.gov/pubmed/6735747

Goldfischer, S., Moore, C. L., … Gartner, L. M. (1973). Peroxisomal and mitochondrial defects in the cerebro-hepato-renal syndrome. *Science (New York, N.Y.)*, *182*(4107), 62–4. Retrieved from http://www.ncbi.nlm.nih.gov/pubmed/4730055

Goodwin, G. W., and Taegtmeyer, H. (2000). Improved energy homeostasis of the heart in the metabolic state of exercise. *American Journal of Physiology. Heart and Circulatory Physiology*, *279*(4), H1490-501. Retrieved from http://www.ncbi.nlm.nih.gov/pubmed/11009433

Grabenbauer, M., Sätzler, K., … Fahimi, H. (2000). Three-dimensional ultrastructural analysis of peroxisomes in HepG2 cells. Absence of peroxisomal reticulum but evidence of close spatial association with the endoplasmic reticulum. *Cell Biochemistry and Biophysics*, *32 Spring*, 37–49. Retrieved from http://www.ncbi.nlm.nih.gov/pubmed/11330069

Grant, P., Ahlemeyer, B., … Baumgart-Vogt, E. (2013). The biogenesis protein PEX14 is an optimal marker for the identification and localization of peroxisomes in different cell types, tissues, and species in morphological studies. *Histochemistry and Cell Biology*, *140*(4), 423–442. https://doi.org/10.1007/s00418-013-1133-6

Grynberg, A., and Demaison, L. (1996). Fatty acid oxidation in the heart. *Journal of Cardiovascular Pharmacology*, *28 Suppl 1*, S11-7. Retrieved from http://www.ncbi.nlm.nih.gov/pubmed/8891866

Guellich, A., Damy, T., … Coirault, C. (2013). Tempol prevents cardiac oxidative damage and left ventricular dysfunction in the PPAR- KO mouse. *AJP: Heart and Circulatory Physiology*, *304*(11), H1505–H1512. https://doi.org/10.1152/ajpheart.00669.2012

Halliwell, B. (1999). Establishing the significance and optimal intake of dietary antioxidants: the biomarker concept. *Nutrition Reviews*, *57*(4), 104–13. Retrieved from http://www.ncbi.nlm.nih.gov/pubmed/10228347

Halliwell, B., Gutteridge, J. M., and Cross, C. E. (1992). Free radicals, antioxidants, and human disease: where are we now? *The Journal of Laboratory and Clinical Medicine*, *119*(6), 598–620. Retrieved from http://www.ncbi.nlm.nih.gov/pubmed/1593209

Hand, A. R. (1974). Letter: Peroxisomes (microbodies) in striated muscle cells. *The Journal of Histochemistry and Cytochemistry : Official Journal of the Histochemistry Society*, *22*(3), 207–9. Retrieved from http://www.ncbi.nlm.nih.gov/pubmed/4132631

Harada, K., Sugaya, T., … Komuro, I. (1999). Angiotensin II type 1A receptor knockout mice display less left ventricular remodeling and improved survival after myocardial infarction. *Circulation*, *100*(20), 2093–9. Retrieved from http://www.ncbi.nlm.nih.gov/pubmed/10562266

Hearse, D. J. (1990). Ischemia, reperfusion, and the determinants of tissue injury. *Cardiovascular Drugs and Therapy*, *4 Suppl 4*, 767–76. Retrieved from http://www.ncbi.nlm.nih.gov/pubmed/2093367

Herzog, V., and Fahimi, H. (1974). Microbodies (peroxisomes) containing catalase in myocardium: morphological and biochemical evidence. *Science (New York, N.Y.)*, *185*(4147), 271–3. Retrieved from http://www.ncbi.nlm.nih.gov/pubmed/4833829

Hicks, L., and Fahimi, H. (1977). Peroxisomes (microbodies) in the myocardium of rodents and primates. A comparative Ultrastructural cytochemical study. *Cell and Tissue Research*, *175*(4), 467–81. Retrieved from

http://www.ncbi.nlm.nih.gov/pubmed/401475

Hill, C., Wurfel, A., … Euler, G. (2013). Inhibition of AP-1 signaling by JDP2 overexpression protects cardiomyocytes against hypertrophy and apoptosis induction. *Cardiovascular Research*, *99*(1), 121–128. https://doi.org/10.1093/cvr/cvt094

Hoepfner, D., Schildknegt, D., … Tabak, H. F. (2005). Contribution of the Endoplasmic Reticulum to Peroxisome Formation. *Cell*, *122*(1), 85–95. https://doi.org/10.1016/j.cell.2005.04.025

Huss, J. M., and Kelly, D. P. (2004). Nuclear Receptor Signaling and Cardiac Energetics. *Circulation Research*, *95*(6), 568–578. https://doi.org/10.1161/01.RES.0000141774.29937.e3

Huybrechts, S. J., Van Veldhoven, P. P., … Cassiman, D. (2008). Identification of a novel PEX14 mutation in Zellweger syndrome. *Journal of Medical Genetics*, *45*(6), 376–83. https://doi.org/10.1136/jmg.2007.056697

Huybrechts, S. J., Van Veldhoven, P. P., … Cassiman, D. (2009). Identification of a novel PEX14 mutation in Zellweger syndrome. *Case Reports*, *2009*(jan21 1), bcr0720080503-bcr0720080503. https://doi.org/10.1136/bcr.07.2008.0503

Hwang, I., Lee, J., … Ha, H. (2012). Catalase Deficiency Accelerates Diabetic Renal Injury Through Peroxisomal Dysfunction. *Diabetes*, *61*(3), 728–738. https://doi.org/10.2337/db11-0584

Islinger, M., Cardoso, M. J. R., and Schrader, M. (2010). Be different-The diversity of peroxisomes in the animal kingdom. *Biochimica et Biophysica Acta - Molecular Cell Research*, *1803*(8), 881–897. https://doi.org/10.1016/j.bbamcr.2010.03.013

Jaeschke, H., and Ramachandran, A. (2011). Reactive oxygen species in the normal and acutely injured liver. *Journal of Hepatology*, *55*(1), 227–8. https://doi.org/10.1016/j.jhep.2011.01.006

Jennings, R. B., and Reimer, K. A. (1991). The Cell Biology of Acute Myocardial Ischemia. *Annual Review of Medicine*, *42*(1), 225–246. https://doi.org/10.1146/annurev.me.42.020191.001301

Kalogeris, T., Bao, Y., and Korthuis, R. J. (2014). Mitochondrial reactive oxygen species: A double edged sword in ischemia/reperfusion vs preconditioning.

Redox Biology, *2*, 702–714. https://doi.org/10.1016/j.redox.2014.05.006

Kamei, A., Houdou, S., … Armstrong, D. L. (1993). Peroxisomal disorders in children: immunohistochemistry and neuropathology. *The Journal of Pediatrics*, *122*(4), 573–9. Retrieved from http://www.ncbi.nlm.nih.gov/pubmed/8463903

Kang, Y. J., Chen, Y., and Epstein, P. N. (1996). Suppression of Doxorubicin Cardiotoxicity by Overexpression of Catalase in the Heart of Transgenic Mice. *Journal of Biological Chemistry*, *271*(21), 12610–12616. https://doi.org/10.1074/jbc.271.21.12610

Kantor, P. F., Dyck, J. R., and Lopaschuk, G. D. (1999). Fatty acid oxidation in the reperfused ischemic heart. *The American Journal of the Medical Sciences*, *318*(1), 3–14. Retrieved from http://www.ncbi.nlm.nih.gov/pubmed/10408755

Karnati, S., and Baumgart-Vogt, E. (2008). Peroxisomes in mouse and human lung: Their involvement in pulmonary lipid metabolism. *Histochemistry and Cell Biology*, *130*(4), 719–740. https://doi.org/10.1007/s00418-008-0462-3

Karnati, S., Lüers, G., … Baumgart-Vogt, E. (2013). Mammalian SOD2 is exclusively located in mitochondria and not present in peroxisomes. *Histochemistry and Cell Biology*, *140*(2), 105–117. https://doi.org/10.1007/s00418-013-1099-4

Keller, G. A., Pazirandeh, M., and Krisans, S. (1986). 3-Hydroxy-3-methylglutaryl coenzyme A reductase localization in rat liver peroxisomes and microsomes of control and cholestyramine-treated animals: quantitative biochemical and immunoelectron microscopical analyses. *The Journal of Cell Biology*, *103*(3), 875–86. Retrieved from http://www.ncbi.nlm.nih.gov/pubmed/3745272

Khoo, N. K. H., Hebbar, S., … Robbins, M. (2013). Differential activation of catalase expression and activity by PPAR agonists: Implications for astrocyte protection in anti-glioma therapy. *Redox Biology*, *1*(1), 70–79. https://doi.org/10.1016/j.redox.2012.12.006

Kino, M., Abelman, W. H., … Osborne, D. G. (1981). Chronic effects of ethanol under partial inhibition of catalase activity in the rat heart: light and electron microscopic observations. *Journal of Molecular and Cellular Cardiology*, *13*(1), 5–21. https://doi.org/10.1016/0022-2828(81)90225-X

Koch, J., Brocard, C., … Erdmann, K. S. (2012). PEX11 proteins attract Mff and human Fis1 to coordinate peroxisomal fission. *Journal of Cell Science*, *125*(Pt

16), 3813–26. https://doi.org/10.1242/jcs.102178

Koch, J., Pranjic, K., … Oswald, B. J. (2010). PEX11 family members are membrane elongation factors that coordinate peroxisome proliferation and maintenance. *Journal of Cell Science*, *123*(Pt 19), 3389–400. https://doi.org/10.1242/jcs.064907

Komatsuzaki, S., Ogawa, E., … Ohura, T. (2015). First Japanese case of Zellweger syndrome with a mutation in *PEX14*. *Pediatrics International*, *57*(6), 1189–1192. https://doi.org/10.1111/ped.12713

Kovacs, W., Charles, K. N., … Faust, P. L. (2012). Peroxisome deficiency-induced ER stress and SREBP-2 pathway activation in the liver of newborn PEX2 knock-out mice. *Biochimica et Biophysica Acta (BBA) - Molecular and Cell Biology of Lipids*, *1821*(6), 895–907. https://doi.org/10.1016/j.bbalip.2012.02.011

Kovacs, W., Tape, K. N., … Faust, P. L. (2009). Peroxisome Deficiency Causes a Complex Phenotype because of Hepatic SREBP/Insig Dysregulation Associated with Endoplasmic Reticulum Stress. *Journal of Biological Chemistry*, *284*(11), 7232–7245. https://doi.org/10.1074/jbc.M809064200

Krebs, J. (1998). The role of calcium in apoptosis. *Biometals*, *11*(4), 375–382. https://doi.org/10.1023/A:1009226316146

Krebs, J., Agellon, L. B., and Michalak, M. (2015). Ca2+ homeostasis and endoplasmic reticulum (ER) stress: An integrated view of calcium signaling. *Biochemical and Biophysical Research Communications*, *460*(1), 114–121. https://doi.org/10.1016/j.bbrc.2015.02.004

Krenz, M., and Robbins, J. (2004). Impact of beta-myosin heavy chain expression on cardiac function during stress. *Journal of the American College of Cardiology*, *44*(12), 2390–2397. https://doi.org/10.1016/j.jacc.2004.09.044

Kvannes, J., Eikhom, T. S., and Flatmark, T. (1995). On the mechanism of stimulation of peroxisomal beta-oxidation in rat heart by partially hydrogenated fish oil. *Biochimica et Biophysica Acta*, *1255*(1), 39–49. Retrieved from http://www.ncbi.nlm.nih.gov/pubmed/7893736

Lalwani, N. D., Reddy, M. K., … Reddy, J. (1983). Evaluation of selected hypolipidemic agents for the induction of peroxisomal enzymes and peroxisome proliferation in the rat liver. *Human Toxicology*, *2*(1), 27–48. Retrieved from

http://www.ncbi.nlm.nih.gov/pubmed/6840792

Langendorff, O. (1895). Untersuchungen am überlebenden Säugethierherzen. *Pfluger, Archiv f[r Die Gesammte Physiologie Des Menschen Und Der Thiere*, *61*(6), 291–332. https://doi.org/10.1007/BF01812150

Langer, M., Lüttecke, D., and Schlüter, K.-D. (2003). Mechanism of the positive contractile effect of nitric oxide on rat ventricular cardiomyocytes with positive force/frequency relationship. *Pflugers Archiv European Journal of Physiology*, *447*(3), 289–297. https://doi.org/10.1007/s00424-003-1187-8

Lasorsa, F. M., Pinton, P., … Palmieri, F. (2008). Peroxisomes as novel players in cell calcium homeostasis. *The Journal of Biological Chemistry*, *283*(22), 15300–8. https://doi.org/10.1074/jbc.M800648200

Lazarow, P. B., and Fujiki, Y. (1985). Biogenesis of Peroxisomes. *Annual Review of Cell Biology*, *1*(1), 489–530. https://doi.org/10.1146/annurev.cb.01.110185.002421

Lee, W.-S., and Kim, J. (2015). Peroxisome Proliferator-Activated Receptors and the Heart: Lessons from the Past and Future Directions. *PPAR Research*, *2015*, 1–18. https://doi.org/10.1155/2015/271983

Lessig, J., and Fuchs, B. (2009). Plasmalogens in biological systems: their role in oxidative processes in biological membranes, their contribution to pathological processes and aging and plasmalogen analysis. *Current Medicinal Chemistry*, *16*(16), 2021–41. Retrieved from http://www.ncbi.nlm.nih.gov/pubmed/19519379

Li, G., Chen, Y., … Kang, Y. J. (1997). Catalase-overexpressing transgenic mouse heart is resistant to ischemia-reperfusion injury. *The American Journal of Physiology*, *273*(3 Pt 2), H1090-5. Retrieved from http://www.ncbi.nlm.nih.gov/pubmed/9321793

Li, X., Baumgart, E., … Gould, S. (2002). PEX11alpha is required for peroxisome proliferation in response to 4-phenylbutyrate but is dispensable for peroxisome proliferator-activated receptor alpha-mediated peroxisome proliferation. *Molecular and Cellular Biology*, *22*(23), 8226–40. Retrieved from http://www.ncbi.nlm.nih.gov/pubmed/12417726

Li, X., and Gould, S. J. (2002). PEX11 promotes peroxisome division independently of peroxisome metabolism. *The Journal of Cell Biology*, *156*(4), 643–651.

https://doi.org/10.1083/jcb.200112028

Liepinsh, E., Skapare, E., … Dambrova, M. (2013). Activated peroxisomal fatty acid metabolism improves cardiac recovery in ischemia-reperfusion. *Naunyn-Schmiedeberg's Archives of Pharmacology*, *386*(6), 541–550. https://doi.org/10.1007/s00210-013-0849-0

Liu, J., Wang, P., … Yang, Q. (2011). Cardiomyocyte-Restricted Deletion of PPARβ/δ in PPARα-Null Mice Causes Impaired Mitochondrial Biogenesis and Defense, but No Further Depression of Myocardial Fatty Acid Oxidation. *PPAR Research*, *2011*, 372854. https://doi.org/10.1155/2011/372854

Lockhart, M., Wirrig, E., … Wessells, A. (2011). Extracellular Matrix and Heart Development. *Birth Defects Res A Clin Mol Teratol*, *91*(6), 535–550. https://doi.org/10.1002/bdra.20810.Extracellular

Loichot, C., Jesel, L., … Andriantsitohaina, R. (2006). Deletion of peroxisome proliferator-activated receptor- induces an alteration of cardiac functions. *AJP: Heart and Circulatory Physiology*, *291*(1), H161–H166. https://doi.org/10.1152/ajpheart.01065.2004

Lopaschuk, G. D., Ussher, J. R., … STANLEY, W. C. (2010). Myocardial Fatty Acid Metabolism in Health and Disease. *Physiological Reviews*, *90*(1), 207–258. https://doi.org/10.1152/physrev.00015.2009.

Loud, A. V. (1968). A quantitative stereological description of the ultrastructure of normal rat liver parenchymal cells. *The Journal of Cell Biology*, *37*(1), 27–46. Retrieved from http://www.ncbi.nlm.nih.gov/pubmed/5645844

Luo, J., Wu, S., … Yang, Q. (2010). Conditional PPARγ knockout from cardiomyocytes of adult mice impairs myocardial fatty acid utilization and cardiac function. *American Journal of Translational Research*, *3*(1), 61–72. Retrieved from http://www.ncbi.nlm.nih.gov/pubmed/21139806

Luptak, I., Balschi, J. A., … Tian, R. (2005). Decreased Contractile and Metabolic Reserve in Peroxisome Proliferator-Activated Receptor- -Null Hearts Can Be Rescued by Increasing Glucose Transport and Utilization. *Circulation*, *112*(15), 2339–2346. https://doi.org/10.1161/CIRCULATIONAHA.105.534594

Maeda, K., Kimura, A., … Kurosawa, T. (2002). Oral bile Acid treatment in two Japanese patients with Zellweger syndrome. *Journal of Pediatric*

Gastroenterology and Nutrition, *35*(2), 227–30. Retrieved from http://www.ncbi.nlm.nih.gov/pubmed/12187304

Marín-García, J., and Goldenthal, M. J. (2002). Fatty acid metabolism in cardiac failure: Biochemical, genetic and cellular analysis. *Cardiovascular Research*, *54*(3), 516–527. https://doi.org/10.1016/S0008-6363(01)00552-1

Marone, M., Mozzetti, S., … Scambia, G. (2001). Semiquantitative RT-PCR analysis to assess the expression levels of multiple transcripts from the same sample. *Biological Procedures Online*, *3*(1), 19–25. https://doi.org/10.1251/bpo20

Maxwell, M., Bjorkman, J., … Crane, D. I. (2003). Pex13 inactivation in the mouse disrupts peroxisome biogenesis and leads to a Zellweger syndrome phenotype. *Molecular and Cellular Biology*, *23*(16), 5947–57. Retrieved from http://www.ncbi.nlm.nih.gov/pubmed/12897163

Mendis, S., Puska, P., and Norrving, B. (2015). *WHO | Global atlas on cardiovascular disease prevention and control*. *WHO*. Geneva, Switzerland: World Health Organization.

Michiels, C., Raes, M., … Remacle, J. (1994). Importance of SE-glutathione peroxidase, catalase, and CU/ZN-SOD for cell survival against oxidative stress. *Free Radical Biology and Medicine*, *17*(3), 235–248. https://doi.org/10.1016/0891-5849(94)90079-5

Minners, J., van den Bos, E. J., … Sack, M. N. (2000). Dinitrophenol, cyclosporin A, and trimetazidine modulate preconditioning in the isolated rat heart: support for a mitochondrial role in cardioprotection. *Cardiovascular Research*, *47*(1), 68–73. Retrieved from http://www.ncbi.nlm.nih.gov/pubmed/10869531

Misra, P., Viswakarma, N., and Reddy, J. (2013). Peroxisome proliferator-activated receptor-α signaling in hepatocarcinogenesis. *Subcell Biochem.*, *69*, 77–99.

Miyata, S., Minobe, W., … Leinwand, L. A. (2000). Myosin heavy chain isoform expression in the failing and nonfailing human heart. *Circulation Research*, *86*(4), 386–90. Retrieved from http://www.ncbi.nlm.nih.gov/pubmed/10700442

Morita, E., Yasue, H., … Nakao, K. (1993). Increased plasma levels of brain natriuretic peptide in patients with acute myocardial infarction. *Circulation*, *88*(1), 82–91. Retrieved from http://www.ncbi.nlm.nih.gov/pubmed/8319360

Morrison, A., Yan, X., … Li, J. (2011). Acute rosiglitazone treatment is cardioprotective against ischemia-reperfusion injury by modulating AMPK, Akt, and JNK signaling in nondiabetic mice. *American Journal of Physiology - Heart and Circulatory Physiology*, *301*(3).

Moser, A. E., Singh, I., … Moser, H. W. (1984). The cerebrohepatorenal (Zellweger) syndrome. Increased levels and impaired degradation of very-long-chain fatty acids and their use in prenatal diagnosis. *The New England Journal of Medicine*, *310*(18), 1141–1146. https://doi.org/10.1056/NEJM198405033101802

Mukoyama, M., Nakao, K., … al., et. (1991). Brain natriuretic peptide as a novel cardiac hormone in humans. Evidence for an exquisite dual natriuretic peptide system, atrial natriuretic peptide and brain natriuretic peptide. *The Journal of Clinical Investigation*, *87*(4), 1402–12. https://doi.org/10.1172/JCI115146

Nagaraj, S. H., Gasser, R. B., and Ranganathan, S. (2007). A hitchhiker's guide to expressed sequence tag (EST) analysis. *Briefings in Bioinformatics*, *8*(1), 6–21. https://doi.org/10.1093/bib/bbl015

Nascimento, J., Mota, C., … Garrido, C. (2015). D-Bifunctional Protein Deficiency: A Cause of Neonatal Onset Seizures and Hypotonia. *Pediatric Neurology*, *52*(5), 539–543. https://doi.org/10.1016/j.pediatrneurol.2015.01.007

Neely, J. R., and Morgan, H. E. (1974). Relationship Between Carbohydrate and Lipid Metabolism and the Energy Balance of Heart Muscle. *Annual Review of Physiology*, *36*(1), 413–459. https://doi.org/10.1146/annurev.ph.36.030174.002213

Neuhaus, A., Kooshapur, H., … Erdmann, R. (2014). A Novel Pex14 Protein-interacting Site of Human Pex5 Is Critical for Matrix Protein Import into Peroxisomes. *Journal of Biological Chemistry*, *289*(1), 437–448. https://doi.org/10.1074/jbc.M113.499707

Neuspiel, M., Schauss, A. C., … McBride, H. M. (2008). Cargo-Selected Transport from the Mitochondria to Peroxisomes Is Mediated by Vesicular Carriers. *Current Biology*, *18*(2), 102–108. https://doi.org/10.1016/j.cub.2007.12.038

Nguyen, S. V., and Claycomb, W. C. (1999). Hypoxia Regulates the Expression of the Adrenomedullin and HIF-1 Genes in Cultured HL-1 Cardiomyocytes. *Biochemical and Biophysical Research Communications*, *265*(2), 382–386.

https://doi.org/10.1006/bbrc.1999.1674

Nishikimi, T., Maeda, N., and Matsuoka, H. (2006). The role of natriuretic peptides in cardioprotection. *Cardiovascular Research*, *69*(2), 318–328. https://doi.org/10.1016/j.cardiores.2005.10.001

Noguer, M. T., and Martinez, M. (2010). Visual Follow-Up in Peroxisomal-Disorder Patients Treated with Docosahexaenoic Acid Ethyl Ester. *Investigative Opthalmology & Visual Science*, *51*(4), 2277. https://doi.org/10.1167/iovs.09-4020

Nordgren, M., and Fransen, M. (2014). Peroxisomal metabolism and oxidative stress. *Biochimie*, *98*, 56–62. https://doi.org/10.1016/j.biochi.2013.07.026

Novikoff, A., and Shin, W. (1964). No TThe endoplasmic reticulum in the Golgi zone and its relations to microbodies, Golgi apparatus and autophagic vacuoles in rat liver cells.itle. *J. Microscopie*, *3*, 187–206.

Oberley, T. D., Oberley, L. W., … Elwell, J. H. (1990). Immunohistochemical localization of antioxidant enzymes in adult Syrian hamster tissues and during kidney development. *The American Journal of Pathology*, *137*(1), 199–214. Retrieved from http://www.ncbi.nlm.nih.gov/pubmed/2372042

Ofman, R., Dijkstra, I. M. E., … Kemp, S. (2010). The role of ELOVL1 in very long-chain fatty acid homeostasis and X-linked adrenoleukodystrophy. *EMBO Molecular Medicine*, *2*(3), 90–97. https://doi.org/10.1002/emmm.201000061

Okubo, K., Hori, N., … Matsubara, K. (1992). Large scale cDNA sequencing for analysis of quantitative and qualitative aspects of gene expression. *Nature Genetics*, *2*(3), 173–179. https://doi.org/10.1038/ng1192-173

Oliver, P. M., Fox, J. E., … Maeda, N. (1997). Hypertension, cardiac hypertrophy, and sudden death in mice lacking natriuretic peptide receptor A. *Proceedings of the National Academy of Sciences of the United States of America*, *94*(26), 14730–5. Retrieved from http://www.ncbi.nlm.nih.gov/pubmed/9405681

Opaliński, Ł., Kiel, J. A. K. W., … van der Klei, I. J. (2011). Membrane curvature during peroxisome fission requires Pex11. *The EMBO Journal*, *30*(1), 5–16. https://doi.org/10.1038/emboj.2010.299

Opie, L. H. (2004). *Heart physiology : from cell to circulation*. Lippincott Williams &

Wilkins.

Orth, T., Reumann, S., … Hu, J. (2007). The PEROXIN11 protein family controls peroxisome proliferation in Arabidopsis. *The Plant Cell*, *19*(1), 333–50. https://doi.org/10.1105/tpc.106.045831

Paker, A. M., Sunness, J. S., … Raymond, G. V. (2010). Docosahexaenoic acid therapy in peroxisomal diseases: Results of a double-blind, randomized trial. *Neurology*, *75*(9), 826–830. https://doi.org/10.1212/WNL.0b013e3181f07061

Peters, J. M., Lee, S. S., … Gonzalez, F. J. (2000). Growth, adipose, brain, and skin alterations resulting from targeted disruption of the mouse peroxisome proliferator-activated receptor beta(delta). *Molecular and Cellular Biology*, *20*(14), 5119–28. Retrieved from http://www.ncbi.nlm.nih.gov/pubmed/10866668

Piechaczyk, M., Blanchard, J. M., … Jeanteur, P. (1984). Post-transcriptional regulation of glyceraldehyde-3-phosphate-dehydrogenase gene expression in rat tissues. *Nucleic Acids Research*, *12*(18), 6951–63. Retrieved from http://www.ncbi.nlm.nih.gov/pubmed/6548307

Pol, C. J., Lieu, M., and Drosatos, K. (2015). PPARs: Protectors or Opponents of Myocardial Function? *PPAR Research*, *2015*, 1–19. https://doi.org/10.1155/2015/835985

Qian, G., Fan, W., … Everett, C. (2015). Peroxisomes in Different Skeletal Cell Types during Intramembranous and Endochondral Ossification and Their Regulation during Osteoblast Differentiation by Distinct Peroxisome Proliferator-Activated Receptors. *PLOS ONE*, *10*(12), e0143439. https://doi.org/10.1371/journal.pone.0143439

Qin, F., Lennon-Edwards, S., … Colucci, W. S. (2010). Cardiac-specific overexpression of catalase identifies hydrogen peroxide-dependent and -independent phases of myocardial remodeling and prevents the progression to overt heart failure in G(alpha)q-overexpressing transgenic mice. *Circulation. Heart Failure*, *3*(2), 306–13. https://doi.org/10.1161/CIRCHEARTFAILURE.109.864785

Raedschelders, K., Ansley, D. M., and Chen, D. D. Y. (2012). The cellular and molecular origin of reactive oxygen species generation during myocardial ischemia and reperfusion. *Pharmacology and Therapeutics*, *133*(2), 230–255.

https://doi.org/10.1016/j.pharmthera.2011.11.004

Rao, M. S., Dwivedi, R. S., … Reddy, J. (1988). Induction of peroxisome proliferation and hepatic tumours in C57BL/6N mice by ciprofibrate, a hypolipidaemic compound. *British Journal of Cancer*, *58*(1), 46–51. Retrieved from http://www.ncbi.nlm.nih.gov/pubmed/2901849

Raychaudhury, B., Gupta, S., … Datta, S. C. (2006). Peroxisome is a reservoir of intracellular calcium. *Biochimica et Biophysica Acta - General Subjects*, *1760*(7), 989–992. https://doi.org/10.1016/j.bbagen.2006.02.022

Reddy, J., and Hashimoto, T. (2001). Peroxisomal beta-oxidation and peroxisome proliferator-activated receptor alpha: an adaptive metabolic system. *Annu Rev Nutr*, *21*, 193–230. https://doi.org/10.1146/annurev.nutr.21.1.193

Reddy, J., and Krishnakantha, T. P. (1975). Hepatic peroxisome proliferation: induction by two novel compounds structurally unrelated to clofibrate. *Science (New York, N.Y.)*, *190*(4216), 787–9. Retrieved from http://www.ncbi.nlm.nih.gov/pubmed/1198095

Reddy, J., Rao, M. S., and Moody, D. E. (1976). Hepatocellular Carcinomas in Acatalasemic Mice Treated with Nafenopin, a Hypolipidemic Peroxisome Proliferator. *Cancer Research*, *36*(4).

Reiser, P. J., Portman, M. A., … Schomisch Moravec, C. (2001). Human cardiac myosin heavy chain isoforms in fetal and failing adult atria and ventricles. *American Journal of Physiology. Heart and Circulatory Physiology*, *280*(4), H1814-20. Retrieved from http://www.ncbi.nlm.nih.gov/pubmed/11247796

Rhodin, J. (1954). *Correlation of ultrastructural organization and function in normal and experimentally changed proximal tubule cells of the mouse kidney*. Stockholm, Sweden.

Rienks, M., Papageorgiou, A.-P., … Heymans, S. (2014). Myocardial Extracellular Matrix. *Circulation Research*, *114*(5).

Roels, F. (1976). Cytochemical demonstration of extraperoxisomal catalase. I. Sheep liver. *The Journal of Histochemistry and Cytochemistry : Official Journal of the Histochemistry Society*, *24*(6), 713–24. Retrieved from http://www.ncbi.nlm.nih.gov/pubmed/950458

Roels, F., Geerts, A., … Goldfischer, S. (1982). CYTOPLASMIC CATALASE: CYTOCHEMISTRY AND PHYSIOLOGY. *Annals of the New York Academy of Sciences*, *386*(1 Peroxisomes a), 534–536. https://doi.org/10.1111/j.1749-6632.1982.tb21472.x

Saia, F., Grigioni, F., … Branzi, A. (2010). Management of acute left ventricular dysfunction after primary percutaneous coronary intervention for ST elevation acute myocardial infarction. *American Heart Journal*, *160*(6), S16–S21. https://doi.org/10.1016/j.ahj.2010.10.011

Santos, M. J., Henderson, S. C., … Lazarow, P. B. (2000). Peroxisomal ghosts are intracellular structures distinct from lysosomal compartments in Zellweger syndrome: a confocal laser scanning microscopy study. *Biology of the Cell*, *92*(2), 85–94. Retrieved from http://www.ncbi.nlm.nih.gov/pubmed/10879629

Sassa, T., and Kihara, A. (2014). Metabolism of very long-chain fatty acids: Genes and pathophysiology. *Biomolecules and Therapeutics*. https://doi.org/10.4062/biomolther.2014.017

Schlesinger, J., Schueler, M., … Sperling, S. R. (2011). The cardiac transcription network modulated by gata4, mef2a, nkx2.5, srf, histone modifications, and microRNAs. *PLoS Genetics*, *7*(2). https://doi.org/10.1371/journal.pgen.1001313

Schlüter, K.-D., and Piper, H. M. (2005). Isolation and Culture of Adult Ventricular Cardiomyocytes. In *Practical Methods in Cardiovascular Research* (pp. 557–567). Berlin/Heidelberg: Springer-Verlag. https://doi.org/10.1007/3-540-26574-0_28

Schlüter, K.-D., and Schreiber, D. (2005). Adult ventricular cardiomyocytes: isolation and culture. *Methods in Molecular Biology (Clifton, N.J.)*, *290*, 305–14. Retrieved from http://www.ncbi.nlm.nih.gov/pubmed/15361670

Scholz, T. D., and Segar, J. L. (2008). Cardiac Metabolism in the Fetus and Newborn. *NeoReviews*, *9*(3).

Schrader, M., Costello, J. L., … Islinger, M. (2016). Proliferation and fission of peroxisomes - An update. *Biochimica et Biophysica Acta - Molecular Cell Research*, *1863*(5), 971–983. https://doi.org/10.1016/j.bbamcr.2015.09.024

Schrader, M., and Fahimi, H. (2006). Peroxisomes and oxidative stress. *Biochimica et Biophysica Acta - Molecular Cell Research*, *1763*(12), 1755–1766.

https://doi.org/10.1016/j.bbamcr.2006.09.006

Schrader, M., Grille, S., … Islinger, M. (2013). Peroxisome interactions and cross-talk with other subcellular compartments in animal cells. *Sub-Cellular Biochemistry*, *69*, 1–22. https://doi.org/10.1007/978-94-007-6889-5_1

Schreckenberg, R., Dyukova, E., … Schlüter, K.-D. (2015). Mechanisms by which calcium receptor stimulation modifies electromechanical coupling in isolated ventricular cardiomyocytes. *Pflügers Archiv - European Journal of Physiology*, *467*(2), 379–388. https://doi.org/10.1007/s00424-014-1498-y

Seeger, W., Adir, Y., … Vachiéry, J.-L. (2013). Pulmonary Hypertension in Chronic Lung Diseases. *Journal of the American College of Cardiology*, *62*(25), D109–D116. https://doi.org/10.1016/j.jacc.2013.10.036

Setchell, K. D., Bragetti, P., … Morelli, A. (1992). Oral bile acid treatment and the patient with Zellweger syndrome. *Hepatology (Baltimore, Md.)*, *15*(2), 198–207. Retrieved from http://www.ncbi.nlm.nih.gov/pubmed/1735522

Shimozawa, N., Tsukamoto, T., … Kondo, N. (2004). Identification of a new complementation group of the peroxisome biogenesis disorders and PEX14 as the mutated gene. *Human Mutation*, *23*(6), 552–558. https://doi.org/10.1002/humu.20032

Shipp, J. C. (1964). Interrelation between carbohydrate and fatty acid metabolism of isolated perfused rat heart. *Metabolism*, *13*(9), 852–867. https://doi.org/10.1016/0026-0495(64)90054-X

Simek, C. L., Feldman, M. D., … Kaul, S. (1995). Relationship between left ventricular wall thickness and left atrial size: comparison with other measures of diastolic function. *Journal of the American Society of Echocardiography : Official Publication of the American Society of Echocardiography*, *8*(1), 37–47. Retrieved from http://www.ncbi.nlm.nih.gov/pubmed/7710749

Son, N.-H., Park, T.-S., … Goldberg, I. J. (2007). Cardiomyocyte expression of PPARγ leads to cardiac dysfunction in mice. *Journal of Clinical Investigation*, *117*(10), 2791–2801. https://doi.org/10.1172/JCI30335

Stanley, W. C., Lopaschuk, G. D., … McCormack, J. G. (1997). Regulation of myocardial carbohydrate metabolism under normal and ischaemic conditions. Potential for pharmacological interventions. *Cardiovascular Research*, *33*(2),

243–57. Retrieved from http://www.ncbi.nlm.nih.gov/pubmed/9074687

Steinberg, S. J., Dodt, G., … Moser, H. W. (2006). Peroxisome biogenesis disorders. *Biochimica et Biophysica Acta (BBA) - Molecular Cell Research*, *1763*(12), 1733–1748. https://doi.org/10.1016/j.bbamcr.2006.09.010

Stier, H., Fahimi, H., … Mannaerts, G. P. (1998). Maturation of peroxisomes in differentiating human hepatoblastoma cells (HepG2): possible involvement of the peroxisome proliferator-activated receptor α (PPARα). *Differentiation*, *64*(1), 55–66. https://doi.org/10.1046/j.1432-0436.1998.6410055.x

Stolz, D., Zamora, R., … Watkins, S. C. (2002). Peroxisomal localization of inducible nitric oxide synthase in hepatocytes. *Hepatology*, *36*(1), 81–93. https://doi.org/10.1053/jhep.2002.33716

Strauss, A. W., Powell, C. K., … Sims, H. F. (1995). Molecular basis of human mitochondrial very-long-chain acyl-CoA dehydrogenase deficiency causing cardiomyopathy and sudden death in childhood. *Proceedings of the National Academy of Sciences of the United States of America*, *92*(23), 10496–500. Retrieved from http://www.ncbi.nlm.nih.gov/pubmed/7479827

Strober, W. (2015). Trypan Blue Exclusion Test of Cell Viability. In *Current Protocols in Immunology* (Vol. 111, p. A3.B.1-A3.B.3). Hoboken, NJ, USA: John Wiley & Sons, Inc. https://doi.org/10.1002/0471142735.ima03bs111

Sugamura, K., and Keaney, J. F. (2011). Reactive oxygen species in cardiovascular disease. *Free Radical Biology and Medicine*, *51*(5), 978–992. https://doi.org/10.1016/j.freeradbiomed.2011.05.004

Sugiura, A., McLelland, G.-L., … McBride, H. M. (2014). A new pathway for mitochondrial quality control: mitochondrial-derived vesicles. *The EMBO Journal*, *33*(19), 2142–2156. https://doi.org/10.15252/embj.201488104

Sugiura, T., Matoba, H., … Murakami, N. (1992). Myosin heavy chain isoform transition in ageing fast and slow muscles of the rat. *Acta Physiologica Scandinavica*, *144*(4), 419–423. https://doi.org/10.1111/j.1748-1716.1992.tb09315.x

Suzuki, O., Koura, M., … Matsuda, J. (2011). Use of sample mixtures for standard curve creation in quantitative western blots. *Experimental Animals*, *60*(2), 193–6. Retrieved from http://www.ncbi.nlm.nih.gov/pubmed/21512276

Sylvester, P. W. (2011). Optimization of the Tetrazolium Dye (MTT) Colorimetric Assay for Cellular Growth and Viability (pp. 157–168). https://doi.org/10.1007/978-1-61779-012-6_9

Terlecky, S. R., Koepke, J. I., and Walton, P. A. (2006). Peroxisomes and aging. *Biochimica et Biophysica Acta*, *1763*(12), 1749–54. https://doi.org/10.1016/j.bbamcr.2006.08.017

Tusnády, G. E., and Simon, I. (2001). The HMMTOP transmembrane topology prediction server. *Bioinformatics (Oxford, England)*, *17*(9), 849–50. Retrieved from http://www.ncbi.nlm.nih.gov/pubmed/11590105

Tyagi, S., Gupta, P., … Sharma, S. (2011). The peroxisome proliferator-activated receptor: A family of nuclear receptors role in various diseases. *Journal of Advanced Pharmaceutical Technology & Research*, *2*(4), 236–40. https://doi.org/10.4103/2231-4040.90879

van der Vusse, G. J., van Bilsen, M., and Glatz, J. F. (2000). Cardiac fatty acid uptake and transport in health and disease. *Cardiovascular Research*, *45*(2), 279–93. Retrieved from http://www.ncbi.nlm.nih.gov/pubmed/10728348

Van Veldhoven, P. P. (2010). Biochemistry and genetics of inherited disorders of peroxisomal fatty acid metabolism. *Journal of Lipid Research*, *51*(10), 2863–95. https://doi.org/10.1194/jlr.R005959

Van Veldhoven, P. P., and Mannaerts, G. P. (1994). Assembly of the peroxisomal membrane. *Sub-Cellular Biochemistry*, *22*, 231–61. Retrieved from http://www.ncbi.nlm.nih.gov/pubmed/8146884

Vanden Heuvel, J. P. (2004). Diet, fatty acids, and regulation of genes important for heart disease. *Current Atherosclerosis Reports*, *6*(6), 432–40. Retrieved from http://www.ncbi.nlm.nih.gov/pubmed/15485588

Vijayan, V., Baumgart-Vogt, E., … Immenschuh, S. (2011). Bruton's Tyrosine Kinase Is Required for TLR-Dependent Heme Oxygenase-1 Gene Activation via Nrf2 in Macrophages. *The Journal of Immunology*, *187*(2), 817–827. https://doi.org/10.4049/jimmunol.1003631

Vluggens, A., Andreoletti, P., … Cherkaoui-Malki, M. (2010). Functional significance of the two ACOX1 isoforms and their crosstalks with PPARa and RXRa. *Laboratory Investigation*, *9046*, 696–708.

https://doi.org/10.1038/labinvest.2010.46

Völkl, A., Mohr, H., and Fahimi, H. (1999). Peroxisome subpopulations of the rat liver. Isolation by immune free flow electrophoresis. *The Journal of Histochemistry and Cytochemistry : Official Journal of the Histochemistry Society*, *47*(9), 1111–8. Retrieved from http://www.ncbi.nlm.nih.gov/pubmed/10449531

Wagner, G. P., Kin, K., and Lynch, V. J. (2012). Measurement of mRNA abundance using RNA-seq data: RPKM measure is inconsistent among samples. *Theory in Biosciences*, *131*(4), 281–285. https://doi.org/10.1007/s12064-012-0162-3

Wallner, S., and Schmitz, G. (2011). Plasmalogens the neglected regulatory and scavenging lipid species. *Chemistry and Physics of Lipids*, *164*(6), 573–589. https://doi.org/10.1016/j.chemphyslip.2011.06.008

Wanders, R. (2004). Peroxisomes, lipid metabolism, and peroxisomal disorders. *Molecular Genetics and Metabolism*, *83*(1–2), 16–27. https://doi.org/10.1016/j.ymgme.2004.08.016

Wanders, R. (2014). Metabolic functions of peroxisomes in health and disease. *Biochimie*, *98*(1), 36–44. https://doi.org/10.1016/j.biochi.2013.08.022

Wanders, R., Ferdinandusse, S., … Kemp, S. (2010). Peroxisomes, lipid metabolism and lipotoxicity. *Biochimica et Biophysica Acta - Molecular and Cell Biology of Lipids*, *1801*(3), 272–280. https://doi.org/10.1016/j.bbalip.2010.01.001

Wanders, R., and Waterham, H. R. (2006). Peroxisomal disorders: The single peroxisomal enzyme deficiencies. *Biochimica et Biophysica Acta - Molecular Cell Research*, *1763*(12), 1707–1720. https://doi.org/10.1016/j.bbamcr.2006.08.010

Wanders, R., Waterham, H. R., and Ferdinandusse, S. (2016). Metabolic Interplay between Peroxisomes and Other Subcellular Organelles Including Mitochondria and the Endoplasmic Reticulum. *Frontiers in Cell and Developmental Biology*, *3*(January), 83. https://doi.org/10.3389/fcell.2015.00083

Wang, P., Liu, J., … Yang, Q. (2010). Peroxisome proliferator-activated receptor {delta} is an essential transcriptional regulator for mitochondrial protection and biogenesis in adult heart. *Circulation Research*, *106*(5), 911–9. https://doi.org/10.1161/CIRCRESAHA.109.206185

Watanabe, K., Fujii, H., … Aoyama, T. (2000). Constitutive Regulation of Cardiac Fatty Acid Metabolism through Peroxisome Proliferator-activated Receptor Associated with Age-dependent Cardiac Toxicity*. https://doi.org/10.1074/jbc.M000248200

Watanabe, T., and Suga, T. (1988). Suppression of clofibrate-induced peroxisome proliferation in rat liver by nicardipine, a calcium antagonist. *FEBS Letters*, *232*(2), 293–297. https://doi.org/10.1016/0014-5793(88)80756-7

Waterham, H. R., Ferdinandusse, S., and Wanders, R. (2016). Human disorders of peroxisome metabolism and biogenesis. *Biochimica et Biophysica Acta - Molecular Cell Research*, *1863*(5), 922–933. https://doi.org/10.1016/j.bbamcr.2015.11.015

Weng, H., Ji, X., … Iwai, N. (2013). Pex11α deficiency impairs peroxisome elongation and division and contributes to nonalcoholic fatty liver in mice. *American Journal of Physiology. Endocrinology and Metabolism*, *304*(2), E187-96. https://doi.org/10.1152/ajpendo.00425.2012

Winterstein, H. (1904). Ueber die Sauerstoffatmung des isolierten Saeugetierherzens. *Zeitschrift Für Allgemeine Physiologie*, *4*, 339–359.

Wishart, T. M., Pemberton, H. N., … Gillingwater, T. H. (2008). Modified cell cycle status in a mouse model of altered neuronal vulnerability (slow Wallerian degeneration; Wlds). *Genome Biology*, *9*(6), R101. https://doi.org/10.1186/gb-2008-9-6-r101

Wittels, B., and Bressler, R. (1965). Lipid metabolism in the newborn heart. *The Journal of Clinical Investigation*, *44*(10), 1639–46. https://doi.org/10.1172/JCI105270

Wondergem, R., Graves, B. M., … Williams, D. L. (2012). Lipopolysaccharide prolongs action potential duration in HL-1 mouse cardiomyocytes. *AJP: Cell Physiology*, *303*(8), C825–C833. https://doi.org/10.1152/ajpcell.00173.2012

Xu, H. E., Lambert, M. H., … Milburn, M. V. (1999). Molecular recognition of fatty acids by peroxisome proliferator-activated receptors. *Molecular Cell*, *3*(3), 397–403. Retrieved from http://www.ncbi.nlm.nih.gov/pubmed/10198642

Yamamoto, K., Völkl, A., … Fahimi, H. (1988). Catalase in guinea pig hepatocytes is localized in cytoplasm, nuclear matrix and peroxisomes. *European Journal of*

Cell Biology, *46*(1), 129–35. Retrieved from http://www.ncbi.nlm.nih.gov/pubmed/3396586

Yang, P.-C., and Mahmood, T. (2012). Western blot: Technique, theory, and trouble shooting. *North American Journal of Medical Sciences*, *4*(9), 429. https://doi.org/10.4103/1947-2714.100998

Yasue, H., Yoshimura, M., … Nakao, K. (1994). Localization and mechanism of secretion of B-type natriuretic peptide in comparison with those of A-type natriuretic peptide in normal subjects and patients with heart failure. *Circulation*, *90*(1), 195–203. Retrieved from http://www.ncbi.nlm.nih.gov/pubmed/8025996

Yik, W. Y., Steinberg, S. J., … Hacia, J. G. (2009). Identification of novel mutations and sequence variation in the Zellweger syndrome spectrum of peroxisome biogenesis disorders. *Human Mutation*, *30*(3), E467–E480. https://doi.org/10.1002/humu.20932

Yokota, S., and Asayama, K. (1992). Proliferation of myocardial peroxisomes in experimental rat diabetes: a biochemical and immunocytochemical study. *Virchows Archiv. B, Cell Pathology Including Molecular Pathology*, *63*(1), 43–9. Retrieved from http://www.ncbi.nlm.nih.gov/pubmed/1362021

Yokota, S., and Fahimi, H. (1981). Immunocytochemical localization of catalase in rat liver. *The Journal of Histochemistry and Cytochemistry : Official Journal of the Histochemistry Society*, *29*(7), 805–12. Retrieved from http://www.ncbi.nlm.nih.gov/pubmed/6790603

Yuan, J. S., Reed, A., … Stewart, C. N. (2006). Statistical analysis of real-time PCR data. *BMC Bioinformatics*, *7*(1), 85. https://doi.org/10.1186/1471-2105-7-85

Zaar, K. (1992). Structure and function of peroxisomes in the mammalian kidney. *European Journal of Cell Biology*, *59*(2), 233–54. Retrieved from http://www.ncbi.nlm.nih.gov/pubmed/1493789

Zaar, K., V??lkl, A., and Fahimi, H. (1987). Association of isolated bovine kidney cortex peroxisomes with endoplasmic reticulum. *BBA - Biomembranes*, *897*(1), 135–142. https://doi.org/10.1016/0005-2736(87)90321-X

Zhang, X., Klein, A. L., … Ren, J. (2003). Cardiac-specific overexpression of catalase rescues ventricular myocytes from ethanol-induced cardiac contractile defect. *Journal of Molecular and Cellular Cardiology*, *35*(6), 645–52. Retrieved from

http://www.ncbi.nlm.nih.gov/pubmed/12788382

Zhong, H., and Simons, J. W. (1999). Direct comparison of GAPDH, beta-actin, cyclophilin, and 28S rRNA as internal standards for quantifying RNA levels under hypoxia. *Biochemical and Biophysical Research Communications*, *259*(3), 523–6. https://doi.org/10.1006/bbrc.1999.0815

Zimmerman, J. (1966). The functional and surgical anatomy of the heart. *Annals of the Royal College of Surgeons of England*, *39*(6), 348–66. Retrieved from http://www.ncbi.nlm.nih.gov/pubmed/5957901

9. Index of Abbreviations

3D	three-dimensional
ABCD3, which is also PMP70	ATP-binding cassette sub-family D member 3
ABCD4, also named as PMP69	ATP binding cassette subfamily D member 4
Acox1	peroxisomal acyl-coenzyme A oxidase 1
Acox3	peroxisomal acyl-coenzyme A oxidase 3
ADH	alcohol dehydrogenase
ALDH2	aldehyde dehydrogenase 2
ALDP	adrenoleukodystrophy protein
AMACR	2-methylacyl-CoA racemase
ANOVA	analysis of variance
ANP	atrial natriuretic peptide
ATP	adenosine triphosphate
BLAST	basic local alignment search tool
BNP	brain natriuretic peptide
bp	base pair
BSA	bovine serum albumin
Cat	peroxisomal catalase
CNP	C-type natriuretic peptide
CO_2	carbon dioxide
CoA	coenzyme A
CPT	carnitine palmitoyltransferase
Ct	threshold cycle
CVDs	cardiovascular diseases

CYP2E1	cytochrome P450 2E1
DAB	3,3′-diaminobenzidine
DBP	D-bifunctional protein
DDBJ	DNA Data Bank of Japan
DEHA	di-(2-ethylhexyl)-adipate
DEHP	di-(2-ethylhexyl)-phthalate
DEPC	diethylpyrocarbonate
DHA	docosahexaenoic acid
DMSO	dimethylsulfoxide
DRP	dynamin-related protein
ECM	extracellular matrix
EDTA	ethylene diamine tetraacetic acid
ENA	European Nucleotide Archive
ER	endoplasmic reticulum
ESTs	expressed sequence tags
FAD	flavin adenine dinucleotide
Fis1	mitochondrial fission protein 1
G6P	glucose 6-phosphate
GAPDH	glyceraldehyde-3-phosphate dehydrogenase
GLUTs	glucose transporters
GNPAT	glyceronephosphate O-acyltransferase
GSH	glutathione
GSSG	glutathione disulfide
h	hour
H_2O	water
H_2O_2	hydrogen peroxide

HE	hematoxylin and eosin
HMG-CoA reductase	3-hydroxymethyl glutaryl-CoA reductase
HZ	heterozygote
IF	immunofluorescence
iNOS	inducible nitric oxide synthase
IP	ischemia reperfusion
IRD	infantile Refsum disease
KO	knockout
LA	left atrium
LV	left ventricle
M	marker
MDVs	mitochondria-derived vesicles
MFP	multifunctional protein 1
MI	mitochondria
min	minute
ml	milliliter
MnSOD	mitochondrial superoxide dismutase
Ms	mouse
MTT	methylthiazole tetrazolium
NADPH	nicotinamide adenine dinucleotide phosphate (reduced)
NALD	neonatal adrenoleukodystrophy
NC	negative control
NCBI	National Center for Biotechnology Information
NO	nitrogen monoxide
O_2	dioxygen

ONOO-	peroxynitrite
P2	postnatal day 2
PBS	phosphate-buffered saline
PC	positive control
PCI	percutaneous coronary intervention
PFA	paraformaldehyde
Pmp24	peroxisomal membrane protein 4
PO	peroxisome
PPARs	peroxisome proliferator activated receptors
PPREs	peroxisome proliferator hormone response elements
PTSs	peroxisomal targeting sequences
PUFAs	polyunsaturated fatty acids
RA	right atrium
Rb	rabbit
RC	respiratory chain
RCDP	rhizomelic chondrodysplasia punctata
RGZ	rosiglitazone
ROS	reactive oxygen species
RT-PCR	reverse transcription polymerase chain reaction
RV	right ventricle
RXR	retinoid X receptor
s	second
SD	standard deviation
SDS	sodium dodecylsulfate
SER	smooth endoplasmic reticulum
TBS	Tris-buffered saline

TBST	Tris-buffered saline with Tween-20
TEMED	tetramethylethylenediamine
TPM	transcripts per million
Tris	trishydroxymethylaminomethane
VLCFA	very-long-chain fatty acids
WB	western blot analysis
WT	wild type
X-ALD	X-linked adrenoleukodystrophy
ZS	Zellweger syndrome
ZSD	Zellweger spectrum disorders
α-MHC	α-myosin heavy chain
β-MHC	β-myosin heavy chain
µl	microliter

10. Acknowledgement

My supervisor Prof. Dr. Baumgart-Vogt and I had met in China before I started my PhD study. When she was representing GGL (Giessen Graduate School of Life Science) and interviewing the students in China, we had a very nice interview. Her first impression to me was gentle, elegant, humor and lovely. Actually, she is not only a nice supervisor, but also a careful, strict and hard-working person. I have seen so many excellent characteristics and learned so many things from her. As a female professor, she devoted a lot of her time to research, teaching and student work. As a Ph.D. student, I am lucky to meet a professor, with whom I could discuss the scientific questions in the conference room, in my or her office and even in the kitchen of our building. Many sparkling ideas come out after the discussions. Her perpetual energy and enthusiasm in research have motivated me all the time. She will always be the best example in my research life.

I also want to thank Dr. Claudia Colasante for her kind guidance and enormous help during my doctoral study. She is also an excellent sample of academic professional, who is efficient, hardworking and precise. Also PD Dr. Barbara Ahlemeyer for her kind help and nice cooperation work, she introduced me to use the CLSM and real-time PCR machine, and also gave me many useful tips during my study. Special warm-hearted thanks to Dr. Klaus-Peter Valerius and Dr. Wieland Stöckmann for their frequent help at all times without any hesitation.

This thesis would never have taken shape without the help of technical staffs and I am very grateful to Andrea Textor, Bianca Pfeiffer, Susanne Pfreimer, Elke Rodenberg-Frank and Petra Hahn-Kohlberger for their excellent technical assistance. Also, I want to heartily thank those people who spent their time and shared their knowledge for helping me to complete my thesis with the best possible results: Dr. Srikanth Karnati, Vijith Vijayan Wei Fan and Yu Xiao.

Also my best thanks to those who spent the most time with me and helped me: Shan Wang, Natalie El-Merhie, Rocio Bonilla-Martinez, Eistine Boateng, Lilit Kamalyan and Wenwen Wang.

Further thanks also go to our secretary- Silvia Heller and all lab members in the Department of Anatomy and Cell Biology for their warm and friendly nature.

My study would not have been finished without the help from Prof. Schlüter, also the technician Nadine and Dr. Martin Weber who kindly help me with the experiment. I also want to thank Prof. Böning for providing us the animal material for my research.

Also my deepest thanks to all my family numbers for the forever love and support without any condition.

I would never forget my homeland China, China Scholarship Council for supporting my Ph.D. study. I would like also give my special thanks to Giessen Graduate School of Life Science (GGL), though which I participate a lot of valuable training course.

Der Lebenslauf wurde aus der elektronischen Version der Arbeit entfernt.

The curriculum vitae was removed from the electronic version of the paper.